NANOTECHNOLOGY APPROACHES FOR INHALATION TREATMENT OF FIBROSIS

By

VERA IVANOVA

A Dissertation submitted to the

Graduate School-New Brunswick Rutgers,

The State University of New Jersey In

partial fulfillment of the requirements

for the degree of

Doctor of Philosophy

Graduate Program in Pharmaceutical Science

written under the direction of

Tamara Minko

and approved by

_____

_____

_____

_____

New Brunswick, New Jersey

OCTOBER 2015

ABSTRACT OF THE DISSERTATION NANOTECHNOLOGY APPROACHES FOR INHALATION TREATMENT OF FIBROSIS

By

VERA IVANOVA

Dissertation Director: Professor Tamara Minko, Ph.D.

Idiopathic Pulmonary Fibrosis (IPF) is very insidious and untreatable disease. While many investigations are focused on the pathogenesis of the disease this disorder does not have reliable therapeutic options and an effective therapy has yet to be identified and developed. Pulmonary fibrosis has been mainly treated for secondary symptoms with some success, but unfortunately patients succumb to the disease. While cystic fibrosis is caused by mutation in chlorine transporter gene CFTR, idiopathic pulmonary fibrosis is developed similarly to cancer due to various environmental factors combined with genetic. Antibiotic treatments have prolonged the survival rate of children suffering from cystic fibrosis to forty years. Meanwhile, various treatments for idiopathic pulmonary fibrosis were less successful with general survival rate less than 3 years. All of the current treatments address secondary symptoms rather than the cause of the disease. Therefore, it is very vital to develop new treatment for debilitating fibrotic diseases.

In our study we focused on the pulmonary form of fibrosis. It is natural to use local administration of drugs by inhalation for treating of - respiratory diseases. Some of the respiratory drugs nowadays are being repositioned for local treatment. With successful inhalation devices and monitoring, local delivery to the lungs has higher efficacy due to administering lower doses directly at the site of action and potentially eliminating systemic toxicity.

Nanotechnology is referred to the field that deals with particles in nanometer size range, which gives higher surface area and bioavailability to its desired therapeutic components. Nanoparticles improve treatments by increasing stability, solubility, and providing sustained release of therapeutic agent, which results in reduced dosage frequency and higher patient compliance.

The overall purpose of this work is to develop, characterize and evaluate in vitro and in vivo novel inhalational nanotechnology-based treatment for idiopathic pulmonary - and cystic fibroses. In the dissertation we are planning to focus on the: (1) to design bleomycin animal model of idiopathic pulmonary fibrosis and to test novel inhalational treatment approach using liposomal form of Prostaglandin E2 (PGE2); (2) to develop multifunctional targeted nanosystem for the delivery of siRNA and PGE2 into the lungs of mice with IPF; (3) to develop and evaluate nanosystem containing two drugs with different mechanisms of action for treatment of cystic fibrosis.

DEDICATION

To my advisor, Professor Tamara Minko,

Who is my role model, who has helped and guided me and become an inspiration

To my amazing husband;

Whose patience and love and knowledge supported my journey

To my wonderful parents and grandparents;

Whose unconditional love and warms allowed me to succeed

To my brother Yaroslav Ivanov and his lovely wife Nadiya (my sister); Which are my role models, which love unconditionally and keeps life interesting

ACKNOWLEDGEMENTS

I would not be here without the help of so many wonderful people that directly and indirectly helped me during my career. First, I would like to express deep gratitude to my advisor Professor Tamara Minko. She is truly one of a kind person, a role model, that anyone could wish for as an advisor. I deeply admire her and thankful for her patient guidance, believe in her students, enthusiastic encouragements, useful critiques, passion for research.

I would like to thank my committee members for their valuable time and constructive suggestions: Professors Guofeng You, Leonid Kagan, and Glenn Amatucci. I would like to further thank Dr. Amatucci because he accepted me into his lab after my freshman year of college and the experience of working in his lab solidified my interest in research and his mentorship is awe inspiring. I also would like to express my gratitude to our collaborators and co-authors, Professor Kenneth R. Reuhl, and Dr. David C. Reimer.

I would also like to thank my former and present colleagues for their support and friendship: Dr. Olga Garbuzenko, Dr. Savla, Dr. Min Zhang, Dr. Vatsal Shah, Dr. Oleh Taratula, Dr. Andriy Kuzmov, Milin Shah,. I would like to thank Olga Garbuzenko for her help with animal studies and friendship in the lab. Working with them in the laboratory and going to happy hours, was very delightful.

My special thanks to my colleague and true friend Dr. Ronak Savla for always believing in me, for being my best friend and my "partner in crime". Working with him was a privilege filled with a lot of good times and inspired me to challenge myself to be better.

My special thanks are extended to the office staff in the Department of Pharmaceutics: Marianne Shen; Sharana Taylor; Fei Han; and Hui Pung for their kind assistance and patience in solving my problems.

Also I wish to thank my family for their support and encouragement through every step along the way. I could not have come this far without the love, nonjudgmental support, and belief in me and my work that I have received from my brother, Yaroslav. His personality of enriched kindness, forgiveness to people, instant friendliness, leadership, passion for work, humility is what I cherish and come to rely on.

To my husband, Nader, who remain most special of all, my true believer, and anchor to my sanity. Thank you for supporting me through my graduate work, for always listening to me and making me laugh when I was stressed out, and most of all for your love.

Finally, I would like to extend my gratitude to everyone, who has supported me throughout my life.

The research was supported in part by the R01 HL118312 grant from the National Institute of Heart, Lung and Blood and by the Busch Biomedical Research grant from Rutgers University.

TABLE OF CONTENTS

LIST OF TABLES

LIST OF FIGURES

1 INTRODUCTION

The term fibrosis refers to deposition of excess amount of connective tissue called fibrotic tissue. If certain tissue has frequent injury it will develop scarring. Such scarring consists of accumulation of fibroblasts that invades local tissue and recruits inflammation factors with uncontrollable repair. Fibrosis can develop in several tissues (muscle, heart, liver, kidneys, and lungs). Cardiac fibrosis cause remodeling that is attributed to chronic heart failure, atrial fibrillation, and myocardial infarctions. Renal fibrosis is attributed to exacerbated fibrotic lesions caused by multiple chronic kidney diseases. Hepatic fibrosis is associated with chronic hepatitis B and C viral infections and alcoholism.

Pulmonary fibrosis is used as an umbrella term that consists of numerous parenchymal lung diseases of which sarcoidosis, idiopathic pulmonary fibrosis (IPF) and cystic fibrosis (CF) are the most prevalent. IPF is characterized by fibrotic foci and honeycomb like structures created from fibroblast cells due to depletion of epithelial layer (1). These in turn modulates elasticity of the lungs and proper oxygen exchange. CF is characterized primarily by mucoviscidosis, or thickening of the mucus, which cause pancreatic, liver, and intestine and pulmonary fibrosis as well. Cystic fibrosis is the only one that is derived from autosomal recessive genetic disorder in cystic fibrosis transmembrane conductance regulator (CFTR) gene (2). Most other forms of fibrosis have a distinct environmental component or insult. Also, CF tends to have a multi-organ component compared with other forms of fibrosis.

Thus, each of these fibrotic conditions represents a significant unmet medical need, warranting significant research and clinical study into treatment.

Currently, there are no curable treatments for both cystic and idiopathic pulmonary fibrosis. Cystic fibrosis has been studied for many years. Early diagnosis and treatment regimens prolonged the life expectancy in the US to nearly 37-40 years old (Fig. 1A) (1, 3). However, in other countries, like Russia, lack of proper treatments for cystic fibrosis limits life expectancy at 25 year of age (4). Physicians typically diagnose cystic fibrosis by assessing patient symptoms and confirm using the chloride sweat test, which is the gold standard (5). The rise in the power and decrease in cost of DNA sequencing provides another tool in the diagnostic arsenal for cystic fibrosis. This provides an additional benefit in that physicians can tailor treatment with targeted agents for the specific mutation in the CFTR gene.

Significant lung inflammation is present from very early stages in CF. What initiates the airway inflammation in CF is still debated; it is probably a combination of intrinsic innate immune dysregulation and infection. Misfolding in CFTR gene prevents proper regulation of chlorine exchange resulting in viscous mucus accumulation (6, 7). There is no turnover of the mucus layer covering the epithelial cells by clearance mechanisms, which creates a perfect niche for bacterial infection. The body is incapable of maintaining a proper environment for gas exchange and clearance in the alveoli. Early treatment with antibiotics (such as tobramycin) may suppress *Pseudomonas aeruginosa* bacterial growth (6, 7). Treatment with inhaled N-acetylcysteine and hypertonic saline are aimed at reducing the mucus viscocity (8,

9). In addition, a promising development in the treatment of CFTR channel malfunction has been evaluated by drugs such as ivacaftor and lumafactor, which are the first agents that target the underlying mechanisms of CF. Ivacaftor attaches to mutated CFTR gene and prevents it from early degradation. Meanwhile, lumacaftor attaches to the CFTR protein at transmembrane and allows it to function properly (10, 11). If CFTR dysfunction is corrected at a very early age, it is possible the issue of pneumonia, persistent bacterial insult, and cystic fibrosis may be significantly curtailed in patients with CF.

Unlike CF, IPF is mostly diagnosed later in life and at later stages when it has profoundly spread. IPF is the most lethal fibrosing disease, with a higher mortality rate than of many types of cancer. The reported 5-year survival is only 45% (1). It is distinguished from other interstitial pneumonias by having unique fibrotic foci and honeycombing structure that can be observed by computerized tomography (CT) scan and further confirmed by lung biopsy (1).

Although the pathogenesis of IPF is poorly defined, several hypotheses have been proposed and continue to evolve in response to more detailed characterization of the disease. The pathobiology of IPF is characterized by the presence of alveolar epithelial cell (AEC) injury and apoptosis, which is accompanied by progressive fibrosis. In essence, fibroblasts are present at the injury site where inflammation and healing process is happening. Instead of abating proliferation during injury insult, fibroblasts continue to secrete inflammation signals and metamorphose into myofibroblasts that grow and spread similarly to cancer cells. Slowly these fibrotic

tissue spread over normal alveoli sites and prevent proper oxygen exchange. Elasticity of the local site is lost. Type 1 cells are no longer covering epithelial layer for the gas exchange and type 2 phneumocytes are granulomatous, cannot produce surfactant, and finally have the potential to undergo EMT (1). During this uncontrolled fibrogenesis, many growth factors, extracellular factors, and ECM proteins are overexpressed fueling the positive feedback to the improper wound healing process.

Type II AECs maintain normal alveolar homeostasis via the production of surfactant, the regulation of fluid balance, and the interaction with other structural cells to keep polarity and send important signals such as inhibition of fibroblasts proliferation. One of the cytokines that helps AEC cells to secrete surfactant and prevent epithelial mesenchymal transition (EMT) is prostaglandin E 2 (PGE2) (12). Lack of autocrine signaling factor, PGE2, promulgates EMT pathways and fibrogenesis orchestrated by pleiotropic TGF-β. At the downstream of these pathways are matrix metalloproteinase 3 (MMP3), hypoxia inducible factor (HIF), and chemokine (C-C) motife ligand 2 (CCL2) (13-15). CCL2 promotes accumulation of inflammatory factors at the site, and MMP3 helps to digest basal laminar and invasion of fibroblast to form fibroblasts foci and eventually scarring.

In the last decade, the pharmacological approaches to the management of IPF have changed considerably mirroring the evolving understanding of the disease pathogenesis. Early therapeutic studies in IPF focused on the effects of corticosteroids because of their anti-inflammatory effects and wide use in clinical

practice for a number of fibrotic lung disorders (16). In addition, clinical studies have been performed on sildenafil (phosphodiesterase-5 inhibitor), pulmonary vasodilators, (ET) receptor antagonists, anticoagulants, and tyrosine kinase inhibitors(17-20). Each therapy was evaluated because they target different pathways of IPF pathogenesis. Unfortunately, most therapies did not have statistically significant effect over placebo and some were associated with significant treatment-related morbidity and various potentially severe side effects. This has prompted the approval of pirfenidone in 2014 for treatment of IPF. Pirfenidone is a pyridine compound that has anti-inflammatory, anti-oxidant, and antifibrotic activities that are yet not completely understood (21, 22). Nintedanib was also approved recently for treatment of IPF (23). As with pirfenidone, the nintedanib's mechanism of action is not well understood. Both drugs are not considered to be cures for IPF as the disease may still progress although at a slower pace than without treatment.

Pulmonary delivery enables local delivery of therapeutics targeting respiratory diseases such as asthma, COPD, and cystic fibrosis. Therapeutic agents administered by inhalation don't have to undergo hepatic first pass metabolism and require lower doses. Therefore, non-invasive nature of the pulmonary delivery route ultimately reduces side effects on other organs. The lower dose can lead to significantly reduced costs especially for biologics. The pulmonary route is one of the most acceptable administration routes by patients. Lungs have large surface area (more than $100m^2$) and a rich vasculature, which makes it for attractive systemic delivery(24).

Currently there are three types of inhalational devices that are commercially used: nebulizers; pressured metered dose inhalers (pMDI); and dry powder inhalers (DPI). Dry powder inhalers have storage of drug in powder form, which can be very stable. In the DPI, nanoparticle agglomerates have lower density relative to the dense particles of the same size, resulting in smaller mass median aerodynamic diameter (MMAD), and, thus, enhancing lung deposition (25). However, dry powder inhalers are not the best for children and patients with compromised lung function. Dry powders typically require newer excipients that need toxicological evaluations (25). Most excipients for nebulization are already tested.

Nebulizers can have drugs or nanoparticles in suspension formulation. Nebulizers can be more beneficial for formulations of lipid nanoparticles since they are prepared in water. They provide better dose uniformity and higher delivery efficiency which provides lower initial dose loading (26). Compared with pMDI and DPI formulations, nebulization is able to deliver larger volumes and doses. Generally, pMDIs are used to deliver microgram doses of small molecule drugs such as albuterol (27). These formulations consists of drug molecules with liquid excipients and propellants. DPIs can deliver low milligram doses and typically incorporate lactose as an excipient.

Nanotechnology is a research area that has attracted profound interest in many different fields, including both in inorganic engineering such as semiconductors and as well as in biology from imaging to delivery systems. The generally applied definition of nanoparticle is a substance with at least one dimension between 1-100 nm (28). But more liberal definition allows for the size up to 1000nm. This incredibly

small size of nanoparticles gives it substantially high surface area to volume ratio and therefore increases saturation solubility and dissolution rate (29). This effect makes it a desirable application since there are about 40% poorly soluble drugs currently on the market and 70-90% of pipeline drugs are also low water soluble belonging to Class II and Class IV drugs (28). In terms of medical research, nanomedicine can be used for imaging, improve bioavailability of insoluble drugs, simultaneously deliver multiple drugs, and enhance membrane permeability all due to the nanonization technique. Nanonization is the most attractive approach to improve bioavailability of therapeutic agent, stabilization of amorphous particles, and formation of emulsions which is suitable for inhalational delivery (28).

Nanoparticles can be made with precise characteristics such as size, shape, surface groups, and surface charge. They can have multifunctional aspects such as deliver drugs and biological agents, they can be prodrugs and can be used for diagnostics. There is a great interest in developing nanocarriers with multifunctional properties for treatment of challenging multifactorial diseases such as pulmonary fibrosis. However, there are many challenges involved due to the complexity of synthesis and quality control measurements that have to be developed.

Another therapeutic agent that can be delivered by the nanoparticles is siRNA. siRNA have been showing a promising therapeutic silencing effect on its gene, despite its poor stability in physiological fluid. A newer method in silencing high expression of a gene in pulmonary fibrosis is RNA interference. Gene silencing can be achieved by exogenous administration of short interfering RNA (siRNA) (30). The

applicability in pulmonary fibrosis therapeutic is that there is an overexpression of genes responsible for inflammation and fibrosis. However, siRNA is very instable in the physiological fluid, and thus much be administered in stable nanoparticles that will shield it and deliver at the targeted site.

Consequently, there is growing interest to develop inhalational drug delivery systems for the treatment of pulmonary fibrosis. Nanotechnology is a rapidly growing field in the pharmaceutics field with a predicted profound impact on future therapies. The most basic systems consist of a drug and a nanocarrier, such as colloidal nanoparticles: liposomes, dendrimers, polymers. The main goal is to increase accumulation of drug delivery system at the target site. One way of increasing bioavailability of the therapeutic agent in the lungs is to administer it by nebulizer in the stable nanoparticle formulation with increased half-life.

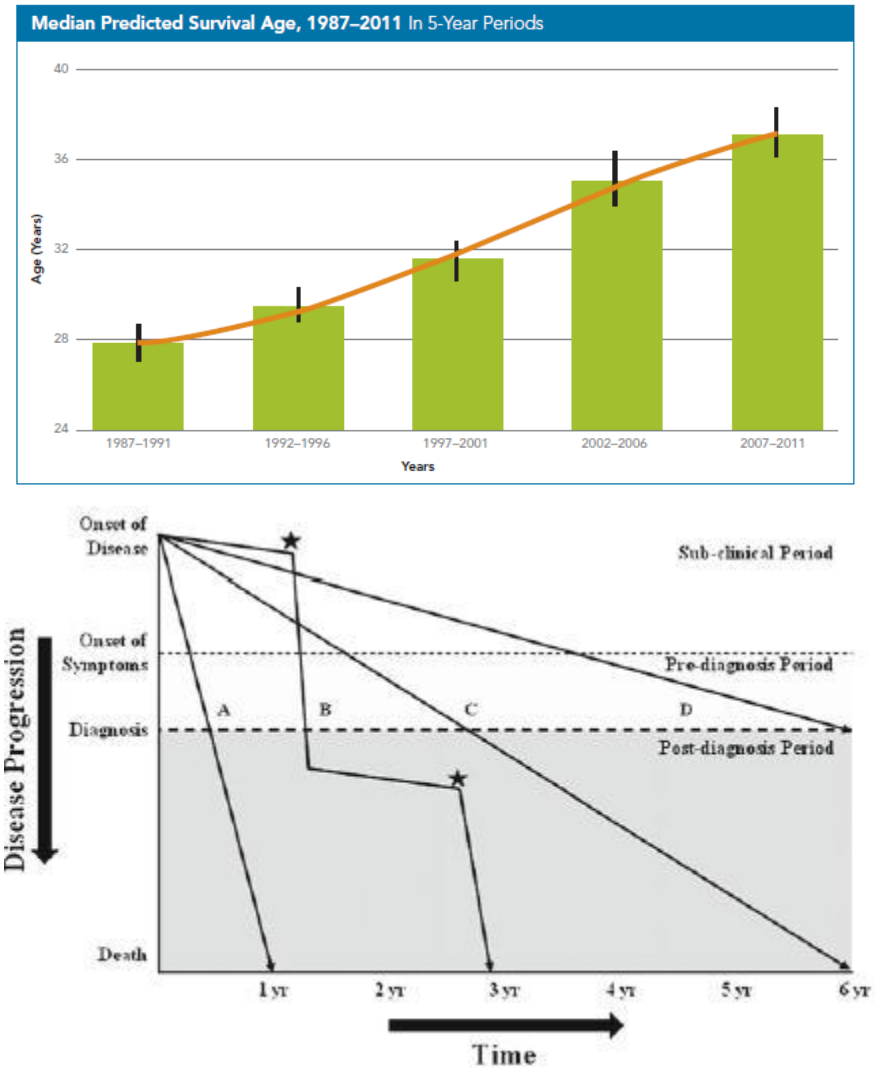

Fig 1. A) 5-year survival age for cystic fibrosis patients. B) 5-year survival rate for IPF patients after diagnosis (31).

2 BACKGROUND AND SIGNIFICANCE

2.1 Idiopathic pulmonary fibrosis (IPF)

Idiopathic pulmonary fibrosis (IPF) was initially discovered in early 1900s and consisted of many different lung diseases. Currently, IPF- is the most common cause of fibrotic lung disease, and unfortunately diagnosis of IPF disease carries poor prognosis. Approximately, out of 10,000 people, one or two are diagnosed with IPF . There is an increased prevalence in elderly patients. The aging population, longer lifespans, and more accurate diagnosis explain the growing number of pulmonary fibrosis cases each year (1). Men are affected twice as often as women. An environmental risk factor was found mostly in people that were exposed to metal or wood dust, and smoking (3). Also, there is a small selection of patients with IPF with a mutation in the vital surfactant protein c (SP-c) gene, which regulates production of surfactant so vital alveoli do not collapse (3, 32, 33).

The name IPF was originally given to the disease because real cause of the disease was not known and it was hard to decipher. Over the past two decades a significant improvement in imaging along with histopathological and clinical data separated IPF from other pneumonias into unidentified interstitial pneumonia not related to other fibrogenic entities. Diagnosis with routine chest X-ray is difficult but detection in loss of volume can be observed in 75% of patients (34-36). Further on, patients can be

referred for high resolution computed tomography HRCT. With an introduction of (HRCT) in the 1990s, the way in which lung diseases are detected has been revolutionized. Definite IPF can be detected when there is a presence of honeycombing (37, 38). Fibrotic tissue in the lungs creates distinct physiological structure consisting of cystic spaces with elastic tense thickened walls that appear like honeycombs (39-41)(Fig. 2.1). When definite detection using HRCT cannot be made, a lung biopsy can be performed to confirm the disease. Lung biopsy should be left for the last resort since it is a difficult procedure for the elderly patients (42). Magnetic resonance imaging (MRI) continues to evolve and may overtime substitute or enhance the prognosis of IPF. It also may evaluate the therapeutic prognosis. One of the main advantages of using MRI over HRCT would be that MR imaging does not use ionized radioactive particles.

2.1.1 Mechanisms of the disease

Early pathological studies emphasized inflammation as the key factor that led the progression of IPF since almost all of fibrotic disorders are strongly linked to pathogenesis of adaptive immune processes. Research showed that T-cells respond to antigens early on in progression and promulgate lung injury and activate autocrine system factors that contribute to IPF progression (43, 44). However, after comprehensive clinical research and animal studies, it was shown, while inflammation occurs, treatments with anti-inflammatory drugs did not prevent disease progression and did not change patient's outcome (45). Some even claim

that since IPF patients do not necessarily respond to steroids, such as corticosteroids treatments, the disease cannot be characterized as immunological.

2.1.1.1 Alveolar epithelial cell injury pathway

An alternative model of IPF pathogenesis have been postulated weighing heavily on repetitive alveolar epithelial cell (AEC) injury accompanied by unresolved wound healing with heavy deposition of matrix formed by newly multiplied myofibroblastic cells. There are several potential mechanisms that are accountable for the progression of IPF. It is believed now that initially injury happens to the alveolar region, which initiates elaboration of local profibrotic factors.

The alveolar epithelial layer is comprised predominantly of two types of epithelial cells called Type I and Type II pneumocytes. Type II cells have a cuboidal morphology and lamellar bodies that maintain its polarity at the basal membrane. Their primary role is to secrete surfactant and also to regenerate epithelium layer after injury, which includes capabilities of differentiation to Type I cells (46-48). Type I cells are much thinner cells which cover 97% of alveoli surface, but are only 40% by mass of the alveolar lining (49). At some places Type I cells are only 25 nm thick, and their membrane is highly specialized in order for oxygen/carbon dioxide exchange to take place more readily.

In IPF, it is believed that acute injury happens to type I alveolar cells leading to their apoptosis. At the same time, type II alveolar cells undergo hyperplasia but are

unable to re-epithelize the rapidly injured sites (Fig. 2.2) (39, 46) Inadequate attempt to re-epithelize maybe one of main factors of fibrosis. Local AEC lining morphology is severely deranged with denuded capillary basement membrane, epithelial necrosis, and extensive Type I alveolar apoptosis (50). Therefore, alveoli regions that have been damaged by vast fibrotic changes in IPF are being replaced with hyperplastic type II cells with abnormal elongated epithelial cells in the sites of type I alveolar cells (51, 52). This abnormal epithelial phenotype happens due to failure of normal re-epithelialization after injury. New alveolar cells do not express Receptor for Advanced Glycation End products (RAGE), which is the specific marker for differentiated type I epithelial cells (53-56). These “faulty” AECs aberrantly secrete profibrotic factors such as highly upregulated transforming growth factor-beta (TGF-β), cytokines, chemokines, and proteases that elicit activation of inflammatory cells and migration of fibroblasts (57) (Fig. 2.2).

During homeostasis, AECs maintain cell-cell contact with the fibroblast on the alveolar wall through which they send inhibitory signals to mesenchyme. Constant output of negative feedback signals prevents epithelial mesenchymal transition (EMT) to occur. AEC dropout occurs when anti-EMT signaling is deregulated (58-61). PGE2 is usually secreted by AECs to produce surfactant and also to inhibit EMT. In IPF, very low levels of PGE2 are observed (62-66). In addition, local site changes mobilize matrix metalloproteinases (MMPs) that disrupt basal lamina of the alveoli. In adequate attempt to re-epithelize maybe is one of main factors of fibrosis.

2.1.1.2 Injured AEC can potentially undergo EMT

AECs have flattened morphology similar to cells that undergo EMT. Therefore, they possess migratory capabilities and when they lose polarity they undergo EMT (67, 68). In EMT process, Type II AECs lose their morphology of cuboidal shape, cell-cell junctions, and apical-basal polarization. The Type II AECs do not differentiate into Type I AECs. Instead Type II AECs convert into cells that have similar morphology to mesenchymal cell types such as fibroblasts. These cells are characterized by having spindles and loss of cell contact (69). In addition, AECs lose E-cadherin expression which is a marker for epithelial cells, and start to express N-cadherins which are seen in mesenchymal cells (70, 71). Also up-regulation of transcription factors implicated in embryogenic EMT seen with up-regulation of Twist, "snail", "snug" genes (72-75). Lung tissue from patients with IPF shows increased expression of Twist and snail (SNAI1) genes, which suggest EMT signaling during IPF.

The main potent inducer of EMT during embryogenesis belongs to superfamily of cytokines TGF-β1, -β2, -β3, and bone morphogenic proteins (BMPs) (76). During embryo development TGF-β/BMP balance regulates epithelial/mesodermal layer creation (77, 78). Up-regulation of TGF-β is seen during developmental signaling as well as during fibrosis. The TGF-β/BMP balance is tilted in favor of TGF-β. BMPs have been implicated in reversing mesenchymal to epithelial transition by antagonizing TGF-β dependent signaling. However, in IPF, BMP expression is very low because they are being inhibited by elevated expression of gremlin 1 protein

(79). Also it was shown that cell-cell contact due to integrins can potentially modify TGF-β signaling response (80, 81). However the aberrant phenotypic change of AECs results in cells that have reduced cell-cell binding. Injured AECs are also seen to express several profibrotic growth factors such as platelet-derived growth factor (PDGF), monocyte chemoattractant protein-1 (MCP-1), connective tissue growth factor (CTGF), endothelin-1, tumor necrosis factor-α (TNF-α), and several MMPs and TIMPs (82-88).

2.1.1.3 Provisional matrix and myofibroblasts proliferation

AECs damage results in swelling of the epithelial cells and increased trans-endothelial permeability. There is an increase in capillary permeability which brings serum derived coagulation factors and serum-derived fibrous exudates that form the provisional matrix upon which fibroblasts initiate proliferation (89, 90). The provisional matrix is activated by factors from AECs and macrophages. The process also activates the extrinsic coagulation pathway. Thrombin gets activated in the injury site and converts serum-derived fibrinogen to fibrin. The fibrin-rich matrix further entraps pro-fibrotic and pro-coagulation factors (91). The accumulation of these factors leads to activation and migration of local interstitial fibroblasts, influx of circulating fibrocytes, and increased EMT. Moreover, thrombin acts as a growth factor for fibroblasts by indirectly activating TGF-β. Epithelial cells and fibroblasts have proteinase-activated receptors (PAR 1) expressed on the cell surface. Thrombin signals, via proteolytic activation of PAR 1, TGF-β and other profibrotic cytokines leads to the stimulation of myofibroblast differentiation (92-94). Other

coagulation factors, such as Factor X and Factor VIIa, have been observed to activate PAR 2 dependent proliferation of fibroblasts (95).

Fibroblasts either derived from serum or inhabitants of interstitial space in IPF sites have pro-fibrotic gene expression. Fibroblasts no longer express phosphatase and tensin homolog (PTEN) of Cav-1 genes as well as PGE2 (96, 97). Also due to strong TGF-β signaling, fibroblasts change their phenotype into highly contractile cells with increased collagen expression called myofibroblasts (98). Tissue remodeling persists, possibly due to rapid multiplication of myofibroblasts with its collagen expression and also aberrant re-epithelialization takes place. Excessive deposition of matrix and highly contractile myofibroblasts results in severely disordered lung tissue with honeycombing pathology and organ failure.

2.1.2 Current Treatments for IPF or Targets for Therapeutic Agents for IPF

Currently, there are no effective treatments recommended by the guidelines. Several specific clinical trials have been made for several drugs and combination of drug treatments. Initially clinical trials evaluated the efficacy of drugs that primarily exert their functions by suppressing inflammatory or immune responses, such as corticosteroids and immunemodulatory agents (16). The results of these trials have all been uniformly disappointing. Over the last decade, the perspective on IPF pathogenesis has profoundly changed and the disease is thought to result from an aberrant reparative mechanism with excessive deposition of extracellular matrix, following an injury that primarily affects the lung epithelium (99, 100). Several drugs

approved for the treatment of different diseases, but with some background for being effective in fibrotic disorders, have also been evaluated in IPF clinical trials.

2.1.2.1 Corticosteroids

Early therapeutic studies in IPF focused largely on the effects of corticosteroids because of their anti-inflammatory effects and wide use in clinical practice for a number of fibrotic lung disorders. Long term corticosteroids treatment did not have any significant effect on patients and resulted in severe side effects (16). Similarly, non-steroidal immunomodulatory drugs such as azathioprine, and cyclosporine A alone or in combination with corticosteroids, showed low-quality evidence of treatment (101). Another large randomized trial called INSPIRE was performed on 800 patients with mild to moderate IPF (102, 103). Patients were treated with interferon gamma-1b (IFN-γ-1b) which finalized the conclusion that there is no statistically significant benefit. Current evidence-based guidelines recommend that patients with IPF should not be treated with IFN-γ.

2.1.2.2 Pulmonary arterial hypertension drugs

Drugs for pulmonary arterial hypertension (PAH) and pulmonary vasculature have also been investigated. Preclinical studies have shown that endothelin 1 (ET-1) is an important contributor to the pathobiology of several fibrotic disorders. ET-1, has been shown to modulate matrix production, leading to increased collagen synthesis by stimulating TGF-β (19, 104). Bosentan and ambrisentan are endothelin receptor

antagonists approved for PAH. Two randomized, double-blind, placebo-controlled studies were performed for bosentan. In the first trial, BUILD-1, a subgroup of patients who lacked honeycombing structure showed some benefit in reducing disease progression and improvements in lung function (105). However, in the second trial, BUILD-3 (106), no differences were observed between the treatment groups with respect to changes from baseline to 1 year in health-related quality of life or dyspnea.

Sildenafil, is known to inhibit phosphodiesterase-5 enzyme (PDE5). PDE5 inhibits degradation of cyclic guanosine monophosphate (cGMP), and stabilizes the second messenger of nitric oxide, which promotes vasodilation (18). Early studies showed a 20% improvement of 6-min walk test distance (6MWD) in 57% of patients (107). These observations prompted the STEP-IPF clinical trials in 180 patients. Unfortunately, the difference in 6MWD was not seen. However, a significant difference was observed in the secondary aftereffects such as partial pressure of oxygen in arterial blood (PaO2), diffusing capacity of the lung for carbon monoxide (DLCO). The treatment also reduced dyspnea, which ultimately improved quality of life (107). While the primary endpoint of this study was not met, the presence of some positive secondary outcomes creates clinical equipoise for further research.

2.1.2.3 Anticoagulants

After inflammation occurs another pathway is propagated such as prothrombotic pathway. Anticoagulant Effectiveness in Idiopathic Pulmonary Fibrosis (ACE-IPF)

trial (sponsored by the IPFnet in the USA) was specifically designed to test the hypothesis that warfarin would reduce rates of mortality, hospitalization, and decline in force vital capacity (FVC). In this double-blind, placebo-controlled trial patients were randomly assigned in a 1:1 ratio to warfarin or matching placebo for a planned treatment period of 48 weeks. Due to a low probability of benefit and an increase mortality observed in the subjects randomized to warfarin (14 warfarin vs. 3 placebo deaths; p = 0.005), the Independent Data and Safety Monitoring Board recommended stopping the study after 145 of the planned 256 subjects were enrolled (72 warfarin, 73 placebo) (20, 108).

2.1.2.4 Tyrosine kinase inhibitors

Tyrosine kinases regulate many genes involved in neoplastic and non-neoplastic diseases. Recently, tyrosine kinase inhibitors (TKIs), such as nintedanib and imatinib have been evaluated for IPF. Nintedanib is an intracellular inhibitor of various tyrosine kinase receptors such platelet derived growth factor receptor (PDGFR), vascular endothelial growth factor receptor (VEGFR), fibroblast growth factor receptor (FGFR) (17, 109). It was approved in 2014. Four different oral doses were tested of nintedanib (50 mg once a day, and 50 mg, 100 mg, or 150 mg twice a day). Both primary and secondary endpoints were met. In the primary endpoint, the group receiving 150 mg of nintedanib had much lower decline of lung function (110). In the secondary endpoint, they had significant lower incidences of acute exacerbations. The side effect profile was very tolerable.

Imatinib has been known to inhibit lung fibroblast-myofibroblast transformation and proliferation as well as extracellular matrix production through inhibition of PDGF and TGF-β signaling (111). A case study in IPF patients was unfortunately less successful. Primary and secondary endpoints were not different from placebo groups and serious side effects were observed (112).

2.1.2.5 Pirfenidone

In 2014, another drug was discovered for pulmonary fibrosis is pirfenidone. It is a pyridine compound with antifibrotic, anti-inflammatory, and antioxidant activities, although it's precise mode of action is unknown. It was initially approved in Europe and Japan. After some time, the efficacy was seen in combinatorial treatment of pirfenidone with azathioprine. While IPF is proven to be very complex disease as cancer, some early studies show that inhibition of pleotropic factor such as TGF-β may have high risk of adverse effects and may not suppress the necessary factors.

2.1.3 Alternative treatment with PGE2

While failure of efficacy in current therapeutic drugs thus far, it necessitates considering novel approaches and conspicuous therapeutics entities. It would be important to take a look on eicosanoids as a new therapeutics therapy for IPF. Eicosanoids are prevalent lipid mediators of the autocrine and paracrine systems in the lungs. Prostaglandin E 2 (PGE2) is the major prostanoid which has a positive feedback action in lungs homeostasis. It has been found as a cytokine that support

AEC homeostasis by sustaining epithelial cell growth, maintaining surfactant secretion, and even suppressing T cell-mediated inflammation (113). Cyclooxygenase-2 (COX-2) converts arachidonic acid ultimately into PGE2, and the limited amount of both contributes to epithelial apoptosis and reduced fibrblast apoptosis.

PGE2 has also distinct autocrine reciprocal signaling effects on the two different cell types: mesenchymal and epithelial. In the epithelial derived tumors there is overexpression of COX-2 which promotes proliferation. However, on the mesenchymal cells, such as fibroblasts, it signals to initiate apoptosis through Fas ligand (FasL) (Fig. 2.3). It was found that during IPF there is a drastic decrease of local production of PGE2. In addition, there is a decreased expression of PGE2 receptor on both epithelial and fibroblasts cells (114-116).

Corticosteroids have been used in pulmonary fibrotic disorder for many years due to their anti-inflammatory effects. However, after visualizing the mechanisms in depth it was found that corticosteroids are very potent inhibitors of COX-2 and the inducible form of PGE synthase enzyme. Low production of PGE2 will not suppress fibroblasts activation and eventual proliferation. Thus corticosteroids may actually potentiate fibrogenesis.

2.1.4 Small interfering RNA (siRNA)

RNA interference (RNAi) has become a very popular in the post-genomic era of therapeutics and has the potential of imparting a new form of therapy to patients. The strong desire to utilize siRNA due to its potency in inhibiting genes lies in its high specificity to the targeted gene. RNA interference process can be initiated by introducing exogenous double stranded RNA (dsRNA) to the cells, animal models, or patients to silence a particular gene. siRNA presence in cytoplasm triggers RNA interference by associating with RNA-induced silencing complex (RISC) in which siRNA base pairs with its complementary mRNA (30, 117, 118). Specifically designed dsRNA possess antisense strand that has complementary sequence to its specific mRNA strand. Upon interaction of dsRNA with its targeted mRNA, mRNA gets rapidly destructed. After mRNA has been degraded, siRNA can be complexed again with another copy of mRNA (119, 120). This way, highly expressed genes can be silenced as in diseases such as cancer and fibrosis where there is a presence of highly expressed pro-disease genes.

Post-transcriptional gene silencing (PTGS) was discovered in plants. Later RNA interference was fully studied in *C. elegans* worms where long 200 bp introduction of siRNA and its cleavage with Dicer was cross examined (121, 122). It was found that exogenous 200 bp double stranded RNA (dsRNA) is further processed into smaller 20-24 base pair dsRNA (123).

There are two types of small RNAs, called micro RNA and siRNA. miRNA are endogenous short interfering RNAs consisting of roughly 200 base pairs in mammalian cells. On the other hand, siRNA is delivered to the cell in its shortened version of 21 base pairs. In the cytoplasm, siRNA gets released in the cytoplasm and gets phosphorylated at 5' ends (124). Then sense and antisense strands are being unwounded by the protein complex called RNA induced silencing complex (RISC). The antisense strand is being read and then presented to mRNA that has complimentary sequence. mRNA sites are paired with 5' end of the antisense strand upon which a nick is created in mRNA that is where the mRNA will have single cleave leading to mRNA degradation (Fig 2.4) (125, 126).

Later on it was found that shorter forms are more efficient due to the fact that they still induce RNAi efficiently in mammalian cells and also don't elicit interferon response observed with the longer nucleotide fragments. This novel silencing approach spurred the modern gene therapy into finding new potential treatments for the incurable diseases.

The Elbashir group was the first one to introduce successfully synthesized short dsRNAs to suppress gene exogeneously (118). siRNAs can be synthetically made into 20-24 bs with sense and anti-sense strands with two overhanging nucleotides that help with RNA interference. The cleavage sites are dependent on the sequence of the dsRNA, and change in one or two sequences can change the cleavage site.

Despite its very high efficiency in suppressing the expression of its complimentary mRNA, siRNA has some obstacles. siRNA is nucleic acid which gives it certain properties such as anionic charge, short half-life of approximately several minutes in the blood (127). Therefore, siRNA cannot be delivered solely as a therapeutic agent. While there is some research involved in making siRNA more stable in the plasma most of them involve chemical modifications of siRNA. Most of the techniques involve modifications such as phorphodiester backbone that demonstrated a decrease in siRNA efficiency (128). Even when siRNA gets next to the desired cells it has problem of being internalized. Cell membranes have anionic charge which naturally would repel negatively charged siRNA yielding poor penetration (129). Lastly, even if siRNA may get internalized in the endosomal process it may have difficult time to be released from endosomes into the cytoplasm. Therefore, siRNA necessitates to be delivered by a carrier system which will protect it from plasma degradation, make easy cellular penetration, and release into the cytoplasm.

2.2 Cystic fibrosis (CF)

Cystic fibrosis (CF) is an autosomal recessive monogenetic disease due to mutation in the cystic fibrosis transmembrane conductance regulator (CFTR). CFTR is a transport channel that transports chloride ion and water in and out of the cell in the lungs. Over 1,800 mutations have been identified, but most are very rare (39). The mutations cause qualitative or quantitative reduction in CFTR activity.

There are estimated to be 70,000 patients with CF, designating it as a rare disease. Due to severe lack of effective therapies, there is high associated morbidity and mortality. The average lifespan for patients is approximately 40 years. Most available therapies only treat the symptoms of cystic fibrosis. Because CFTR is found on the apical surface of many different types of epithelial cells, patients suffer numerous symptoms and have a high medication burden. Because of the reduced CFTR activity in sweat glands, CF patients are unable to recover salt. This forms the basis of the sweat chloride diagnosis test for CF (130).

2.2.1 Cystic fibrosis pathogenesis

Cystic fibrosis is mainly attributed to the function of the CFTR gene. There is recessive mutation occurs in the CFTR gene that prevents proper transport of chloride ion. In addition, CFTR is a transporter of the sodium and bicarbonate. Transport of bicarbonate may be the primary culprit in the gastrointestinal (GI) pathologies of the disease. The recessive mutation causes 1800 mutations in the gene, with higher prevalence in some than others (131). Overall, the mutations cause both the qualitative and quantitative reduction in CFTR activity.

CFTR is a membrane of ATP binding cassette (ABC) family of transmembrane glycoproteins. It has a molecular weight of 170kDa and composed of 1480 amino acids (131). The protein structure consists of two six alpha helices transmembrane domains and two nucleotide-binding domains (NBDs) on the cytoplasmic side, one regulatory domain. CFTR channel works by undergoing ATP hydrolysis in the first

NBD upon which the channel opens, likewise channel closes when ATP hydrolysis happen to the second NBD domain. More than 70% of the mutations happen due to the deletion of phenylalanine at position 508 of the CFTR protein, termed ΔF508 CFTR (Fig. 2.5) (132). This form only retains 30% of its activity of its wild type form due to improper folded proteins undergo recycled turn over even before reaching the cell membrane (2).

CFTR dysfunction in the pancreas leads to numerous effects such as autodigestion, malabsorption of fat soluble vitamins, poor growth, gallstones, and hepatobiliary disease. This requires treatment with pancreatic enzyme supplementation. Many of the manifestations of CF are due to an inability of duct lumens to hydrate macromolecules. There is pathologic evidence to suggest that in most organs, damage arises from ductal or glandular plugging by macromolecules that have precipitated in concentrated secretions. For example, mucus secretions in the bronchi and the intestine are viscid and inspissated, and the crypts are distended as if obstructed. This situation arises as a result of a deficit of ductular fluid flow and altered biochemical and physiologic properties of secretions. GIT obstruction is also common. Prevention requires hydration and pancreatic enzyme supplements and it can be inefficiently managed with stool softeners (lactulose), osmotic agents (PEG), surgery, or hyperosmolar gastrografin enema.

It is widely accepted that morbidity and mortality is primarily due to the respiratory manifestations of the disease. CF patients need to take many therapies for respiratory manifestations. Unfortunately, these therapies only provide symptomatic

benefit and do not correct the underlying cause of disease. CF patients are unable to clear phlegm from their airways. Unlike phlegm in normal patients, the phlegm in CF patients consists primarily of bacteria, inflammatory cells, polymeric DNA and nearly no mucin. Patients must perform chest physiotherapies, take hypertonic saline, and dornase alfa to clear the mucus. Patients also suffer from inflammation, which is treated using prednisone, ibuprofen, and N-acetyl cysteine. Because they are unable to clear mucus, patients tend to have higher incidence of respiratory infections particularly due to pseudomonas infections and must take antibiotics.

Despite the CFTR gene being cloned in 1989, most patients do not have an option for successful treatment of the disease (133). Because of the monogenetic nature, gene therapy held promise for treatment. However, there were numerous shortcomings such as low gene expression levels and failure of repeat administration. Non-efficient gene therapy is not necessarily a setback. CF patients with as little as 10% of normal CFTR function do not develop lung disease (134). In vitro cell mixing experiments have demonstrated that in a cell population with 6-10% of non-CF cells there was complete restoration of CFTR chloride secretion to non-CF levels. However, need full restoration for preventing sodium hyperabsorption. It is unclear if pre-clinical results can be extrapolated to humans. Another consideration for gene therapy is the lifespan of respiratory tract cells. The epithelial cells in the trachea have a lifespan of 6 months whereas those in the lungs have a lifespan of 17 months (134). Therefore, it is likely that the patient would need to be treated several times per year.

2.2.2 Current therapies

Gentamicin in an antibiotic and is administered IV. However, the high dose therapy is limited due to ototoxicity and nephrotoxicity. Ataluren is a small molecule investigational oral drug that works by inducing readthrough of premature but not terminal stop codon. It is also investigated for Duchenne's muscular dystrophy. In a single arm, dose ranging study in 30 patients, ataluren increased apical CFTR in respiratory epithelia and nasal trans-epithelial potential difference. However, there was no statistically significant improvement in lung function.

Recently, Ivacaftor (Kalydeco^{TM}) was approved by the FDA. This is the first medication that targets the CFTR mutation. Although a step in the positive direction, Ivacaftor works in patients with the G551D mutation (Class 3 mutation), which is present in a small minority of patients (1,200 in US, 1,000 in EU, and 180 in Ireland) (135). The G551D mutation is a qualitative reduction in CFTR activity; therefore, ivacaftor is classified as a CFTR potentiator (136). Ivacaftor does not present a viable option for patients homozygous for the common F508del mutation. Annual treatment with ivacaftor cost almost $300,000 per patient, thus imposing a great burden on patients, insurance companies, and the healthcare systems. It is of great interest to ensure optimal therapy with high cost medications. Ivacaftor undergoes CYP3A4 metabolism to two major metabolites: M1 (hydroxymethyl-ivacaftor)is 6X less potent and M6 (ivacaftor carboxylate) is 50X less potent than the parent molecule. Common ADRs from ivacaftor ($\geq$ 8%) are headache, oropharyngeal pain,

upper respiratory tract infection, nasal congestion, abdominal pain, nasopharyngitis, diarrhea, rash, nausea, and dizziness.

There are current clinical trials evaluating a drug candidate, VX-809, that targets the F508del mutation, which is found in a majority of patients (137). The F508del mutation results in a misfolded, yet functional protein. Due to the misfolding, the protein is destroyed prior to reaching the cell membrane. As a result, there is a quantitative reduction in CFTR activ. VX-809 is also being studied in phase 2 clinical trials in combination with ivacaftor for patients either heterozygous or homozygous for the F508del mutation.

2.3 Inhalational route of administration

Pulmonary drug delivery has potential advantages over oral or intravenous route of administration for respiratory diseases. The inhalation route localizes maximum amount of the dose to the lungs while minimizing the dose distribution to the rest of the body where it may potentially cause side effects. A smaller dose can be given to the localized area, the lungs whereas bypassing first pass metabolism in the liver. Smaller dosage also is necessary because most drugs bind to proteins in the blood. Over the past two decades there was a major push in advances in the inhalation devices that made the delivery route more favorable, precise, safe, and with higher patient compliance. In addition, there is a new push in repurposing drugs given by other routes especially that treat lungs diseases, to be administered topically (24). Modern inhalation delivery technology was shown to have greater effects with lower

dose than parenteral route of administration. With precise design of the delivery system combined with particle stability and size, greater pharmacokinetic (PK) and pharmacodynamic (PD) precision can be achieved compared to other routes (24). Therapeutic benefits also can be seen in not only in higher bioavailability but also in benefits in improved compliance with non-invasive delivery.

The human respiratory tract is divided into three regions for inhalational delivery systems respectively: extrathoracic (mouth, oropharynx, and larynx), central airways (the conducting or tracheobronchial airways) and the alveolar or peripheral lungs. The lung peripheral region, or the alveoli, is comprised of a thin layer of cells which has a huge surface area comparable to a ‘tennis court’ (24, 138) (Fig. 2.6). Formulations have to be devised with inhalational devices in mind to avoid deposition in oropharyngeal region (139). Also it is important to put into consideration the location of the disease or the location of the cells that express the receptor of interest. In treating COPD with beta-2 agonists, the muscarinic receptor is located on smooth muscle (140). Thus, after inhalation, the drug should be localized in both small and large airways. However, to treat diseases such as cancer or IPF, peripheral localization of smaller particles is preferred.

2.3.1 Pulmonary devices

Four types of pulmonary delivery devices are commercially available: metered dose inhalers (MDI), nebulizers, and dry power inhalers (DPI) and soft mist inhalers (SMI). Many asthma and COPD drugs, such as beta-agonist, steroids, anticholinergics, and

antibiotics, are currently available in the nebulizer, MDI, DPI (141). Being the oldest aerosol delivery system, nebulizers have evolved from jet nebulizers to ultrasonic nebulizers. In general, nebulizers utilize compressed air or ultrasonic power to break up a liquid formulation containing drugs into inhalable aerosol droplets. Nebulizer formulation is one of the easiest to develop because drugs can be simply dissolved or dispersed in water or saline. In order to avoid airway irritation, the solution should be isotonic. The evolution of nebulizers offers smaller sizes, improved aerosol performance, and delivery efficiency. When compared to MDI and DPI, nebulizers are usually bulkier and, require longer administration time (26).

The pressured (pMDI) was invented in the 1950s as a portable inhalation device (142). Its design and aerosol generation mechanisms have remained relatively the same since this inception. Currently, they are the most popular inhalation devices. The drug is suspended or solubilized in a propellant formulation consisted of hydrofluoroalkanes propellants (24, 142). There is also a need of excipients that stabilizes the solutions which often need to be optimized with respect to drug's properties, propellant solvency, and safety to the patient. Actuation through the metering valve causes rapid expansion of the propellant, generating aerosol droplets. pMDIs are small, and thus portable; multi-dose; and usually have fairly uniform dosing. However, application of pMDI technology is limited by the requirement of breath coordination, high oral deposition, and limited dose per actuation since the upper limit on delivered dose is dictated by the metered volume of the propellant (24, 138).

The DPI is an inhalational device that administers more complex dry powder formulation in aerosol. Excipients are required to stabilize the powder and prevent adhesive tendencies of the powder. One of the most common stabilizers used is lactose, which might cause an issue for lactose intolerant patients (143). DPI aerosolizes dry powder formulations without the need for breath coordination, which accounts for more than 90% of MDI misuse (144). However, due to strong interparticle forces, drug delivery by DPI is highly dependent on inspiratory flow rate, which varies greatly. In addition, moisture ingress can pose stability issues (145).

2.3.2 Topical lung treatments for respiratory diseases

First justification for pulmonary delivery was done by repositioning asthma beta 2 agonist drugs for inhalation route rather than by oral and injection routes (146). Oral administration of epinephrine required higher doses to be effective because little was reaching lungs. Epinephrine has non-selective binding and found to cause increased blood pressure in patients taking it for asthma. In its inhalatory model of albuterol there is fast onset of action observed with smaller dosage and no systemic side effects (147). Therefore, the higher alternative drug dose may have cost and side effects implications while inhaled dose can be much lower in cost yet achieve greater effect. Prostacyclin analogs of iloprost when administered IV lacks pulmonary selectivity leading to systemic side effects (e.g. hypotension, nausea, vomiting, jaw pain, headache) (148). Repositioned aqueous formulation via nebulizer, Tyvaso®, four times daily showed better patient compliance (148). Another major application is for treating respiratory infections in patients with chronic

lung diseases such as cystic fibrosis. Severe respiratory infections are a major cause of morbidity and mortality in cystic fibrosis (149, 150). Therefore higher concentration antibiotic tobramycin (TOBI Novartis) was formulated into aqueous solution for twice-a-day nebulizer delivery to reduce severe systemic side effects (151). Inhaled antibiotics have been reformulated into liposomes to have prolonged release of antibiotics to fight highly resistive biofilms that are currently in the late stage clinical trials: amikacin (Arikace Insmed) and ciprofloxacin (Lipoquin and Pulmaquin, Aradigm) (151) .

2.4 Nanotechnology

Over the past 10 years pharmaceutical companies have ventured into nanotechnology applications for the improved drug delivery. Nanoparticles are essentially colloidal delivery systems that can deliver effective small doses to the site of action. In 2007, FDA issued its Nanotechnology Task Force Report that has defined nanotechnology as to manufacture, measure, and manipulate particles in the range of one to 200 nanometers (28, 152). They have nanotechnology attributes such as high surface area which can have high solubility, high functionalization, and high permeability. It is written in particle sciences journal that by 2015 it is estimated that 80% of pharmaceutical industry will be associated with the nanotechnology (153).

The characteristic features of nanoparticles lies in the particle size, shape, and surface properties. Nanoparticles are colloidal dispersions and their size directly

affects the bioavailability of active pharmaceutical ingredients (API) and the safety. Nanoparticles have very high surface area-to-volume ratio per given mass for the particles (154). Therefore, nanoparticles can deliver drugs by faster dissolution and increased bioavailability solving the problem of low bioavailability of the insoluble drugs. Nanoparticle formulations also deliver lower dose of drug since they have faster dissolution.

Nanoparticles are attractive drug delivery systems because they can have customized and complex properties. The most common nanoparticles being researched are dendrimers, polymers, liposomes, mesoporous silica to name a few. These nanoparticles can be designed so that they can be loaded with hydrophilic and lipophilic drugs, antibodies, peptides, nucleic acids, targeting moieties, and other cargoes. The highly specialized structure demonstrates improved pharmacokinetics, controlled release, and ability to deliver combinatorial treatments. The global market for nanotechnology is a rapidly growing field that was recently totaled at $147 billion in 2007, and is projected to grow with a huge impact in drug delivery field (155).

2.4.1 Liposomes

Liposomes became the most versatile and commonly investigated vesicle systems since the time they were first discovered in 1965 (156). Bangham and colleagues first observed phospholipid materials similar to biological cell membrane that are able of self-assembling into vesicles (157). These spherical lipid vesicles contain a

bilayer where the hydrophobic tails are facing each other and create a barrier encapsulating a volume of aqueous medium. Polar phospho groups are facing outward and inward into the lumen of the vesicle. Aqueous medium usually consists of suspending medium but it can be interchanged by dialysis.

Shortly after in 1970s liposomal delivery system has been investigated in biotechnology field due to its highly desirable characteristics: particularly biocompatibility, biodegradability, low toxicity, structural variability, and desirable size. Liposomes can self-assemble creating flexible membrane that can embed lipophilic or polymeric molecules within the membrane, as well as, conjugate large variety of functional groups to its lipid molecules within (Fig. 2.7) (156). In its secluded internal volume, liposomes can hold encapsulated hydrophilic drugs or detection markers that can be released in specific well defined conditions. Liposomes protect encapsulated molecules from degradation that can passively target organs with discontinuous easily permeable membrane barrier. Also they have relatively high drug to lipid ratio which allows them safely load more drug inside as supposed to some other nanoparticles. This led to widespread use in biochemical sciences, drug delivery, immunoassays, proteomics, cosmetics, and even to industrial-scale applications (156). Therefore, due to their structural and functional characteristics, liposomes have been used widespread and are being regarded as the cornerstone of today's bionanotechnology.

2.4.1.1 Liposome properties and characteristics and preparation

From morphological perspective, liposomes are mainly classified by their size and number of membrane bilayers (lamellae). Despite many different ways of preparations that were developed over several decades, mainly, liposomes are characterized based on four different types of preparations which are based on different size of liposomes (multilamellar (MLV), giant unilamellar (GUV), large unilamellar (LUV), and small unilamellar (SUV)) (158, 159). Multilamellar liposomes are more complex in preparation requiring thin-film hydration which produces micron size MLV with high variability in size, size distribution and lamellarity (158, 160). On the other hand unilamellar liposomes can be rapidly and efficiently prepared by solvent-injection method; whereas, ethanolic solution is slowly injected into an aqueous phase. A direct transfer of lipid mixture from organic solvent into the aqueous buffer is observed. Liposomes prepared in this way, typically, display a well-defined size distribution, polydisperity, and encapsulation efficiency (156, 158, 161). Also the size can be adjusted by extrusion with selected membrane size and dialysis later removes residual ethanol.

Liposomes preparation is known to be a free energy system. Another free energy system is micelle, which have critical micelle concentration (CMC) of about 10-4mM (162-164). Liposomes have unique properties, unlike micelles, when they are self-assemble into phospholipid bilayer, they decrease their solubility in the hydrophilic surrounding medium and increase four orders of magnitude their CMC. This free energy-driven process is recognized as one of the most powerful mechanisms in

bottom-up engineering. In liposomes, however, this free energy span is about 104s when compared to 10-4s in the micelles (165).

Liposomes can be made from phospholipids such as neutral phosphatidylcholine and also from negatively charged phosphatidic acid, phosphatidylglycerol, phosphatidylserine, and phosphatidylethanolamine vary in fatty acid chain length in the hydrophobic region (166-168). Positively charged stearylamine can be also incorporated to make cationic liposomes (167). The nature of fatty acid hydrophobic chains is responsible for elasticity of the liposomes due to each unique double bond containing saturated chain. In addition incorporation of cholesterol makes liposomes more stable. Therefore, more unique formulations can be studied for each unique drug application.

2.4.1.2 Stability

The physicochemical properties of liposomes, such as net surface charge, hydrophobicity, size fluidity, and packing of the lipid bilayer, influences their stability and the type of proteins that bind to them. When delivered into the bloodstream, conventional liposomes have relatively short half-life because they get entrapped by the serum components of the mononuclear phagocyte system (MPS) or complements complex systems (168, 169). Opsonins, such as beta 2-glycoprotein and C-reactive protein, bind to the surface of the liposome which MPS recognizes and engulfs liposomes (170). This mechanism has been exploited for one of the earliest liposomal delivery system of antifungal drug amphotericin B, which delivers

to macrophages where fungus is hosted (171). Complement system factors that bind to microbial cells and initiate cell lysis, also bind to liposome. When complement C5b-9 complex binds to liposomes it produces lytic pores which release liposomes contents into the blood stream (172, 173). In addition, liposomes tend to bind to HDL and LDL and thus releasing its contents. However, there are also dysopsonins in the blood that bind to foreign objects and prevent phagocytosis (168). Studies have shown that a balance between blood opsonic proteins and suppressive proteins has been found to regulate the rate of liposome clearance (169).

To overcome instability issues of conventional liposomes, several physicochemical properties, such as size, charge and saturation can be fine-tuned. One of the earliest attempts to reduce fluidity of the liposome bilayer was to incorporate cholesterol to increase the packing of the phospholipids and to reduce transfer of phospholipids to HDL. Senior et al demonstrated that liposomes with unsaturated phospholipid (higher liquid crystalline transition temperature) tails are more stable than their saturated counterparts (174).

In addition, size and charge of the liposomes directs the interaction with opsonins and MPS clearance in the liver. MLVs (500-5000nm) are recognized more rapidly and have much shorter half-life than SUVs (168). Also neutral liposomes have longer circulation span as opposed to charged ones. While negatively charged liposomes may have slightly shorter half-lives, positive liposomes not only get faster recognition by phagocytes but also can be toxic. Chonn et al discovered that

negative liposomes primarily activate complement system via classical pathway, and positively charged liposomes via alternative pathway (170).

2.4.1.3 "Stealth" liposomes

Several different compounds have been investigated to coat liposomes with inert compounds that create spatial barrier from serum proteins binding and create steric stabilization. Several glycoproteins and, gangliosides that mimic erythrocyte membrane proteins have been investigated. The hydrophilic polymer, polyethylene glycol (PEG), is the most successful and well-studied polymer for coating liposomes. PEG is a flexible polymer that can insert itself at the surface of the liposomes and create a barrier for the opsonins to attach whereby creating long lasting circulating liposomes that passively extravasate into interstitial space and accumulate predominately in the tumor by the enhanced permeability and retention (EPR) effect (168).

PEG is a linear polyether diol with many favorable properties for medical delivery, such as it is biocompatible, soluble in both organic and aqueous solvents, non-cytotoxic, has good excretion kinetics, and has low immunogenicity (168, 175). Also, unlike glycolipids, its molecular weight and structure can be modified for various purposes, while easier and cheaper to make. Surface modification of liposomes with PEG can be achieved in several ways: adsorbing onto the surface, covalently binding, or by incorporating PEG-lipid conjugate during preparation.

PEGylated liposomes have a drastic increase in blood circulation of the drugs. Also PEGylated liposomes do not aggregate after formation and therefore improve stability. X-ray analysis showed that PEG extends at 50A which creates interbilayer repulsion forces (168, 176). In addition this coverage does not allow for opsonins to bind and therefore are less cleared. Currently there are some drug formulations of PEGylated liposomes that are on the market such as liposomal doxorubicin. For example, cisplatin form in Pegylated liposomes, Lipoplatin, composed of PC, DPPG, CHOL, and PEG2000-DSPE has a half-life of 6-117 hours (177). It also has no serious side effects especially as basic cisplatin drug nephrotoxicity.

2.4.1.4 Liposomes for gene delivery

Liposomal delivery systems are the most efficient delivery gene delivery systems known. Gene transfection was studied with many synthetic delivery systems, yet liposomes were found to have greatest transfection efficiency. For delivering negatively charged siRNA, positively charged liposomes are used. Numerous cationic liposomes were studied which depends or three factors. Positively charged head group in a appropriate relationship to the negatively charged siRNA and a linker, which is important in determining the biodegradability of the liposome. Linker also anchors the cationic group inside liposome. Cationic liposomes mainly consist of DOTAP, DOTMA, or DOPE (161, 168). However, it was found that cationic liposomes can be somewhat toxic. So incorporation of relatively short PEG or PEG combination with targeted moiety lowers cytotoxicity and improves cellular internalization.

2.4.2 Solid lipid nanoparticles (SLN)

In the early 1950s, lipid nanoemulsions were developed for parenteral nutrition. Liquid oils, such as vegetable oils or middle chain triglycerides were used in a range of 10-20% of lipid phase of formulation accompanied with stabilizers, such as phospholipids (178). Later on it was realized that lipid nanoemulsions can be used as drug carriers to enhance stabilization formulations and enhance bioavailability of lipophilic drugs. Several formulations were commercialized, such as Diazepam-Lipuro®. When compared to different formulations of Diazepam, Diazepam-Lipuro demonstrated much lower systemic toxicity. Diazepam is embedded in the lipid core of the nanoemulsion, which restricts its lytic group having contact with erythrocytes to cause systemic toxicity (179). With nanoemulsions having big advantages are toxicological safety, large scale production by high pressure homogenization process, and also relatively high lipid content. However, the disadvantage is that for most drugs the release is relatively rapid, unless the drug is very lipophilic (178). Therefore, a new idea of substituting liquid oils with solid lipids was introduced two decades ago.

Solid lipid particles are produced by spray drying techniques that yields micro size. High pressure homogenization and ultrasonification techniques are applied to reduce the size of the particles and increase its surface area (180). Solid lipid nanoparticles are made of lipid matrix composition and are highly bioavailable and physiologically tolerable and possess little acute or chronic toxicity. Additional advantages are their relatively easy scalability of production without use of organic

solvents, their ability to protect the drugs from degradation, and ability to control drug release.

Two main methods are thoroughly researched to yield the best performance of solid lipid nanoparticles with suitable properties: cold homogenization and hot homogenization (178). In the hot pressure homogenization (HPH) technique the procedure is carried out at the temperature above the melting point of the lipid. It is regarded at homogenization of the lipid emulsion since the lipids need to be liquid in order for homogenization to take place. There are two phases of the reaction: lipid melt and the aqueous surfactant phase. Both phases are heated to the same temperature which is based on the solid lipid melting point. Then both phases are mixed by high-shear mixing device. Higher temperature decreases viscosity of the inner phase and allows for small particles to be formed (178). However, some drugs may not be able to incorporate due to high temperature degradation. In addition, larger particles can be formed with higher homogenization pressure and number of cycles due to particle coalescence. After high pressure homogenization nanoemulsion needs to be rapidly cooled on ice.

Cold high pressure homogenization technique was developed to overcome temperature induced degradation of several drugs (181, 182). Drug is being dispersed in the melt of bulk lipid which gets rapidly cooled by means of dry ice or liquid nitrogen. High cooling method helps distribution of drug. Solid lipid melt is subjected to milling by means of ball or mortar milling which produce microparticles. Then solid lipid microparticles are subjected to high pressure homogenization in cool

emulsifier solution. Cold homogenization technique produces larger particle size and broader size distribution (181, 182).

SLNs are composed of three key ingredients of solid lipids, emulsifiers, and water. The term solid lipid pertains to lipids that are solid at room temperature and body temperature. Generally, critical parameters for different SLN formulations depends on lipid and emulsifier compositions. Solid lipids include triglycerides (e.g. tristearin), partial glycerides (e.g. imwitor), fatty acids (e.g. stearic acid), steroids (e.g. cholesterol) and waxes (e.g. cetyl palmitate) (178). Higher melting lipid and lipids with longer fatty acid chains results in larger nanoparticle sizes. This can be explained by the higher viscosity of the dispersed phase. In addition, increasing lipid concentration above 10% of the dispersion, results in larger particles formation, presence of microparticles, and overall broader particle size distribution.

Emulsifiers help to decrease particle size by reducing the surface tension and thus allowing for particle partitioning to occur. Decrease in particle size also produces increase in surface area, which occurs very rapidly during homogenization. During this process an excessive amount of emulsifiers should be present because new uncovered surfaces can produce agglomeration. Typically 5 w%-10w% should be used to prevent agglomeration (183). All classes of emulsifiers and coemulsifiers have been evaluated in stabilizing SLNs (184). Ionic surfactants (e.g. epikurin 100, taurodeoxycholate, and monooctylphosphate) tend to produce smaller SLN dispersions rather than nonionic surfactants (e.g. Tween 80 and butanol) (185). It has been found that combination of emulsifiers, or emulsifier and coemulsifier, is

better in preventing agglomeration and decrease toxicity of rapidly distributing surfactants like SDS. It was found that increasing emulsifier concentration would decrease nanoparticle size but at the same time would increase toxic side effects. Also emulsifier selection is more limited for parenteral administrations (185).

2.4.3 Nanostructured lipid carriers (NLC)

In contrast to liposomes and SLNs, nanostructured lipid carriers (NLCs) are synthesized using both solid and liquid lipids. The highly pure lipids used in the making of SLNs result in a low energy crystal matrix. Small molecules are able to reside within the voids of the matrix. NLC structure limits drug and shows a burst drug release. Within a mixture of different lipids, NLCs have more imperfections and higher loading capacity and lower drug release rates. When the liquid lipid used for NLCs is trapped in the solid lipid crystal matrix, it solubilizes the lipophilic drug and does not seem to affect the solid lipid crystal structure.

Both SLNs and NLCs are made from lipids designated as Generally Recognized as Safe (GRAS), which overcomes the toxicity concerns with inorganic nanoparticle drug delivery systems. Also these lipids carriers do not use organic solvents during preparation, which helps to reduce environmental and cost concerns (186).

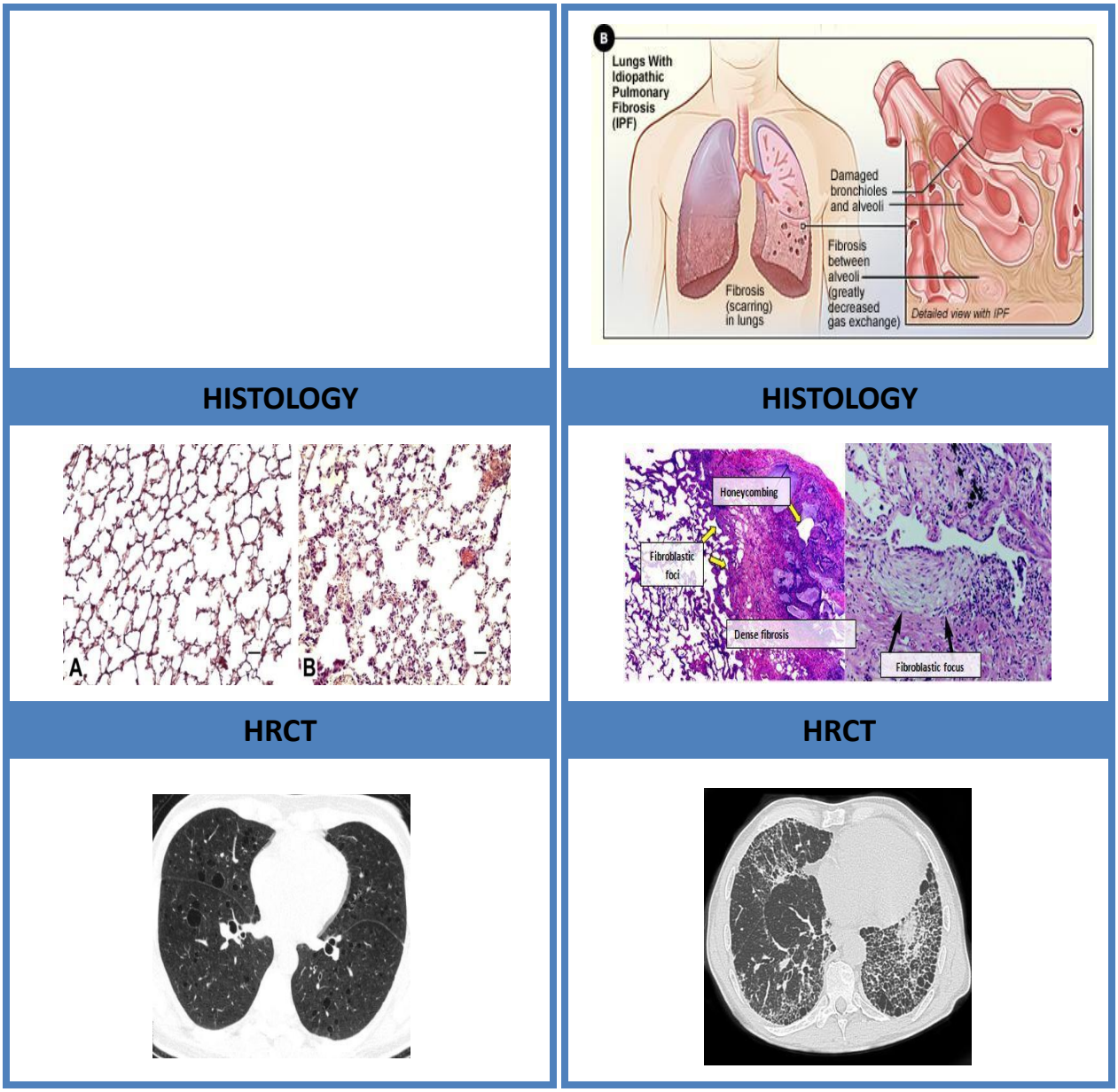

Fig. 2.1 A) Left diagram of healthy lungs vs. B) IPF lungs through cartoon drawing, H&E histology staining, and HRCT (Reproduced from Ref. (187) (1)).

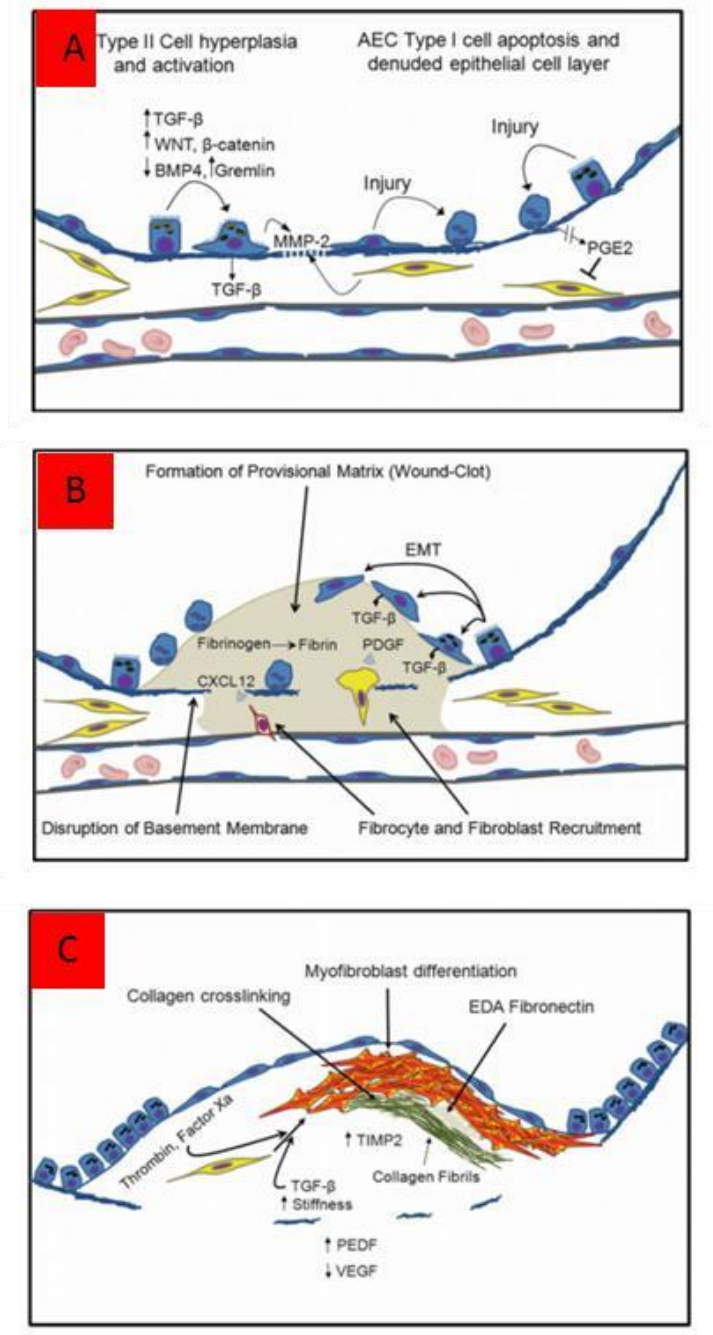

Fig. 2.2 Three main pathways of IPF. A) AEC injury, B) Epithelial-mesenchymal transition (EMT) of epithelial cells, C) Matrix formation and myofibroblast proliferation. (Reproduced from Ref. (39).

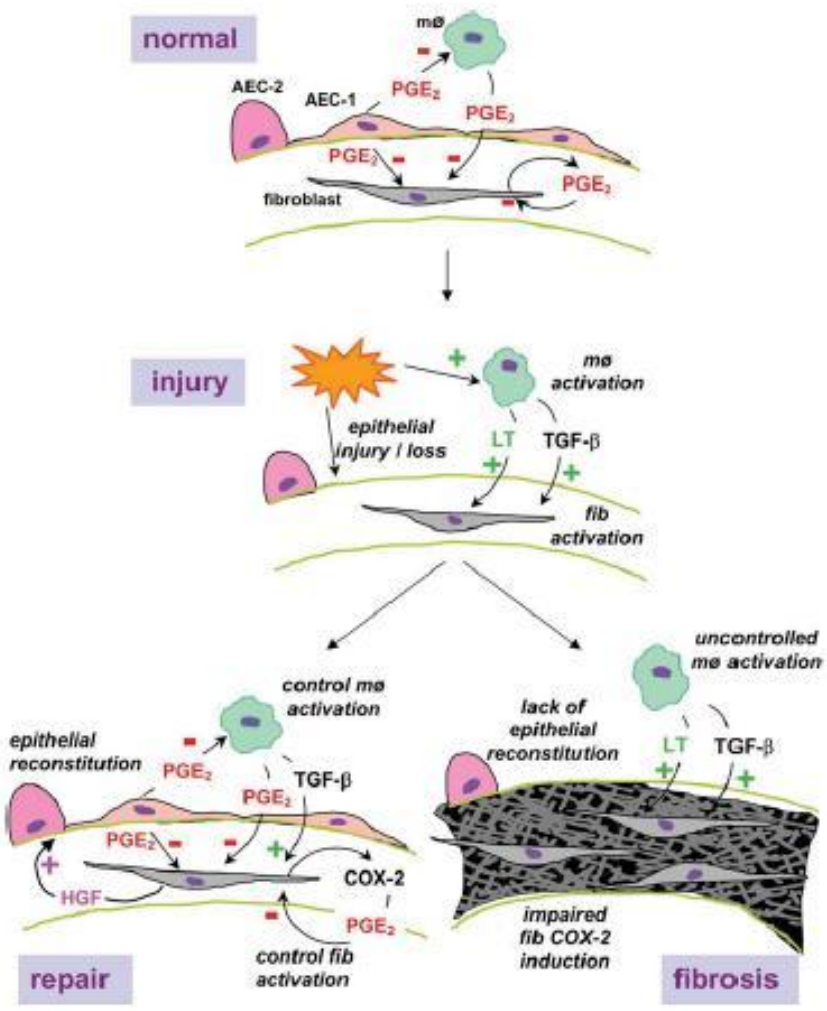

Fig. 2.3 PGE2 role in the pathogenesis of the pulmonary fibrosis. (Reproduced from Ref. (114)).

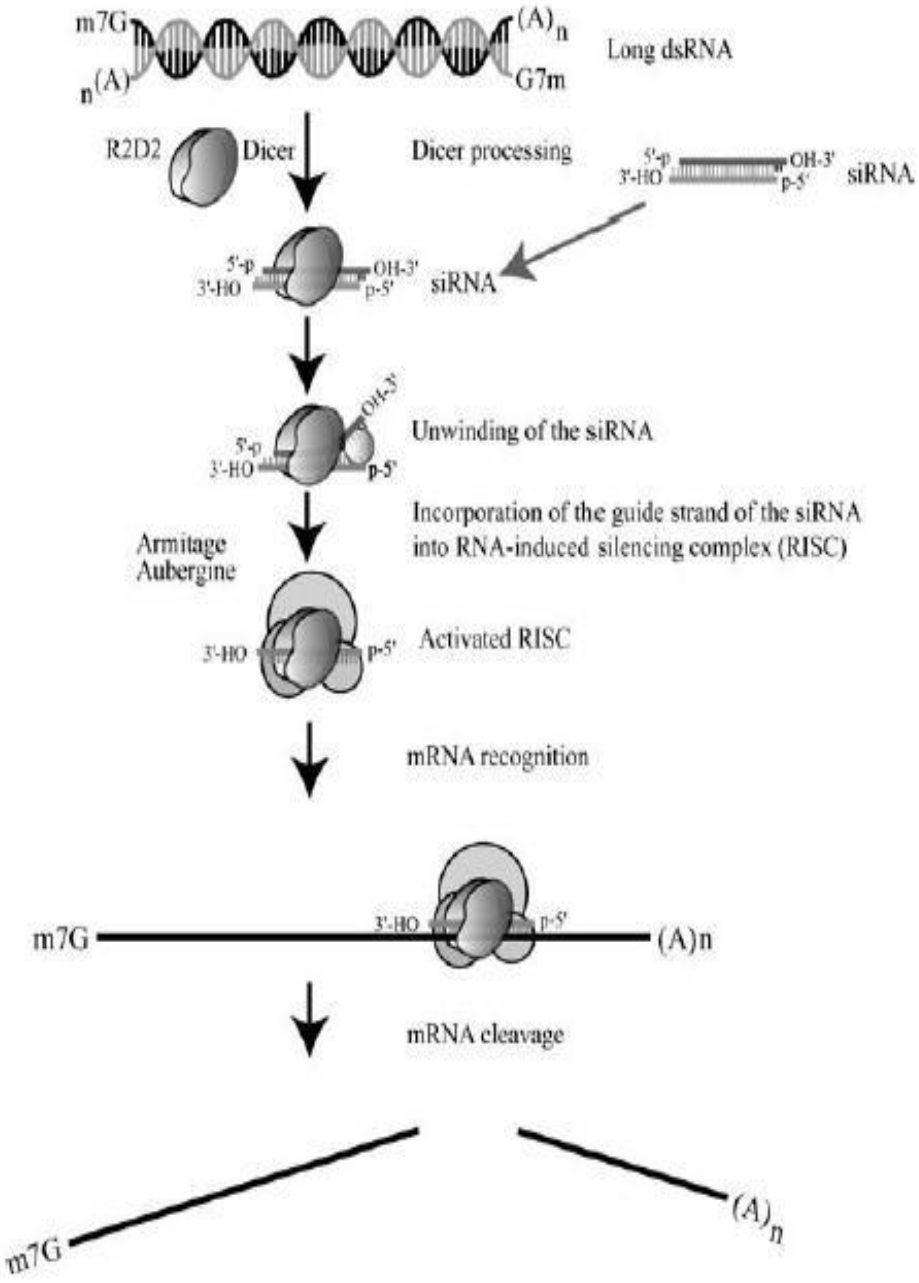

Fig. 2.4 siRNA pathway (Reproduced from Ref. (30)).

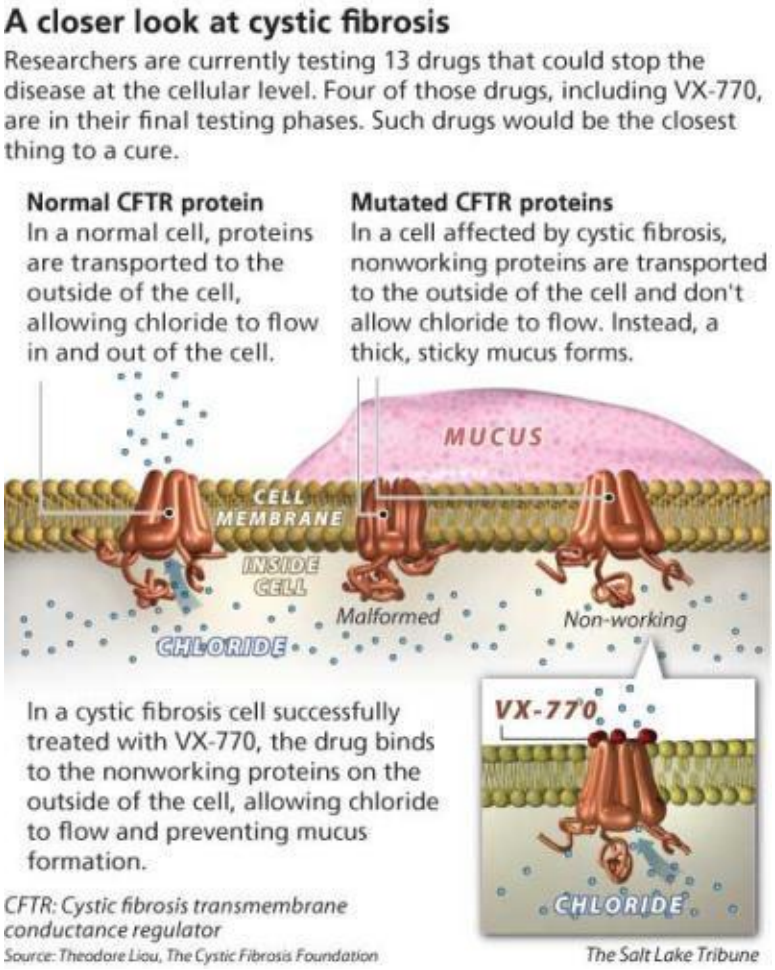

Fig. 2.5 CFTR transporter in cystic fibrosis (Reproduced from Ref.).

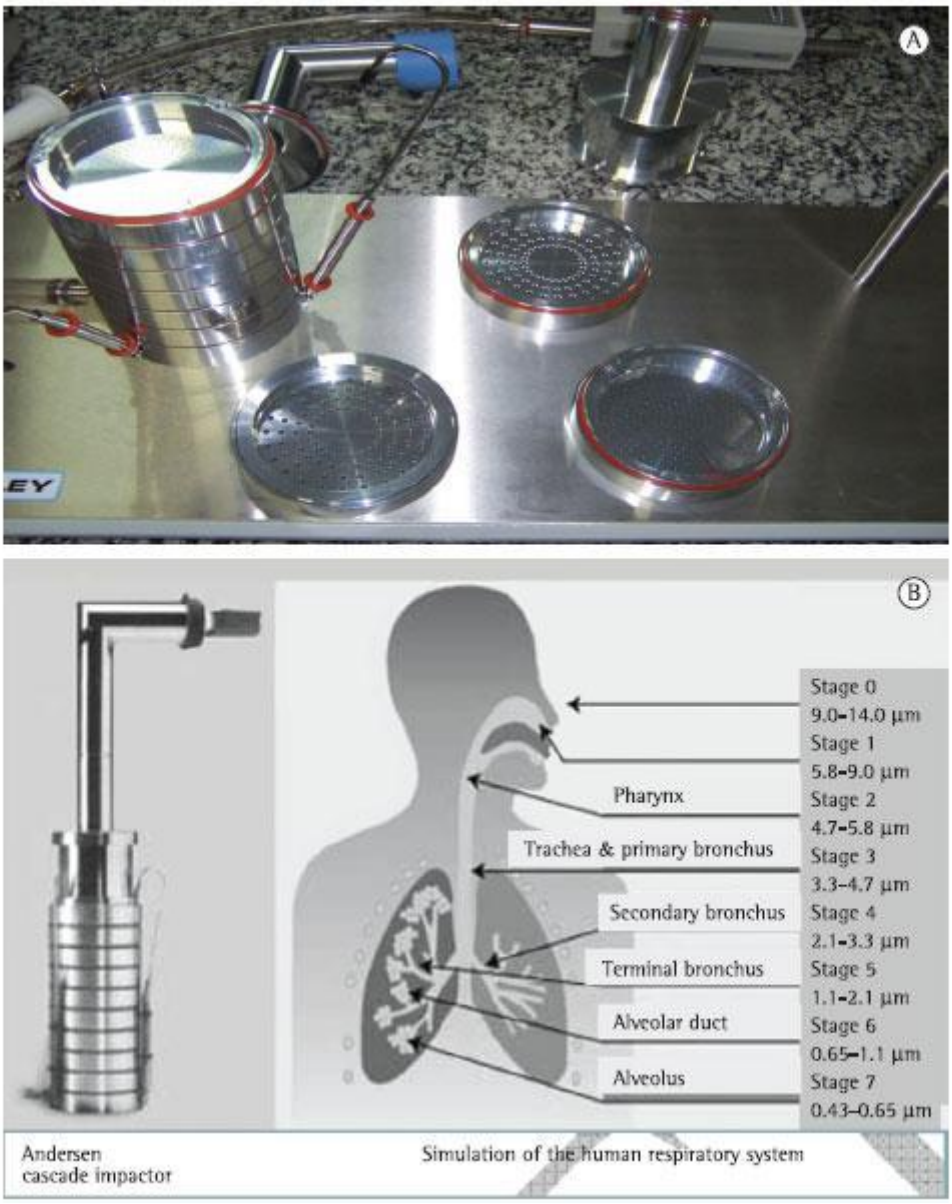

Fig. 2.6 A) Image of Andersen cascade impactor. B) Device and the correspondence to different levels of deposition (Reproduced from Ref. (188)).

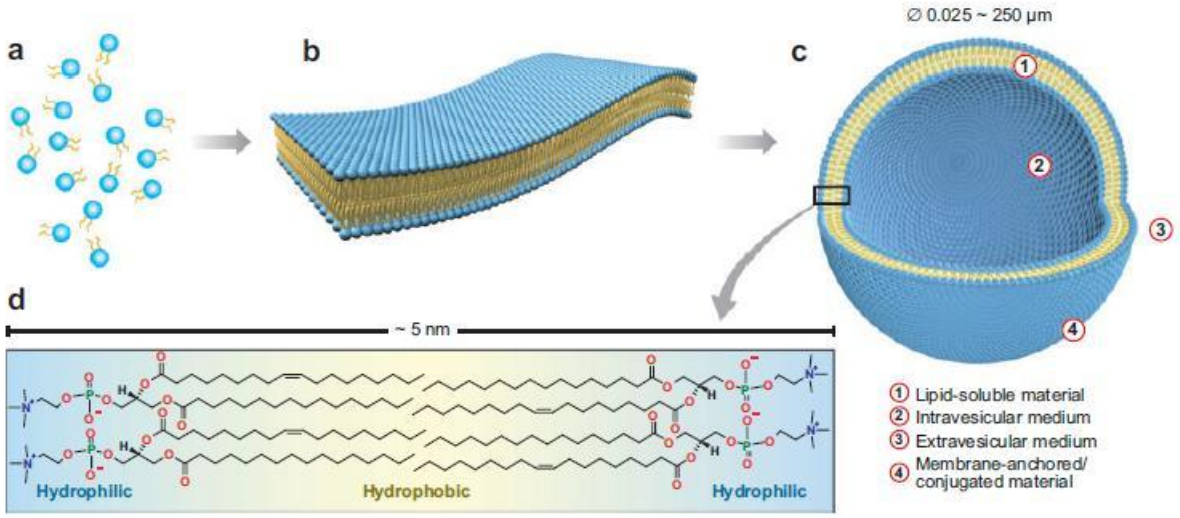

Figure 1

Schematic illustration of the fundamental self-assembly process from individual phospholipid molecules (*a*) to bilayer membrane leaflets (*b*), followed by transformation into liposomes (*c*). A single bilayer is typically ~5 nm thick and consists of neatly arranged individual lipid molecules with their hydrophobic tails facing each other and their hydrophilic headgroups facing toward the internal and external aqueous medium (*d*). Apart from the structural characteristics of the lipid molecules themselves, the properties and functionality of liposomes are largely defined by their size and the composition of the four distinct regions highlighted in panel *c*. Various natural and synthetic lipid molecules are available for the preparation of bilayer membranes and liposomes (140).

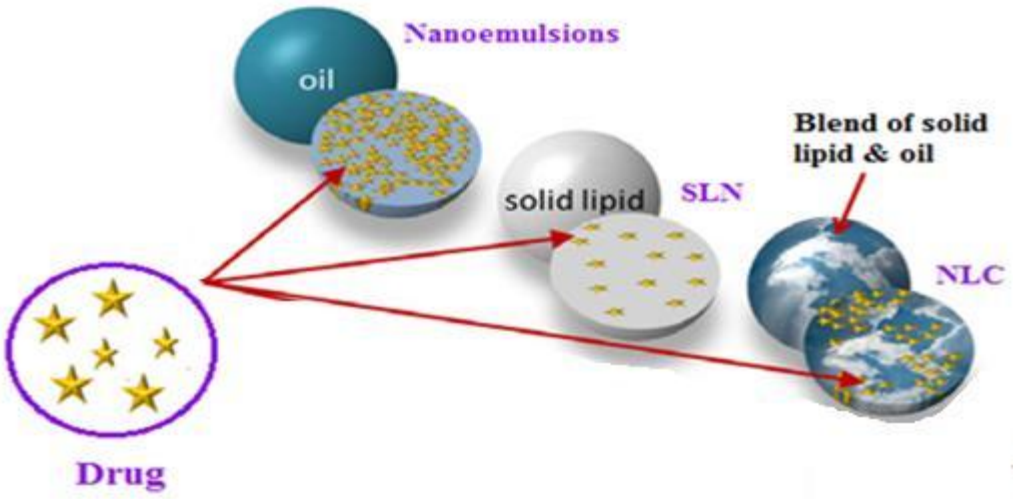

Fig. 2.8 Lipid nanoparticles (Reproduced from Ref. (189).

3 SPECIFIC AIMS

3.1 Specific Aim 1

To examine treatment of mice with idiopathic pulmonary fibrosis (IPF) by inhalation delivery of liposomal prostaglandin E2 (PGE2).

The goal of the present investigation is to deliver liposomal form of PGE2 by inhalation to the lungs of mice with IPF. We hypothesized that the local pulmonary delivery of PGE2 by liposomes can be used for the effective treatment of IPF. To test this hypothesis, we designed and evaluated the bleomycin induced murine model of IPF treated by liposomal drug delivery system which carries PGE2 topically to the lungs. It was shown that after inhalation delivery, liposomes accumulated predominately in the lungs. In contrast, intravenous administration led to the accumulation of liposomes mainly in kidney, liver, and spleen. Liposomal PGE2 normalized the disturbances in the expression of many genes involved in the development of IPF, substantially restricted inflammation and fibrotic injury in the lung tissues, prevented decrease in body mass, limited hydroxyproline accumulation in the lungs and finally eliminated mortality of animals after intratracheal injection of bleomycin. In summary, our data provide evidence that pulmonary fibrosis can be effectively treated by the inhalation administration of liposomal form of PGE2 locally into the lungs. The results of the present investigations make liposomal form of PGE2 an attractive drug for the effective inhalation treatment of IPF.

3.2 Specific Aim 2

To develop a nanoscale-based system suitable for the local inhalation co-delivery of siRNA and PGE2 for treatment of IPF.

In this specific aim, we will design and test solid lipid nanoparticles (SLN) containing both prostaglandin E2 (PGEs) and siRNA in order to deliver them locally to the lung by inhalation. Inhaled therapeutics has recently played an important role in local therapy of various lung diseases including IPF. However, the efficiency of therapeutic agents delivered via inhalation is limited by the complexity of devices used and difficulties in formulation of suitable dosage forms. Furthermore, unlike asthma drugs, biological therapeutics including siRNA cannot be administered without an appropriate dosage form due to their fast degradation and poor cellular penetration. PGE2, a cyclooxygenase-derived lipid mediator, has attracted considerable attention for its role in the development and progression of IPF and as a possible therapeutic agent for this disease. Previously, we found that chemokine CCL12, matrix metalloproteinase MMP3 and hypoxia inducible factor HIF1A are key proteins responsible for the development of inflammation and IPF. We hypothesize that inhibition of these proteins by the local inhalation co-delivery of PGE2 and multiple siRNAs targeted to mRNA encoding these proteins can be successfully used for effective treatment of IPF. This specific aim is aimed at developing an appropriate nanoscale-based complex of drug and siRNAs for such inhalation co-delivery and verifying the hypothesis.

3.3 Specific Aim 3

To study nanostructured lipid carriers for inhalation co-delivery of two drugs for inhibition of transmembrane conductance regulator (CFTR) pathway of cystic fibrosis (CF).

The goal of this aim is to encapsulate two anti-CF drugs, ivacaftor and lumacaftor, within the matrix of nanostructured lipid carriers (NLCs) and evaluated these formulations. It was found that NLCs possess attractive properties such as not complicated synthesis, narrow size distribution, high drug loading potential, stability, biocompatibility, and capability to enter cells. Plain and loaded NLCs were characterized for their colloidal properties such as size, size distribution, drug loading efficiency, *in vitro* drug release, cytotoxicity and genotoxicity. Also, CFTR gene and protein expressions were evaluated after incubation of cells with NLCs. Changes in the size distribution of nanoparticles were evaluated before and after nebulization of the delivery system. It was found that synthesized nanoparticles possessed a narrow size distribution, spherical shape and low cyto- and genotoxicity. Nebulization led to minimal changes in the size and dispersion of nanoparticles. It was concluded that the proposed NLCs are perspective candidates for the inhalation delivery of one or several drugs for treatment of pulmonary manifestations of CF.

4 TO EXAMINE TREATMENT OF MICE WITH IDIOPATHIC PULMONARY FIBROSIS BY INHALATION DELIVERY OF LIPOSOMAL PROSTAGLANDIN E2

4.1 Introduction

Idiopathic pulmonary fibrosis (IPF), a chronic, progressive, and often fatal form of interstitial lung disease, is the most common form of idiopathic interstitial pneumonias (181). IPF causes the loss of lung epithelial cells, substitution of normal functional tissue, elevated accumulation of fibroblasts and myofibroblasts, extracellular matrix deposition, alteration of lung architecture, pulmonary hypertension leading to substantial impairment of respiration and gas exchange often resulting in patient morbidity and mortality (190, 191). Treatment of IPF still represents a major clinical challenge since this disorder does not have reliable therapeutic options and an effective therapy has yet to be identified and developed (190, 192, 193). Surgery and lung transplantation are considered to be the most radical but risky treatments, while oxygen therapy represents a major alleviating treatment of IPF. Consequently, the development of a novel effective treatment of this devastating disease represents a very important and urgent task.

Prostaglanding E2 (PGE2), a cyclooxygenase-derived lipid mediator, attracts considerable attention for its role in the development and progression of IPF and as a possible therapeutic for this disease. An importance of PGE2 for treatment of IPF

is based on the very specific and unique role that PGE2 plays in the lungs making “the lung as a privileged site for the beneficial actions of PGE2” (194). Outside the lungs in other organs and tissues, PGE2 often acts as a potent pro-inflammatory mediator and is involved in pathogenesis of many inflammatory diseases. In contrast, in the lungs, PGE2 limits the immune-inflammatory response, inhibits specific lung fibroblast functions, their proliferation and synthesis of matrix proteins such as collagen and therefore can potentially be used for the treatment of IPF (194-198). Moreover, it was recently shown that a synthetic analog of PGE2 (16,16-dimethyl-PGE2) was tested using mouse model of pulmonary fibrosis (intratracheal administration of bleomycin) and showed a promising results as a potential treatment option for IPF (199).

Systemic delivery of PGE2, as well as other drugs intended to fight lung diseases, has several disadvantages including but not limited to low accumulation in the lungs and possible adverse side effects on other organs and tissues. In contrast, local inhalation delivery of PGE2 directly to the lungs has the potential to enhance the treatment of IPF by increasing its local concentration in the lungs and preventing or at least limiting its penetration into the bloodstream and accumulation in other healthy organs. However, free native PGE2 cannot be delivered into the lungs by inhalation requiring a special dosage form or delivery system that can be inhaled. We showed that liposomes and some other nanoscale-based particles can be used for local inhalation delivery to the lungs of drugs, antisense oligonucleotides and siRNA, vitamins and imaging agents (200-203). It was found that liposomes remain in the lungs after the inhalation delivery limiting penetration of the payload into the

blood stream and accumulation in other organs. Therefore, we hypothesize that the local pulmonary delivery of liposomes containing PGE2 can be used for the effective treatment of IPF and will limit its adverse side effects on other organs. To test this hypothesis, we designed and tested the bleomycin induced murine model of IPF liposomal drug delivery system which delivers PGE2 topically to the lungs.

4.2 Materials and methods

4.2.1 Materials

Egg phosphatidylcholine and cholesterol were purchase from Avanti Polar Lipids (Alabaster, AL). PGE2 was obtained from Apichem Chemical Technology Co., Ltd. (Shanghai, China), bleomycin was purchased from Sigma Aldrich (Ronkonkoma, NY). Hairless SKH1 6-8 weeks old mice were purchased from Charles River Laboratories (Wilmington, MA). All mice were maintained in micro-isolated cages under pathogen free conditions in the animal maintenance facilities of Rutgers, The State University of New Jersey and were handled according to the animal protocol approved by the Institutional Animal Care and Use Committee.

4.2.2 Liposomal composition of PGE2

Liposomes were prepared as previously described (200, 201, 204, 205). Briefly, to prepare liposomes, egg phosphotidyl choline and cholesterol were dissolved in 4.0 ml of chloroform at 55:45 ratio (all compounds were obtained from Avanti Polar

Lipids, Alabaster, AL). The clear lipid solution was evaporated at 25 ºC under reduced pressure. A thin layer was formed and rehydrated using 2.0 ml of 0.3 M sodium citrate buffer (pH=4.0). The lipid mixture was sonicated continuously for 3.0 hours. Liposomes were extruded gradually through 100 nm and 200 nm polycarbonate membranes at room temperature using an extruder device from Northern Lipids, Inc. (Vancuver, BC, Canada). PGE2 was incorporated in the membranes of liposomes in the ratio of 1:1. Liposomes were separated from non-encapsulated PGE2 by dialysis against 100 volumes of 0.9% NaCl. The encapsulation efficacy of PGE2 in liposomes was ~90-95%. The final phospholipids concentration was 10 mg/ml. Aliquots of each liposomal formulation were labeled with near infrared fluorescent dye Cy5.5 Mono NHS Ester (GE Healthcare, Amersham, UK). A fluorescent dye was dissolved together with lipids in chloroform. Approximate excitation/emission maxima of Cy5.5 were 675 nm/694 nm. Portions of liposomes were labeled with osmium tetroxide (0.5%) that was added to the rehydration buffer. The size of liposomes was measured by dynamic light scattering using 90 Plus Particle Sizer Analyzer (Brookhaven Instruments Corp., New York, NY). Aliquot of 40 µL of each sample was diluted in 2 mL of saline. Zeta potential was measured on PALS Zeta Potential Analyzer (Brookhaven Instruments Corp, New York, NY). Samples were taken as is and their volume was 1.5 mL. All measurements were carried out at room temperature. Each parameter was measured in triplicate, and average values were calculated. Mean diameter of liposomes was about 500 nm.

4.2.3 Animal model of IPF and treatment

Experiments were performed on healthy 6-8 weeks old SKH1-hr hairless mice (25-35 g) obtained from Charles River Laboratories (Wilmington, MA). Veterinary care followed the guidelines described in the guide for the care and use of laboratory animals (AAALAC) as well as the requirements established by the animal protocol approved by the Rutgers Institutional Animal Care and Use Committee (IACUC). All mice were contained in micro-isolated cages under pathogen free conditions at room temperature with humidity of 40 ± 15% and light/dark cycle on 12 h per day in the animal maintenance facility. Mice were anesthetized via intraperitoneal injection with 80 mg/kg ketamine and 10-12 mg/kg xylazine (Butler-Schine Animal Health Inc, Dublin, Ohio). Once anesthetized, the mouse was placed on the tilting rodent work stand (Hallowell EMC, Pittsfield, MA) in supine position and restrained in position by an incisor loop. The tongue was then extruded via rotation with a cotton tip applicator. The larynx was visualized using a modified 4 mm ear speculum attached to an operating head of an ophthalmoscope (Wellch Allyn, Skaneateles Falls, NY). The modified speculum, acting as a laryngoscope blade, in an inverted fashion provided dorsal displacement of the tongue and magnification of the laryngeal opening as described (200, 201). Bleomycin was administered intratracheally in doses of 0.5, 1.0, 1.5, and 2.0 U/kg. Mice were treated with liposomal PGE2 twice a week for three weeks starting with the second day after the bleomycin administration. Liposomal bleomycin was injected intravenously or inhaled. Previously, developed instillation containing a Collison nebulizer connected to four-port, nose-only exposure chambers was used for inhalation delivery of liposomal

PEG2 (201). Liposomes were aerosolized at the flow rate of 2 L/min for ten min. Animal weight was measured every day within all experimental period. After the treatment, all mice were anesthetized with isoflurane and euthanized. The organs (lungs, heart, liver, kidney, spleen, and brain) were excised and used for further analysis.

4.2.4 Gene expression

Mouse lungs were extracted, frozen and homogenized. RNA was isolated using an RNeasy kit (Qiagen, Valencia, CA) according to manufacturer's protocol. First-strand cDNA was synthesized with Ready-To-Go You- Prime First-Strand Beads (Amersham Biosciences, Piscataway, NJ) with 1 µg of total cellular RNA (from 10^7 cells) and 100 ng of random hexadeoxynucleotide primer (Amersham Biosciences, Piscataway, NJ). After synthesis, the reaction mixture was immediately subjected to quantitative polymerase chain reaction (QPCR). A standard Mouse Fibrosis RT Profiler™ PCR Array panel from SABiosciences (Quiagen, Valencia, CA) was used. The assay was performed on lung samples from healthy mice (control), mice with lung fibrosis and mice with lung fibrosis treated with liposomal PGE2. QPCR was performed using SYBER Green Master Mix as detection agent. Fold change of the gene expression was measured using SABioscience internet software which compares the expression of testing genes with that of housekeeping genes and expresses fold change in gene expression as $\Delta\Delta$Ct values ($\Delta\Delta Ct = \Delta Ct_{treated} - \Delta Ct_{control}$). PCR specificity was verified by melting curve and gel electrophoresis. In addition to the pull of genes provided in mouse fibrosis array, the expression of

genes encoding Hypoxia Inducible Factor 1α (*HIF1A*), von Hippel-Lindau (VHL) and β-actin (B-ACTIN, internal standard) was measured as previously described (202, 205).

4.2.5 Immunohistochemistry

To confirm PCR data, the expression of some proteins was measured. To visualize the expression of proteins, immunohistochemical staining was conducted on paraffin-embedded slides of tumor tissue. Slides were deparaffiized in xylene for 5 min followed by progressive rehydration in 100%, 95%, 70%, and 50% ethanol for 3 min during each step. Endogenous peroxidase activity was blocked by incubating slides in 3% H_2O_2 solution in methanol at room temperature for 10 min and washing in 300 mL PBS two times for 5 min. The slides were then stained with anti-mouse monoclonal antibodies for VEGF, CCL12, MMP3 and HIF1A proteins. Antibodies against VEGF (labeled with Alexa Fluor 488 fluorescence dye) and MMP3 (labeled with FITC) were obtained from Biolegend, San Diego, CA. Antibodies against CCL12 and HIF1A (both labeled with FITC) were purchased from Biorbyt, Cambridge, UK and from Novus Biologicals, Littleton, CO, respectively. All antibodies were used in in the dilution of 1:100. The slides were stained using Vector M.O.M. Immunodetection Kit (Vector Lab., Inc., Burlingame, CA), visualized and photographed by a fluorescence microscope (Olympus IX71, Center Valley, PA).

4.2.6 Hydroxyproline assay

Fourteen days after bleomycin instillation, lungs were harvested and homogenized in distilled water and Biovision hydroxyproline assay kit (Biovision, Mount View, CA) was used to perform the test. Homogenized lung tissues were hydrolyzed in 12 N HCl at 120 ºC for 3 h in pressure tight vials. After this, 10 µl of samples were allocated to the 96 well plate and dried under vacuum. Oxidation buffer with chloramines T was added to each sample at room temperature for 5 min, and the samples were incubated in dimethylaminobenzaldehyde (DMAB) reagent for 90 min at 60 ºC. Samples were cooled and the absorbance at 560 nm was measured using a microtiter plate reader. Six concentrations of hydroxyproline standard dilutions (from 0 to 1 µg/well) were used to plot a hydroxyproline standard curve.

4.2.7 Histopathologic analysis

At the end of the experiments, the animals were euthanized; the lungs were extracted and immediately fixed in 10% phosphate-buffered formalin. Samples were subsequently dehydrated and embedded in Paraplast®. Five-micrometer sections were cut and stained with hematoxylin-eosin as previously described (206) and analyzed.

4.2.8 Content of liposomes in different organs

The distribution of fluorescent-labeled liposomes was examined in mouse lungs, heart, liver, spleen, kidneys, and brain. The organs were excised, rinsed in saline, and fluorescence was registered by IVIS imaging system (Xenogen Corporation, Alameda, CA). Visible light and fluorescence images were taken and overlaid. The intensity of fluorescence was represented on composite light/fluorescent images by different colors with blue color reflecting the lowest fluorescence intensity and red color – the highest intensity. Images of each organ were then scanned and total fluorescence intensity was calculated as previously described (200, 201, 204). Preliminary experiments showed a strong linear correlation between the total amounts of labeled substance accumulated in the organ and calculated total fluorescence intensity. The fluorescence was expressed in arbitrary units with 1 units represented approximately 2×10^{10} photons/s/sr/cm^2. The method allows a quantitative comparison of the concentration of the same fluorescent dye between different series of the experiments. The mass of all organs was measured. The fluorescence intensity was normalized for organ weight.

4.2.9 Internalization of liposomes by lung cells

Internalization of osmium-labeled liposomes by lung cells was studied by electron transmission microscopy in lung tissue sections fixed prior to microscopy using standard techniques as previously described (204, 205, 207, 208). Briefly, lung tissue slices were fixed for 2 hours in Trump's EM Fixative (combination of low

concentration of both formaldehyde and glutaraldehyde in 0.1 M Milloning's Phosphate buffer pH 7.3). Postfixation was carried out in 1% Osmium Tetroxide in buffer for 1 hour followed by dehydration in graded Ethanol series and embedded in Spurr's Low Viscosity Resin. Sections were prepared using a diamond knife by LKB-2088 Ultramicrotome (LKB-Produkter / Bromma, Sweden). Observation and micrographs were made with a JEM-100CXII Electron Microscope. (JEOL LTD., Tokyo, Japan).

4.2.9 Statistical analysis

Data obtained were analyzed using descriptive statistics and single-factor ANOVA, and are presented as a mean+-SD from five independent measurements. We analyzed data sets for significance with Student's *t* test and considered *P* values of less than 0.05 as statistically significant.

4.3 Results

4.3.1 Selection of bleomycin dose

In order to select an appropriate dose of bleomycin, four doses (0.5; 1.0; 1.5; 2.0 U/kg) were tested. Bleomycin was injected intratracheally and mice were observed within 21 days after the instillation. The dose of 2.0 U/kg led to the death of 100% of animals within 21 day (Fig. 4.1A). The doses of 1.5 and 1.0 U/kg induced death of 50 and 25% of animals, respectively. The lowest tested dose (0.5 U/kg) did not

induce animal death. Based on the results of these observations, 1.5 U/kg dose of bleomycin was selected for the future experiments.

4.3.2 Validation of IPF model

Changes in animal body mass, hydroxyproline content in the lung tissue and lung histology were used as hallmarks of the development of IPF in experimental animals after the injection of 1.5 U/kg bleomycin. It was found that three weeks after the injection, the body mass of animals decreased for 1.3 fold ($P < 0.05$) when compared with its initial value (Fig. 4.2A). At the same experimental point, the concentration of hydroxyproline in the lungs increased in 2.6 times (Fig. 4.2B). Histological analysis of lung tissue showed that control lung demonstrated widely patent alveoli without inflammation or edema (Fig. 4.3A). The bronchi were also patent. Lungs of animals injected with bleomycin (Fig. 4.3B) showed consolidation of the pulmonary architecture, with early fibrotic thickening of the alveolar walls, ablation of the alveolar space, and edema. Chronic inflammatory cells and fibroblasts were readily apparent within the affected areas. Taken together these data clearly confirm the development of marked lung fibrosis in experimental animals subjected to bleomycin.

4.3.3 Body distribution and accumulation of liposomes in the lungs

The average size of liposomes used in the present study for inhalation was 500-600 nm. Previously we demonstrated that liposomes retains predominately in the lungs

for a long period of time after inhalation (200, 201). In order to confirm the preferential accumulation of used in the present study liposomes in the lungs, we studied organ content of fluorescently labeled liposomes using the IVIS imaging system (Fig. 4.4). Inhalation delivery was compared with intravenous injection of similar liposomes. It was found that 24 hours after intravenous injection, liposomes predominately accumulated in the kidneys and liver while substantially less content of liposomes was found in the spleen, heart and lungs. Only trace amount of liposomes registered in the brain. In contrast, after inhalation delivery, liposomes predominately retained in the lungs with minimal amounts found in other organs including the liver, kidneys spleen, heart and brain. These data confirmed the favorable distribution of inhaled liposomes and formed the basis for the use of such liposomes as carriers to deliver PGE2 locally to the lungs, for the prevention of their entrance into the bloodstream and accumulation in other organs, and limitation of possible adverse side effects of PGE2. In order to study the penetration of liposomes in lung cells after inhalation, lipid membrane of liposomes was labeled by osmium tetroxide and visualized in slices of lung tissues by transmission electron microscopy (Fig. 4.4C). These data clearly showed that liposomes did penetrated lung cells after inhalation and accumulated in the cytoplasm.

4.3.4 Treatment of IPF with liposomal form of PGE2

In order to estimate anti fibrotic effect of liposomal PGE2, we investigated the influence of this preparation on the body mass, hydroxyproline content in the lungs and mortality of animals with IPF induced by a single intratracheal injection of

bleomycin. It was found that treatment with liposomal PGE2 prevented the decrease in the body mass of experimental animals induced by bleomycin injection (Fig. 4.2A). The difference between body mass in untreated animals with IPF (Fig. 4.2A, bar 2) and animals injected with bleomycin and treated with liposomal PGE2 (Fig. 4.2A, bar 3) was statistically significant ($P < 0.05$). A therapeutic action of liposomal PGE2 was also confirmed by the measurement of hydroxyproline content in the lungs. It was found that treatment of animals injected with bleomycin by liposomal PGE2 statistically significantly ($P < 0.05$) decreased the accumulation of hydroxyproline in lung tissues in 1.3 fold (Fig. 4.2B). However, the content of hydroxyproline in the lung tissues still was significantly ($P < 0.05$) higher (~2 times) when compared with intact control (compare bars 3 and 1 in Fig. 4.2B). Inhalation treatment of animals with liposomal PGE2 substantially limited lung tissue damage induced by bleomycin (Fig. 4.3C). Some mild thickening of the alveolar septa was noted focally, and in some areas fibrosis could still be observed. However, both the extent and severity of the fibrotic process were reduced in this group. Edema was minimal and only focal inflammation was presented. Finally, inhalation treatment of animals with pulmonary fibrosis by liposomal PGE2 completely prevented the mortality of experimental (Fig. 4.1B).

4.3.5 Gene and protein expression

In order to examine mechanisms of the development of fibrosis induced by intratracheal injection of bleomycin and protective effect of liposomal PGE2 deliver to the lungs by inhalation, we studied the profiles of the expression of 84 key genes

involved in dysregulated tissue remodeling during the repair and healing of wounds and development of fibrosis. The data obtained using the standard Mouse Fibrosis RT Profiler™ PCR Array panel showed that after injection of bleomycin, 24 studied genes were upregulated in more than 5 times while 7 out of 84 genes were downregulated more than 5 folds (Fig. 4.5A). Data showed that transforming growth factor (TGF)-mediated cell signaling was impaired in mice after the injection of bleomycin. While the expression of genes encoding different types of TGF proteins was practically unaffected, the expression of proteins associated with TGF receptors and their second messenger (*ENG*, *TGFBR2* and *SMAD6* genes, Fig. 4.5A, #5, 65, and 73, respectively) was significantly downregulated. In addition to TGF signaling, the expression of genes encoding vascular endothelial growth factor (*VEGF*), integrin alpha-1 (*ITGA1*), calveolae protein (*CAV1*) signal transducer and activator of transcription 6 (*STAT6*) were also decreased (Fig. 4.5A, #45, 54, 68, and 83, respectively). In order to confirm data obtained by the QPCR, the expression of VEGF protein was also examined in lung tissues using imunostaining of tissue sections (Fig. 4.6). The data obtained confirmed QPCR results and showed that VEGF protein expression was substantially decreased after injection of bleomycin. In contrast, the expression of genes encoding the following functional groups of proteins was substantially increased after bleomycin injection: plasminogen and plasminogen activator (*PLG* and *PLAU*, Fig. 4.5A, #10 and 11), several matrix metalloproteinases (*MMP13*, *MMP1A*, *MMP3*, *MMP8*, *and MMP9*, Fig. 4.5A, #15, 17, 19, 20, and 21) as well as tissue inhibitor of metalloproteinases (*TIMP1* – Fig. 4.5A, #22), angiotensinogen and a member of the TGF-beta family (*AGT* and *BMP7*,

Fig. 4.5A, #26 and 27), chemokines (*CCL11* and *CCL12*, Fig. 4.5A. #33 and 34), gamma interferon (*IFNG*, Fig. 4. 4A, #36), several interleukins (*IL10*, *IL13*, *IL1B*, *IL4*, and *IL5*, Fig. 4.5A, #37, 38, 40, 41, and 24, respectively) and interleukin 13 receptor (*IL13RA2*, Fig. 4.5A, #53), inhibin (*INHBE*, Fig. 4. 5A, #43), tumor necrosis factor and its ligand (*TNF* and *FASL*, Fig. 4.5A, #44 and 69), integrin (*ITGB8*, Fig. 4.5A, #62) and transforming growth factor-beta-induced factor (*TGIF1*, Fig. 4.5A, #84). Immunohistochemical measurement of the expression of chemokine CCL12 and matrix metalloproteinase MMP3 confirmed that bleomycin injection induced overexpression of both proteins. In addition to genes included in the mouse fibrosis array, the expression of hypoxia inducible factor 1 alpha (HIF1A) and von Hippel-Lindau (VHL) genes and proteins were analyzed by RT-PCR and immunohistochemical staining, respectively. It was found that injection of bleomycin led to the overexpression of *HIF1A* and suppression of *VHL* genes (Fig. 4.7). Analysis of the expression of HIF1A protein supports RT-PCR finding and show that the expression of this protein was also upregulated after bleomycin injection (Fig. 4.6). It is remarkably, that treatment of mice with liposomal PGE2 delivered by inhalation after injection of bleomycin almost completely eliminated the mentioned disturbances in gene and protein expression (Fig. 4.5B, 6 and 7).

4.4 Discussion

Data obtained in the present study showed that intratracheal injection of bleomycin in dose of 1.5 U/kg induces extensive lung fibrosis. As expected, the development of fibrosis was initiated by a marked pulmonary inflammation with following transition of

such inflammation into fibrosis. The reality of this process was supported first of all by founded morphological features of inflammation and overexpression of several genes involved in the development of inflammation. In fact, several chemokines, inflammatory cytokines and interleukines were overexpressed after injection of bleomycin. It was previously shown that chemokines are important in the pulmonary recruitment of granulocytes and are essential in the pathogenesis of bleomycin-induced lung fibrosis. (209) Moreover, interferon-gamma, an inflammatory cytokine, was implicated in the development of fibrosis in inflamed tissues. (210) The gene encoding this protein was also overexpressed after injection of bleomycin. In addition, all analyzed genes encoding interleukins were overexpressed in the lungs after bleomycin treatment. It is well known that interleukins are important mediators of inflammation and remodeling in the lungs. In particular, it was found that the overexpression of interleukin IL10 in the lung causes mucus metaplasia, tissue inflammation, subepithelial fibrosis and airway remodeling via IL13-dependent and -independent pathways. (211) It seems that IL13-depended pathway was definitely involved in the development of fibrosis after inflammation in the present study. The registered overexpression of the *IL13* gene as well as gene encoding IL3 receptors (*IL13RA2*) supports this suggestion. Interleukin 13 is considered as a major inducer of fibrosis in several different pathologies accompanied by fibrosis (212-215). The activation of inflammation and its transition to fibrosis was associated with the overexpression of several matrix metalloproteinases (collagenases/gelatinases). It is possible that such activation was compensatory and directed to the degrading of fibrillar collagens in order to limit their accumulation during pulmonary fibrosis.

However, the activation of these enzymes might also enhance tissue damage during IPF (216-218). Therefore, the present experimental data supports the hypothesis that pulmonary “fibrosis is preceded and provoked by a chronic inflammatory process that injures the lung and modulates lung fibrogenesis, leading to the end-stage fibrotic scar” (217).

It is generally assumed that the transforming growth factor-beta (TGFB) family of receptors may play an important role in the initiation of the signal transduction that leads to mitogenic responses and initiation of fibrosis by induced myofibroblast differentiation (195, 213, 219-222). However, the present experimental data showed that this signal transduction pathway probably did not have a valuable impact on the development of pulmonary fibrosis in the present study because genes encoding proteins and receptors involved in this pathways were either practically unchanged or downregulated after the injection of bleomycin. Only transforming growth factor-beta-induced factor and bone morphogenetic protein-7 is (a member of the TGFB superfamily) was substantially upregulated in these conditions, suggesting that other than TGFB receptor-initiated signaling pathways might be involved in the development of fibrosis. A second important mediator of inflammation and fibrosis, tumor necrosis factor (TNF), a multifunctional proinflammatory cytokine secreted predominantly by monocytes/macrophages, was upregulated alone with tumor necrosis factor ligand superfamily member 6 (encoding by the *FASL* or *TNFSF6* gene) after injection of bleomycin. These proteins are known as mediators of the transition from pulmonary inflammation to fibrosis as well as apoptosis inducers (223-225) .

Several other signal transduction pathways activated in the lung tissues after injection of bleomycin including inhibins, angiotensinogens and integrins, might also be involved in the development of pulmonary fibrosis and tissue damage in the present experimental conditions (211, 220, 226-228). It is generally believed that fibrosis is accompanied by hypoxia and major hypoxic signaling pathways initiated by HIF1A and VHL proteins contribute in the development and compensation of fibrotic damage (229-237). In many cases, it was found that tissue hypoxia promotes fibrosis and HIFA-associated signaling pathways of hypoxia are involved on the development to fibrosis in the liver and lungs. We found that injection of bleomycin induces overexpression of HIF1A gene and protein and inhibit the expression of its counterpart – the VHL gene. This supports the conception of the involvement of HIF1A signaling pathways in the development of lung fibrosis after bleomycin injection. It was found that, independently from HIF1A, pVHL protein encoded by the *VHL* gene might be directly involved in the development of IPF, (237) it is unlikely that this mechanism was involved in the present study because the *VHL* gene was suppressed in lung tissues after injection of bleomycin. It was also found that the overexpression of HIF1A protein can promote the development of IPF via TGF-beta-signaling pathways (236). However, it is unlikely that such a pathway was involved in the present study because, as discussed above, genes encoding proteins and receptors involved in this pathway were either practically unchanged or down-regulated after the injection of bleomycin.

In the present experimental work, the first time, we showed that treatment of pulmonary fibrosis by liposomal PGE2 delivered by inhalation led to the substantial

elimination of all studied symptoms of IPF developed after intratracheal injection of bleomycin. The data show that liposomal PGE2 delivered locally to the lungs eliminated the increase in the mouse body mass, substantially limited hydroxyproline content in the lungs, disturbances in the mRNA and protein expression, restricted lung tissue damage and completely prevented animal mortality. These preventive effects of PGE2 can be a result of its ability to limit fibroblast proliferation, activation, migration, collagen secretion, myofibroblast differentiation (194-198). Similar results were recently obtained after treatment of bleomycin-induced IPF in mice by continuous subcutaneous infusion of free non-bound synthetic analog of PGE2. (199) In an independent study, orally induced losartan, an angiotensin II type 1 receptor antagonist, led to the similar effect by increasing the level of PGE2 in the lungs (238). These experimental data support our findings and underline a high perspective of treatments IPF based on the increase in the level of PGE2 in the lung tissues. It is highly possible that the normalization of the expression of many genes encoding proteins responsible for inflammation and fibrosis after bleomycin injection that was found in the present study might play a central role in the prevention of lung injury and animal mortality. Suppression of HIF1A protein by liposomal PGE2 might also played a role in the limitation of fibrotic damage of lung tissue. The exact mechanisms of the protective action of liposomal PGE2 require a special more detail study that is planned in our laboratory.

4.5 Conclusions

The data obtained provide evidence that pulmonary fibrosis can be effectively treated by the inhalation delivery of liposomal form of PGE2 locally into the lungs. The results of present investigations make liposomal form of PGE2 an attractive drug for effective inhalation treatment of idiopathic pulmonary fibrosis.

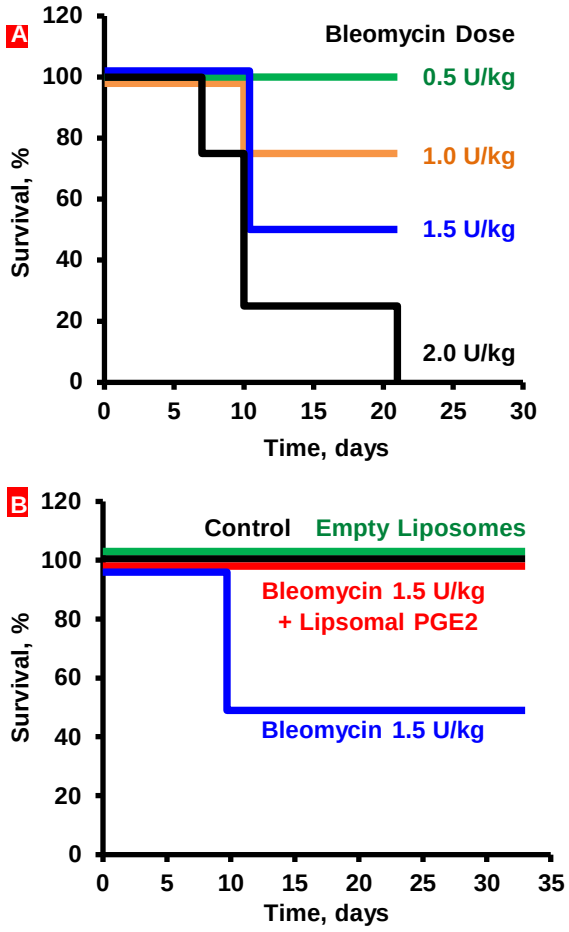

Fig. 4.1. Survival of mice (Kaplan-Meier survival plot) after inhalation exposure to bleomycin. A – Selection of bleomycin dose. Mice were instilled intratracheally once with different concentrations of bleomycin. The dose of 1.5 U/kg that led to death of 50% of animals was selected. B – Inhalation treatment of mice with experimental lung fibrosis by liposomal PGE2 (Lip PGE2) prevents animal mortality. Inhalation of healthy mice with empty liposomes did not influence on animal survival. Lung fibrosis was induced by intratracheal instillation of 1.5 U/kg of bleomycin. Mice were treated with liposomal PGE2 twice a week for three weeks starting one day after the bleomycin administration.

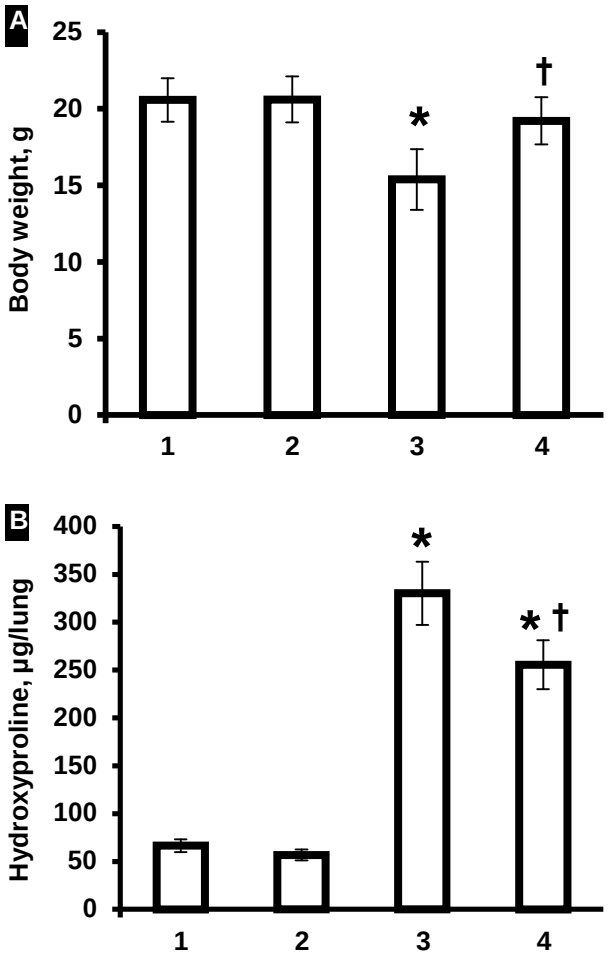

Fig. 4.2. Influence of inhalation treatment with liposomal PGE2 on body weight (A) and hydroxyproline content in the lungs (B). Lung fibrosis was induced by intratracheal instillation of 1.5 U/kg of bleomycin. Mice were treated with liposomal PGE2 twice a week for three weeks starting one day later after the bleomycin administration. At the end of treatment, lungs were harvested, homogenized and hydroxyproline content in the lungs was measured. 1 – Healthy mice (control); 2 – Healthy mice treated by inhalation with empty liposomes; 3 – Mice instilled with bleomycin (1.5 U/kg); 4 – Mice instilled with bleomycin (1.5 U/kg) and treated by inhalation with liposomal PGE2. Means ± S.D. are shown. *$P < 0.05$ when compared with control (1). $^{\dagger}P < 0.05$ when compared with mice with fibrosis (2).

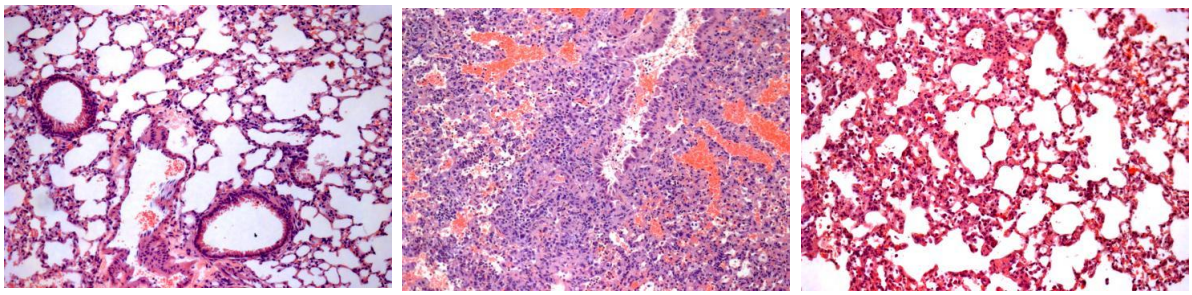

A. Healthy mice (control)

B. Mice injected with bleomycin (1.5 U/kg)

C. Mice injected with bleomycin (1.5 U/kg) and treated by inhalation with liposomal PGE2

Fig. 4.3. Lung histology. A- Healthy mice (control). B-Lung fibrosis was induced by intratracheal instillation of 1.5 U/kg of bleomycin. C-Mice were treated with inhalation of liposomal PGE2 within 3 weeks twice a week starting one day later after the bleomycin administration. At the end of experiment, lungs were harvested and fixed in 10% phosphate-buffered formalin. Samples were subsequently dehydrated and embedded in Paraplast®. Sections (5 µm) were cut, stained with hematoxylin and eosin. Representative images are shown (10X magnification).

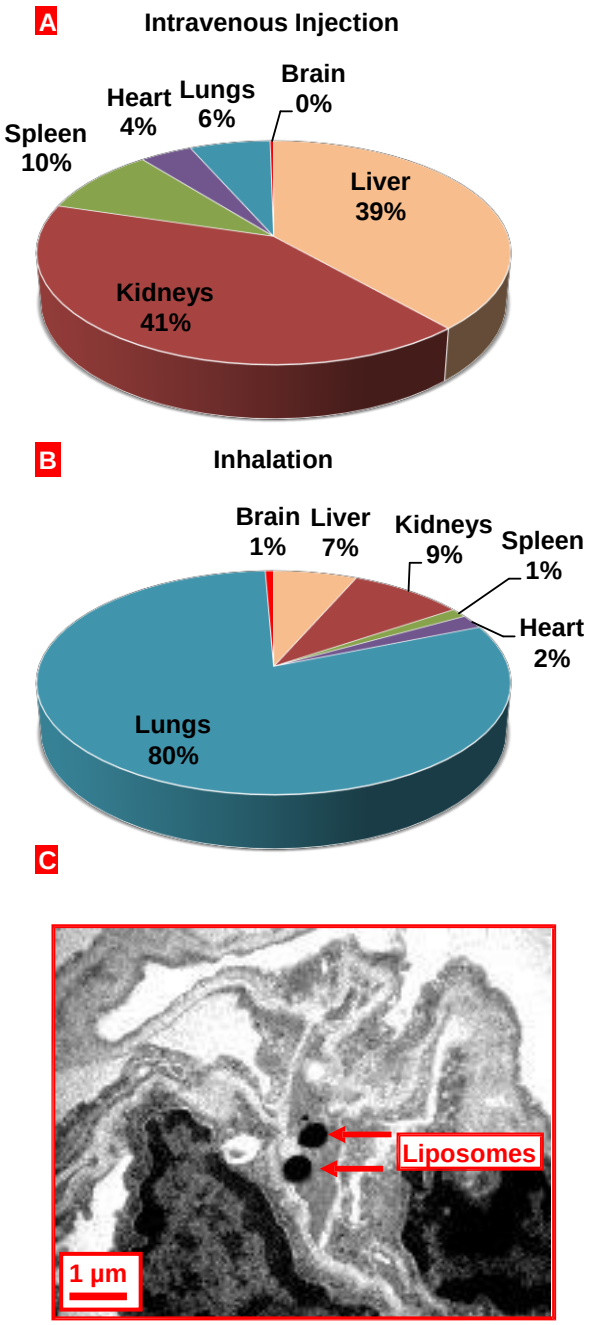

Fig. 4.4. Inhalation delivery of liposomes to mouse lungs. A, B - Relative tissue content of liposomes delivered to mice by intravenous instillation (A) or inhalation (B). Liposomal content was registered in organs 24 h after inhalation. C - Localization of liposomes in the mouse lung tissues after the inhalation delivery. Liposomes were labeled by osmium tetroxide and visualized by electron transmission microscopy.

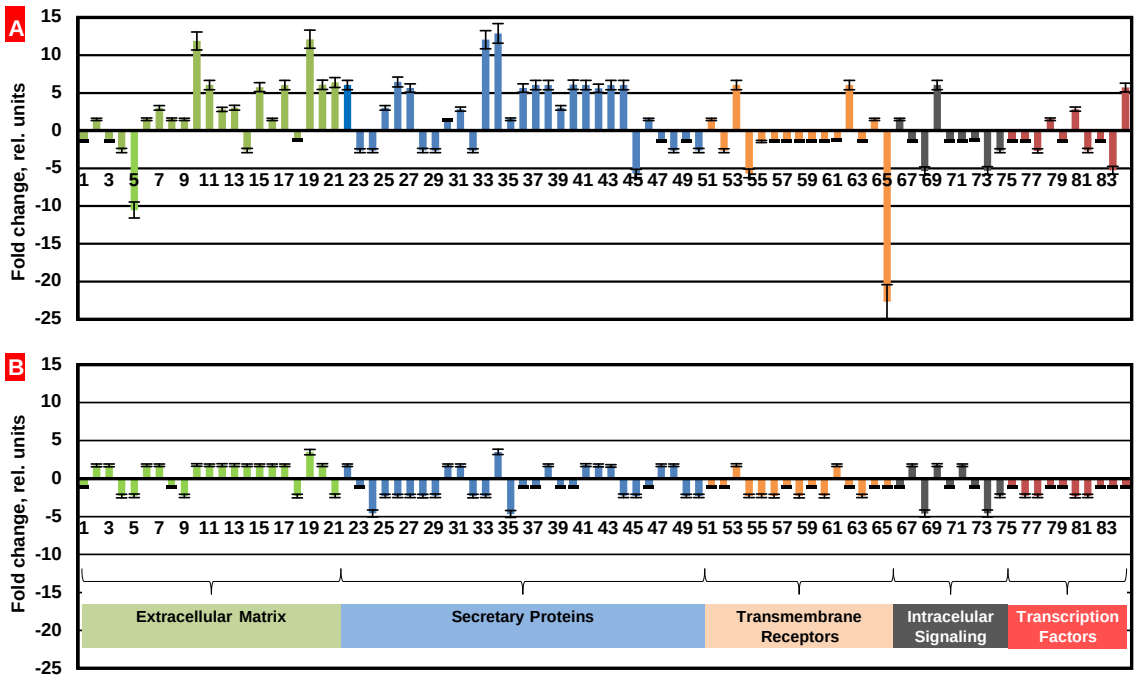

Number	Gene Name	Number	Gene Name	Number	Gene Name	Number	Gene Name
1	ACTA2	22	TIMP1	43	INHBE	64	TGFBR1
2	COL1A2	23	TIMP2	44	TNF	65	TGFBR2
3	COL3A1	24	TIMP3	45	VEGFA	66	AKT1
4	DCN	25	TIMP4	46	TGFB1	67	BCL2
5	ENG	26	AGT	47	TGFB2	68	CAV1
6	LOX	27	BMP7	48	TGFB3	69	FASL
7	THBS1	28	CTGF	49	PDGFA	70	ILK
8	THBS2	29	EDN1	50	PDGFB	71	SMAD2
9	PLAT	30	EGF	51	CCR2	72	SMAD3
10	PLAU	31	GREM1	52	CXCR4	73	SMAD6
11	PLG	32	HGF	53	IL13RA2	74	SMAD7
12	SERPINA1A	33	CCL11	54	ITGA1	75	SMAD4
13	SERPINE1	34	CCL12	55	ITGA2	76	CEBPB
14	SERPINH1	35	CCL3	56	ITGA3	77	JUN
15	MMP13	36	IFNG	57	ITGAV	78	MYC
16	MMP14	37	IL10	58	ITGB1	79	NFKB1
17	MMP1A	38	IL13	59	ITGB3	80	SNAI1
18	MMP2	39	IL1A	60	ITGB5	81	SP1
19	MMP3	40	IL1B	61	ITGB6	82	STAT1
20	MMP8	41	IL4	62	ITGB8	83	STAT6
21	MMP9	42	IL5	63	LTBP1	84	TGIF1

Fig. 4.5. Gene expression measured by the Quantitative Polymerase Chain Reaction (QPCR). The QPCR was performed using a standard Mouse Fibrosis RT Profiler™ PCR Array panel. Lung fibrosis was induced by intratracheal instillation of 1.5 U/kg of bleomycin. Mice were treated by inhalation delivery of liposomal PGE2 twice a week for three weeks starting one day later after the bleomycin administration. A – Mice instilled with bleomycin (1.5 U/kg); B – Mice instilled with bleomycin (1.5 U/kg) and treated by inhalation with liposomal PGE2.). Means ± SD are shown.

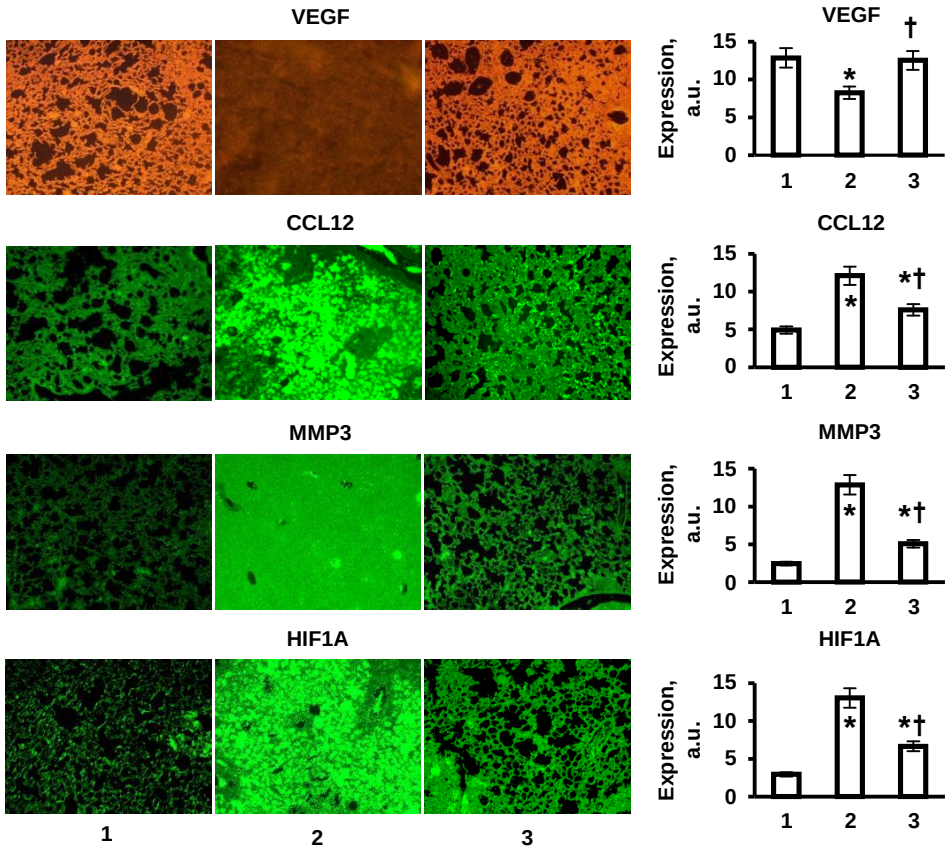

Fig. 4.6. Expression of proteins (immunohistochemistry) in lung tissues. Representative images of tissue sections stained with antibodies against VEGF, CCL12, MMP3 and HIF1A proteins (10X magnification) and average expression of corresponding proteins. High intensity of the color indicates high protein concentration. Lung fibrosis was induced by intratracheal instillation of 1.5 U/kg of bleomycin. Mice were treated with liposomal PGE2 twice a week for three weeks starting one day later after the bleomycin administration. 1 - Healthy mice (control); 2-Mice instilled with bleomycin (1.5 U/kg); 3 - Mice instilled with bleomycin (1.5 U/kg) and treated by inhalation with liposomal PGE2. Means ± SD from are shown. *P < 0.05 when compared with healthy mice (control). †P < 0.05 when compared with mice instilled with bleomycin.

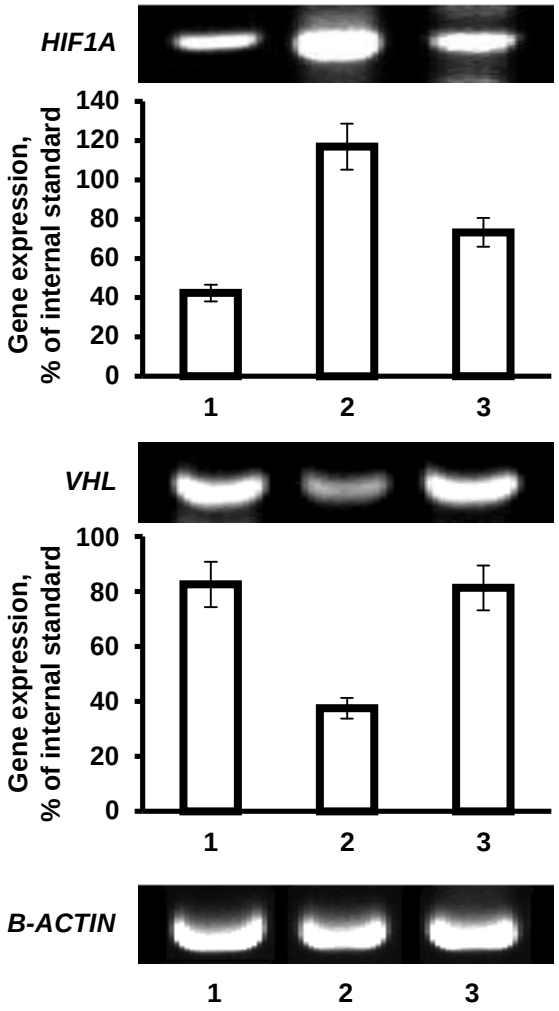

Fig. 4.7. Gene expression analyzed by RT-PCR. Representative images of gel electrophoresis of RT-PCR product and average expression of genes encoding hypoxia inducible factor 1α (HIF1A), von Hippel-Lindau (VHL) and β-actin (B-ACTIN, internal standard) proteins. 1 - Healthy mice (control); 2-Mice instilled with bleomycin (1.5 U/kg); 3 - Mice instilled with bleomycin (1.5 U/kg) and treated by inhalation with liposomal PGE2. Means ± SD from are shown. *P < 0.05 when compared with healthy mice (control). †P < 0.05 when compared with mice instilled with bleomycin.

5 TO DEVELOP A NANOSCALE-BASED SYSTEM SUITABLE FOR THE LOCAL INHALATION CO-DELIVERY OF siRNA AND PGE2 FOR TREATMENT OF IPF

5.1 Introduction

Idiopathic pulmonary fibrosis is debilitating disease that is often detected in the later stage when symptoms cannot be ignored. Lung tissue is unique in a sense that there is no presence of nervous intervention and thus lungs able to have chronic asymptomatic insult. Many different classes of drugs have been examined for therapeutics based on the pathology pathways of the disease that are known. Initially it was believed that inflammation is the primary cause of the disease, however, treatment with inflammatory medications have not been effective. In addition, other therapies for pulmonary disease have been examined such as tyrosine kinase inhibitors, pulmonary arterial hypertension (PAH) drugs, corticosteroids, and more, all of which unfortunately fell short (101, 107).

Previously we have investigated treating pulmonary fibrosis with liposomal Prostaglandin E2 (PGE2). PGE2 belongs to eicosanoid family of autocrine system. Locally in the alveoli region, epithelial cells secrete PGE2 to maintain basellamelar polarity, to maintain proper surfactant secretion, and homeostasis in alveoli. However, when fibrotic invades, new manifested myofibroblast do not secrete PGE2 and cannot sustain alveoli pockets (114).

Local inhalation treatment to the lungs provides maximal dose at the targeted site bypassing first metabolism, rapid clearance and systemic toxicity. Inhalational liposomes with PGE2 already showed great improvement treating pulmonary fibrosis versus intravenous treatment. Inhalation treatment prepared for nebulization is regarded safe to use because they are water base. Also they show less irritation as suppose to the dry powder in the respiratory tract.

Nanoparticles, such as liposomes, have been used for improving delivery of the drug by making them less cytotoxic and more stable. PGE2 in physiological fluid is very unstable with a short half-life (114). It is rapidly degraded to the other forms of eicosanoid family of mediators. Therefore, incorporation in the lipid nanoparticles increases the life span of PGE2.

In addition nanoparticles can deliver combinatorial treatments by being able to carry different drugs. Another therapeutic agent, siRNA, needs to be protected in nanoparticles. siRNA therapy provides a good promise in nucleic-acid-based therapeutics. As PGE2, siRNA can be relatively unstable if not modified. Also siRNA has negative charge and high molecular weight (13,000) which prevents it penetrating cells (30, 118, 239). Therefore, it remains challenging to deliver siRNA efficiently. siRNA can be used to silence the highly expressed genes such MMP3, CCL12, and HIF-1a that were observed in the previous studies.

In this study, a different class of biodegradable solid lipid nanoparticles is evaluated for combinatorial drug delivery system. SLNs prepared from lipids that remain solid

at body temperature. Solid lipid nanoparticles have been utilized for imaging; drug carries with the benefits of using physiological lipids that are biodegradable and safe (178, 180, 240, 241). Despite its numerous utilizations, SLNs have not been thoroughly evaluated for the inhalational delivery of siRNA.

We propose new treatment for pulmonary fibrosis incorporating lipophilic PGE2 inside and siRNA on the hydrophilic side. Lipid nanoparticles can be used as drug delivery system that can be the potential treatment to meet both challenges. Utilization of nanoparticles engineered for slow and controlled release of functional PGE2 and siRNA may decrease the treatment frequency and increase patient compliance, and overall increasing patient compliance.

5.2 Materials and methods

5.2.1 Materials

Analytical grade methanol, chloroform, butanol were purchased from Fisher Scientific (Pittsburgh, PA). Precirol ATO 5, triasterin, Compritol 888 ATO was kindly donated by Gattefosse (Paramus, NJ). Bleomycin was purchased from Sigma Aldrich (Ronkonkoma, NY). Tween 80, Pluronic 68, and Tween 20 were purchased from Sigma-Aldrich (St. Louis, MO). Dimethyl sulfoxide (DMSO), sodium dodecyl sulfate (SDS), sodium hydroxide (10 N solution, 30% w/w), and phosphate buffered saline (PBS) were purchased from Fisher Scientific (Fair Lawn, NJ). SYBR® Gold nucleic acid gel stain was purchased from Life Technologies (Carlsbad, CA). 1,2-

distearoyl-s n-glycero-3-phosphoethanolamine-N-[Amino(Polyethylene Glycol) 2000] ammonium salt (DSPE-PEG-NH2), and soy L-α-phosphatidylcholine (soy PC) were purchased from Avanti Polar Lipids (Alabaster, AL). PGE2 was purchased from Selleckchem (Houston, TX).

5.2.2 Synthesis of SLN formulations

SLNs were prepared by hot melt homogenization method. Briefly, DSPE-PEG and soybean lecithin, and Precirol ATO 5 were dissolved in water solution of methanol:water 1:2 ratio with cosurfactant of butanol 0.5%. This mixture was allowed to heat to 70 °C and homogenized by high-speed homogenizer (PRO Scientific Inc., Oxford, CT) for 5 min. Then this mixture (receiver solution) was allowed to cool to 35-40 °C, at which point siRNA/DOTAP complex in CHF/MeOH/H2O solution was added. siRNA was solution was made by mixing 1:1 charge ratio of siRNA to cationic lipid DOTAP (5 wt% of siRNA). Then Compritol 888 ATO (10 mg/mL) and PGE2 (10mg/ml) dissolved in CHF was added to receiver solution. Organic solvents were allowed to evaporate under stirring for 8 h leading to nanoparticle precipitation at which point it was sonicated by an ultrasonicator (Model 120 Sonic Dismembrator, Fisher Scientific, Fairlawn, NJ) for 30 s. For SLN preparation without siRNA, addition step of siRNA to receiver solution was omitted. siRNA sequences that were carefully selected and studied are: MMP3 #1, (5‘-CGAUGAUGAACGAUGGACA-3’); MMP3 #2, (5‘-GUGGUACCCACCAAGUCUA-3’); MMP3 #3, (5‘-GAAAUCAGUUCUGGGCUAU-3’); CCL12 #1 (5’-CUCAUAGCUACCACCAUCA-3’); CCL12 #2, (5‘-CCAGUCACGUGCUGUUAUA-3’);

CCL12 #3 (5'-GGACCAUACUGGAUAAGGA-3'); HIF1A #1, (5'-AGAUGACGGCGACAUGGUU-3'); HIF1A #2, (5'-CUCCAAGUAUGAGCACAGU-3'); HIF1A #3, (5'-CAGUUACGAUUGUGAAGUU-3').

5.2.3 Nebulization

SLN, PGE2-SLN, siRNA-PGE2-SLN were subjected to nebulization using an ultrasonic nebulizer (eFlow, PARI Pharma GmbH, Starnberg, Germany). SLN formulations were added to the nebulization holding chamber. The mist was collected in a 50 mL centrifuge tube. Running time was adjusted for each nanoparticle formulations accordingly and all samples were run until the nebulizer was operated to dryness. The volume was adjusted to 10 mL. The nebulization efficiency (NE) was calculated as:

Samples were collected for particle size analysis using Malvern Zetasizer NanoSeries (Malvern Instruments, Malvern, UK). Each experiment was performed in triplicate.

5.2.4 Stability during nebulization

The stability of various SLN formulations was studied for a month. Nanoparticles size and zeta potential and drug encapsulation was measured over time intervals.

Also SLNs concentration remained in the nebulizer reservoir during nebulization time were analyzed. Aliquots were withdrawn at scheduled time intervals for HPLC analysis respectively. The output of the nebulizer was examined for the weight loss before and after nebulization at time intervals. Each experiment was performed in triplicate.

The prostaglandin E2 concentrations were determined by the chromatography system consisted of a Waters 1525 with a Binary pump, Waters 2487 Dual wavelength absorbance detector, Waters 717 plus autosampler, and Breeze workstation (Waters Corp, Milford, USA). The stationary phase consisted of a YMC-Pack ODS-AQ 312 (150×6.0 mm ID, s-5 mm, 120A) column with a guard column. The mobile phase consists of a mixed solvent of 0.017 M phosphoric acid and acetonitrile (40:60) with an isocratic flow rate of 1.0 mL/min at 30°C. The average retention time for PGE2 was around 13 min. The percentage recovery was calculated. PGE2 was quantified at 235 nm.

5.2.5 Drug loading (DL) and encapsulation efficiency (EE)

Due to the high hydrophobic natures of PGE2, the amount of free drugs in the water phase drug is negligible. In order to measure the amount of encapsulated drugs, the SLN formulations were mixed with 4× volume of methanol and centrifuged at 3,500 rpm for 15 min. The supernatant was collected and the concentration of PGE2 was analyzed as described above. The DL and EE were calculated using the following equations:

Where: , and denote weight of drug encapsulated within SLNs, weight of drug added during synthesis, and weight of lipids (Precirol ATO 5, lecithin, Compritol 888 ATO), respectively.

5.2.6 In vitro siRNA release

siRNA encapsulation and sustained release from SLN was performed on SLN dispersed in PBS or PBS with 1% PF68 in 10 ml flask at 37C. At time intervals 500 µl was collected and centrifuged for 3 min at 13,200 rpm to collect SLN, while volume was replenished by equal amount of PBS. The suspension was added to SYBERGOLD (1:500) dilution. Fluoresecent intensity was measured and compared to standard curve at 537nm. The encapsulation ratio is calculated by 100×(siRNA mass)/(total mass of SLN complexation). Then this amount was counted as 100% of cumulative release.

5.2.7 Cell Culture

Human lung (A549), CRL-1490, and Chinese hamster ovary cells (CHOK1) were

purchased from ATCC (Manassas, VA). The A549 cells were grown in RPMI 1640 medium (Lonza, Walkersville, MD) supplemented with 10% fetal bovine serum (Life Technologies, Carlsbad, CA) and 1.2 mL/100 mL penicillin-streptomycin (Life Technologies, Carlsbad, CA). CHO-K1 cells were grown in F12-K medium supplemented with 10% fetal bovine serum (Life Technologies, Carlsbad, CA). CRL-1490 cells were grown in MEM media with 10% fetal bovine serum from Lonza, Walkersville, MD. All cells were grown in a humidified atmosphere of 5% CO2 (v/v) at 37 °C. All experiments were performed on the cells in the exponential growth phase.

5.2.8 Cellular internalization

Nanoparticles were incubated with lung epithelial cells A549 and CRL-1490 cells. A549 cells were seeded at a density of 10^5 cells/well in 6 well-plates at 37 °C and 5% CO_2 for 24 h. Cells were incubated with nanoparticles for 24 h with 50 µL of SLN combinations. SLN with fluoresein (absorption 322n, emission 515nm) and/or with siGLO(emission at 565 nm). Afterwards, the medium was removed from each well, cells were washed with DPBS buffer, and fresh medium was added to each well. Cell nucleus was stained with DAPI (emission at 461 nm). Fluorescent microscopic visualizations were performed on Leica TCS SP2 AOBS confocal laser scanning microscope (Leica Microsystmes, Wetzlar, Germany).

5.2.9 Cytotoxicity and Genotoxicity

The cytotoxicity was determined by a modified MTT (3-(4,5-dimethylthiazol-2-yl)-2,5-diphenyltetrazolium bromide) assay as previously described (242). Briefly, A549 cells were seeded in a 96 well/plate at a density of 10×10^4 cells/well, and allowed to attach to the wells for 24 h. Then, cells were maintained for predetermined time period of 1-3 days at different concentrations of SLN formulations (0.1-5.0 mg/mL lipid concentration). Control cells were treated with an equal volume of fresh medium. After treatment, the medium was removed and replaced with fresh medium and MTT solution. After 3 h incubation, a solubilizing solution was added and the plates were stored 24, 48 hr. The absorbance intensity was measured the following day by Tecan infinite M200Pro (Grudig, Austria) at absorbance wavelengh of 570nm and corrected wavelengh of 630nm. The CometAssay® HT kit (Trevigen, Gaithersburg, MD) was used as a sensitive genotoxicity test for the detection of DNA damage induced by non-cytotoxic concentrations of SLNs as previously described (243). The extent of DNA breakage was calculated as the percent of DNA in the comet tail using CometScore™ software (TriTek Corp., Sumerduck, VA).

5.2.10 Gene expression

CRL-149, A549 cells were used for the studies of cytotoxicity, genotoxicity, cell internalization. Cells were incubated with different nanoparticle formulations with the concentration of 500 µg/mL for 72 h. Then cells were washed twice with PBS. RNA was isolated from cells using RNeasy kit (Qiagen, Frederick, MA) following the

manufacturer's protocol. Further, RNA samples were subjected to RQ1 RNase free DNase treatment at 37 °C for 30 min to avoid genomic DNA contamination. Then 3 µg of each RNA were subjected to quantitative polymerase chain reaction to convert following Qiagen Protocol. First, mRNA was converted to cDNA and diluted with nuclease free water. Quantitative PCR was performed using SYBER Green Master Mix as detection agent. Fold change of the gene expression was measured using SABioscience internet software which compares the expression of testing genes with that of housekeeping genes and expresses fold change in gene expression as $\Delta\Delta$Ct values ($\Delta\Delta Ct = \Delta Ct_{treated} - \Delta Ct_{control}$). PCR specificity was verified by melting curve and gel electrophoresis.

5.2.11 Statistical analysis

Data were analyzed using descriptive statistics and single factor ANOVA, and are presented as a mean ± SD from five to ten independent measurements. We analyzed data sets for significance with Student's t test and considered *P* values of less than 0.05 as statistically significant.

5.3 Results

5.3.1 Physicochemical characterization of SLNs

SLN formulations (SLN, PGE2-SLN, siRNA-SLN) had similar size distribution profiles in the range of 120-150 nm. SLN with siRNA were slightly bigger than 150

nm. The SLNs were very uniform as seen with their narrow size distribution (Fig. 5.1). In addition, nanoparticles showed relatively low polydispersity index (PDI) indicating high stability of the nanoparticles at desired size range and low level of agglomeration. The uniformity and stability of the nanoparticles makes them more robust when they are subjected to shear forces during nebulization and more consistent lung deposition in deeper airways.

5.3.2 Effects of nebulization on particle size

There are several parameters to take under consideration when determining optimal therapeutic efficacy of inhalation formulations. The design of nebulizer and its respective flow rate is very important. In addition, drug formulation is a critical factor in successful delivery of the therapeutic agent to the target region of the lungs. Solid lipid nanoparticles can be designed to deliver therapeutic agents without having detrimental effects on its physical stability and loading efficiency by the shear forces that are generated by extrusion through the jet orifice.

In our study, SLNs formulations were compared before and after nebulization. The size and PDI before nebuization were 120±11nm and 0.11±0.045, and after nebulization 135±15nm and 0.2±0.05, which shows no obvious destructions from the shear forces applied (Fig. 5.1). However, the size and PDI in the mist seemed to be broader due to possible partial agglomeration.

5.3.3 Drug loading and encapsulation efficiency

It is known that solid lipid nanoparticles are highly effective in incorporating lipophilic drugs into its lipid core. PGE2 is a lipophilic molecule that has a very short half-life. However, we found that SLNs protected encapsulated PGE2 against degradation or leakage during inhalation (Fig 5.2). PGE2-SLNs were studied for encapsulation efficiency. PGE2 encapsulation efficiency was 100 % due to its readily miscibility and solubility into the lipid core during preparation. An optimal drug loading was found to be around 5%.

5.3.4 siRNA loading and encapsulation efficiency

SLNs containing siRNA were analyzed for the encapsulation efficiency of nucleic acids. After the nanoparticles were prepared, they were subjected to dialysis overnight. Then siRNA-SLNs formulations were analyzed using fluorescent dye SYBRGold for encapsulation efficiency. It was found that roughly 85% of siRNA are efficiently encapsulated by SLNs. Then sustained release of siRNA was evaluated in PBS (pH 7.4) using surfactant Pluronic 68. Samples were taken at the designated time intervals and evaluated by SYBRGold for siRNA release. We found that initially there was a burst release of approximately 20% of siRNA. After thus initial burst, a more gradual and sustained release was registered that reached a plateau at approximately 75% of encapsulated dose of siRNA (Fig. 5.3). When the cumulative release reached the plateau, nanoparticles were subjected to chloroform, then diluted with water, and remaining of siRNA was released. Release of the remaining

siRNA can be achieved more readily in vivo physiological lung fluids consisted of biodegradable enzymes, such as lipases.

5.3.5 SLN Cytotoxicity and Genotoxicity

The cytotoxicity of synthesized delivery systems was studied on A549 cells with various SLN formulations by the MTT assay. A549 cell line was employed for cytotoxicity studies because this cell line commonly used for representing structural and biochemical properties of human type II epithelial cells. Secondly, prostaglandin E2 is expected to have positive therapeutic effect on epithelial cells rather than fibroblasts. Therefore, we did not have to employ SLNs to fibroblasts nor measure cytotoxicity. However, briefly studies showed that MTT assay cannot be performed on fibroblast cells due to their metabolic mechanism.

A549 cells were subjected to SLN, PGE2-SLN, siRNA-SLN, PGE2-siRNA-SLN treatments for 24 h and 48 h. The viability of cells treated with SLN and PGE2-SLN was over 95% (Fig. 5.4). This indicates that the SLN and PGE2 have negligible cytotoxicity. In addition low doses of PGE2 are safe and beneficial for alveolar epithelial cells. However, there was slightly lower viability (85%) observed in cells treated with nanoparticles with siRNA.

Even if therapeutic show low cytotoxity and used in essentially non-toxic concentrations, they still potentially can induce genotoxic effects over the time when used repetitively. In most cases Genotoxicity is usually measured by the

quantitation of micronuclei formation after treatment with a test compound. The term micronucleus describes the small nucleus that forms whenever a chromosome or a fragment of a chromosome is not incorporated into one of the daughter nuclei during cell division. Testing for micronucleus formation is used to screen for potential genotoxic compounds. After cytotoxicity analysis, we study genotoxicity of the synthesized nanoparticles in concentrations closed to their IC_{50} doses. The commercially available COMET Assay was performed to verify genotoxicity of SLN. During this assay, micronuclei appear as tails on the slide images after electrophoresis. Hydrogen peroxide was used as the positive control and induced a median of 50% DNA in the tail. The negative control showed a median of approximately 25% DNA in the comet tail, which can be considered the normal genetic makeup of non-treated cells (Fig. 5.5). At non-cytotoxic concentrations, treatment with SLNs resulted in approximately 37% of DNA in the tail that was substantially less when compared with the positive control.

5.3.6 Cellular internalization

Fibroblasts were used to study of cellular internalization of the SLN nanoparticles (SLN-PGE2-siRNA). In these srudies, fluorescently labeled commercially available siGLO siRNA was used. Cells were incubated with nanoparticles overnight. After the incubation, cells were washed with PBS and incubated with DAPI for nucleolus staining. Cellular internalization was analyzed by a confocal microscope. We found that SLN nanoparticles were efficiently internalized by the cells (Fig. 5.6).

5.3.7 Gene expression

A549 and CRL-1490 cells were used for gene expression analysis and were treated with 10 µg/mL of bleomycin. Control cells were treated with fresh media. Upregulation of CCL12 gene was registered in CRL-1490 cells treated with bleomycin (5.6 times) and MMP3 gene (6.87 times) (Fig. 5.7). Since fibroblasts increase the expression of profibrotic factors MMP3 and CCL12, these fibroblasts were incubated with SLNs with siRNAs formulations. Three different sets of each MMP3, CCCL12, and HIF-1a siRNAs were evaluated for the best silencing efficiency (Fig.5.8). After analysis one sequence for each gene was chosen for future *in vivo* studies.

5.4 Discussion

Currently there is no effective treatment for pulmonary fibrosis. Consequently, the development of novel therapeutic approaches for treatment of this disease represents an urgent and important task. In addition, the delivery route of therepautics is very important for treatment of pulmonary disorders. As the fibrotic tissue is developed in the lungs, one could not expect a high efficacy of drugs after their systemic administration. Therefore, topical inhalation treatment not only can be more efficient but also may limit adverse side effects upon other healthy organs. With new innovative approaches in inhalational devices, better formulations, and their evaluations, many drugs are being repurposed for inhalational treatment.

Inhalation therapy is commonly used for respiratory diseases such as asthma and chronic obstructive pulmonary disease. Tobramycin Inhalation solution (TOBI®) is administered by nebulization for treatment of Pseudomonas infection and break down DNA in mucus in cystic fibrosis patients, respectively (244). In addition, inhalational route of administration was considered to be effective for the systemic administration of unstable and hard to deliver macromolecules such as insulin (245, 246). Recently, afrezza, inhalational insulin, was approved for treating diabetes that demonstrates faster onset of action and more patient compliance when compared with traditional injectable insulin (247).

During inhalational formulation studies, shear force generated from jet orifice has a detrimental effect on physical characteristics. Stability concerns and leakage problems are common for many nanoparticle formulations (248). For others, such as polymers, cytotoxicity becomes a primary concern (249). Therefore, increasing attention has been directed at lipid nanoparticles such as SLN for pulmonary delivery system.

SLN have been shown in present study to be able to delivery both lipophilic drug (PGE2) and siRNA into alveolar epithelial cells and fibroblasts. Also SLN formulations showed good nebulization efficiency. As in our previous studies, efficient delivery of liposomal PGE2 drastically alleviates bleomycin induced fibrosis in the mouse model. In addition, several new proteins were discovered to be highly upregulated during fibrogenesis: MMP3, HIF-1a, and CCL12. Fibroblast proliferation, migration, and differentiation into myofibroblasts depend on various growth factors, cytokines, and chemokines. CCL12 is a monocyte chemoattractant

protein-1 (MCP-1) that induces TGFβ1 and its process of procollagen gene expression (250, 251). Moore et al. studied the knock out CCL12 receptror mouse model (CCR2-/-) on developing mouse IPF (252). It was shown that CCR2-/- mice are protected from FITC-induced pulmonary fibrosis. In addition, only CCL12 was the main ligand from its CCL family responsible for the neutralization fibrogenesis. In our study it also showed that during bleomycin treatment fibroblast cells have 5 fold higher expression of CCL12. However, incubation with CCL12 siRNA in SLN drastically decreased the expression of CCL12 chemokine.

MMP3 is another factor that is upregulated in the fibrogenesis. It is responsible for the creation of the collagen matrix during fibrogenesis. It is also primarily expressed by fibroblast and myofibroblast (253). Silencing MMP3 also shows slowdown of the proliferation of the fibroblasts. Another common factor that is present during hypoxia and injury is HIF-1α (97, 254, 255). It is also observed in the elevated expression during IPF. HIF-1a expression was also evaluated by SLN treatment.

It can be concluded that proposed novel combinatorial treatment of IPF by inhalation delivery of efficient and stable nanoparticles containing PGE2 and siRNA can potentially represent an innovative approach for effective cure of this disease or at least limitation of its manifestations.

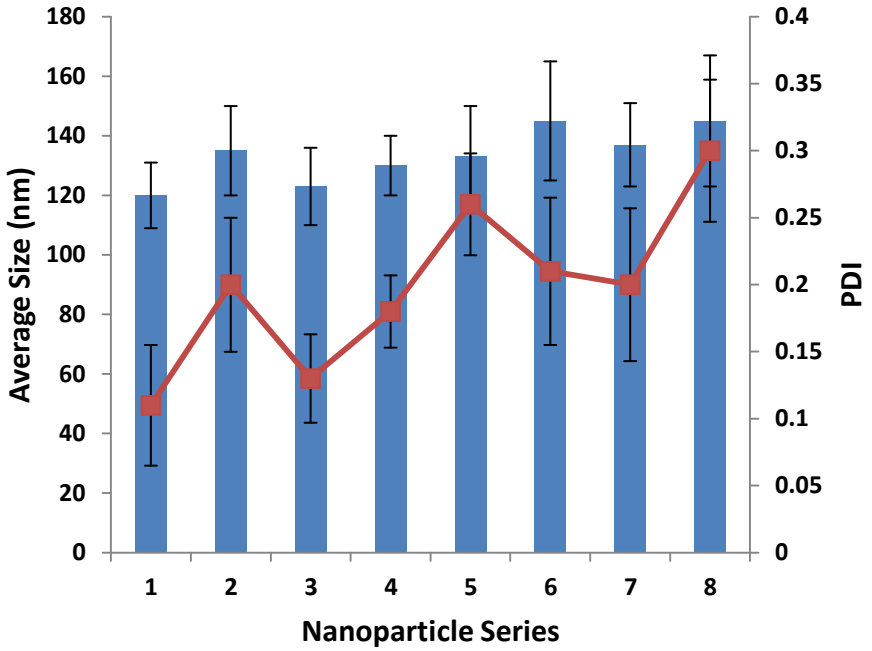

Fig.5.1. Changes in average size and polydispersity index on SLN formulations. 1- empty SLN, 2-empty SLN after nebulization, 3- SLN with PGE2, 4- SLN with PGE2 after nebulization, 5- SLN with siRNA, 6- SLN with siRNA after nebulization, 7- SLN with combinatorial PGE2 and siRNA treatment, 8- SLN with combinatorial PGE2 and siRNA treatment after inhalation.

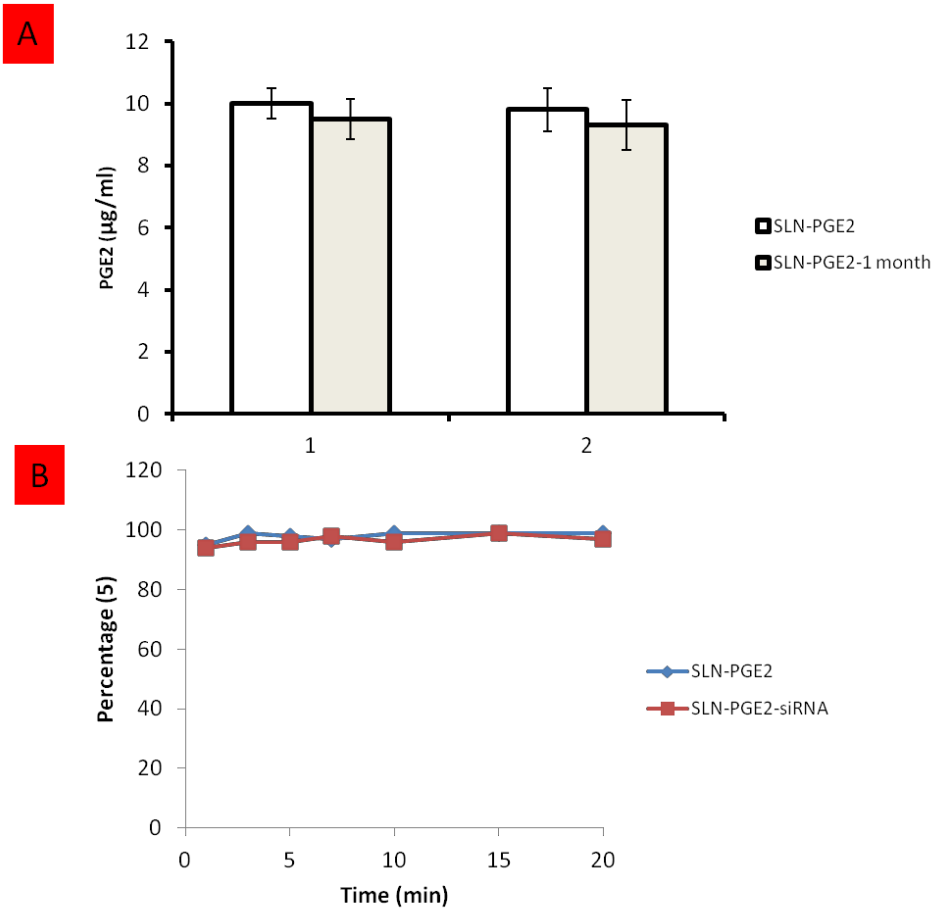

Fig. 5.2. Concentration of PGE2. A) Encapsulation efficiency of PGE2 before and after nebulization and after one month of storage. B) Nebulization efficiency over nebulization time period.

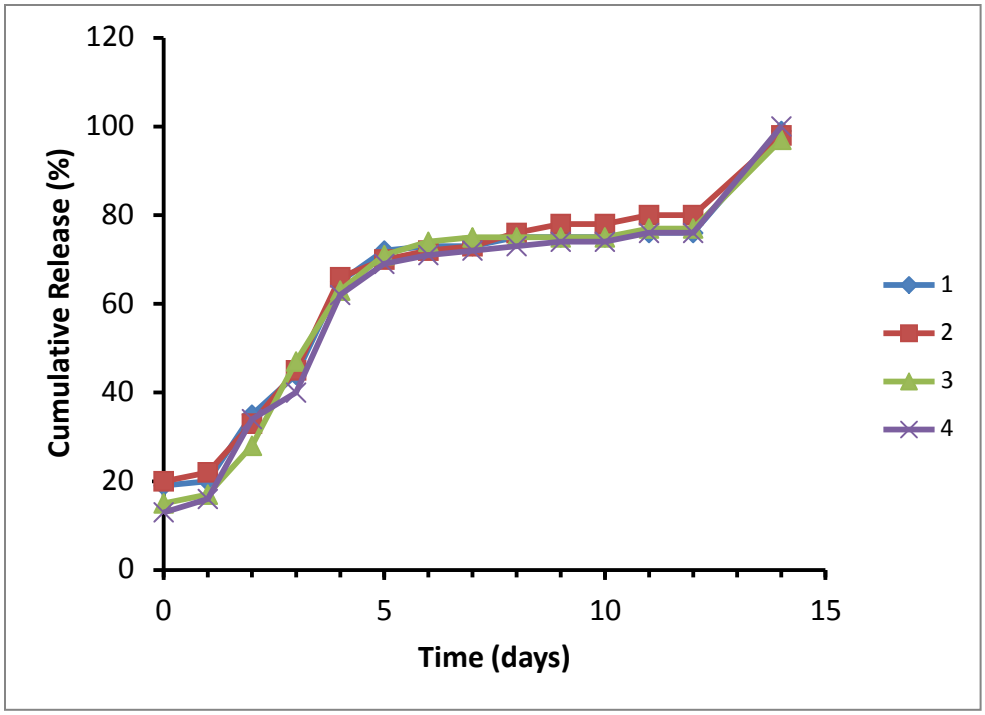

Fig.5.3. Cumulative Release of siRNA from. 1) SLN with 5wt% of MMP3 siRNA, 2) SLN with 5.1wt% of CCL12 siRNA, 3) SLN with 5 wt% of HIF-1α siRNA, 4) SLN with PGE2 and 5 wt% of MMP3 siRNA.

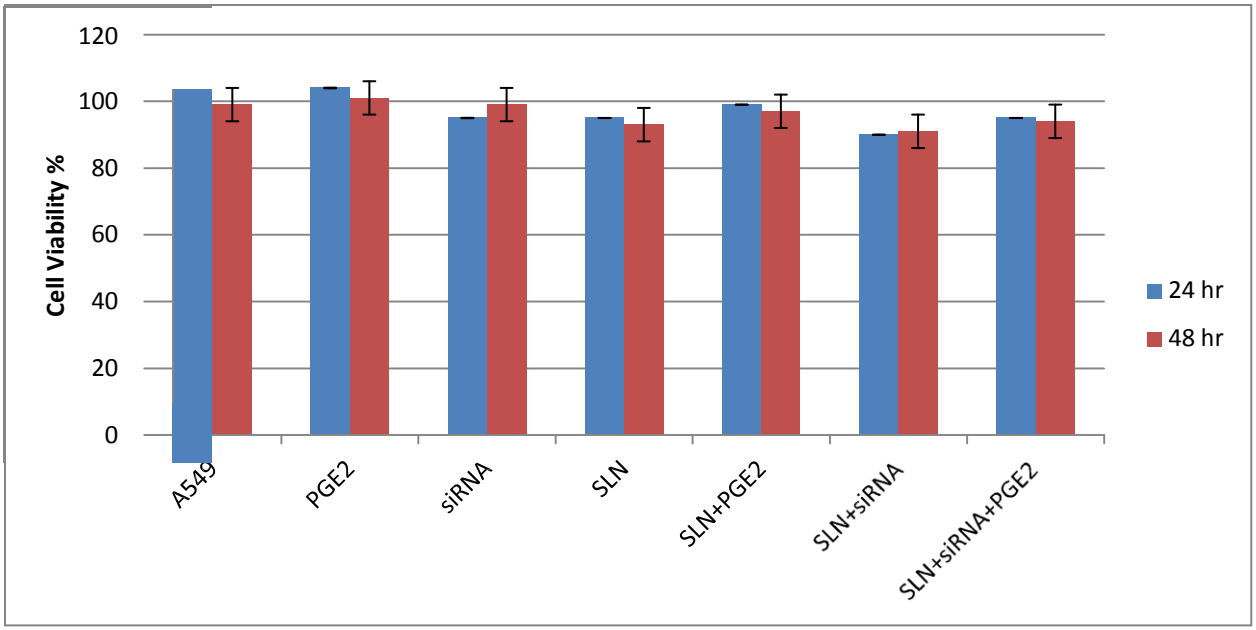

Fig.5.4. Cytotoxicity was investigated by incubating nanoparticles with A549 cells. In the experiments, the cells were exposed to dosages equivalent to the number of particles present in a 100 µg/ml solution of parent SLN. Cell viability was measured for free A549 cells, equivalent PGE2, equivalent free siRNA, 100 µg/ml SLN 102 µg/ml of SLN+PGE2, 100 µg/ml of SLN+siRNA, 100 µg/ml of SLN +PGE2+siRNA.

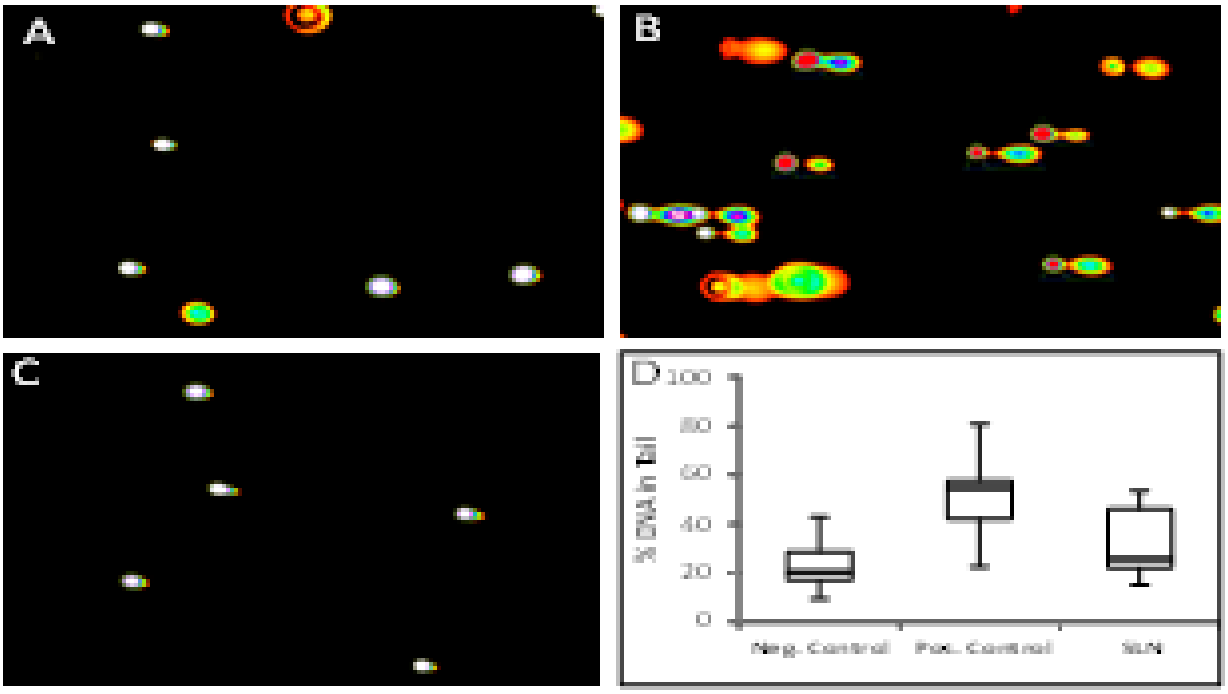

Fig.5.5. Genotoxicity of SLN was evaluated by Comet Assay. CHOK-1 cells were incubated with SLN within 24 h.

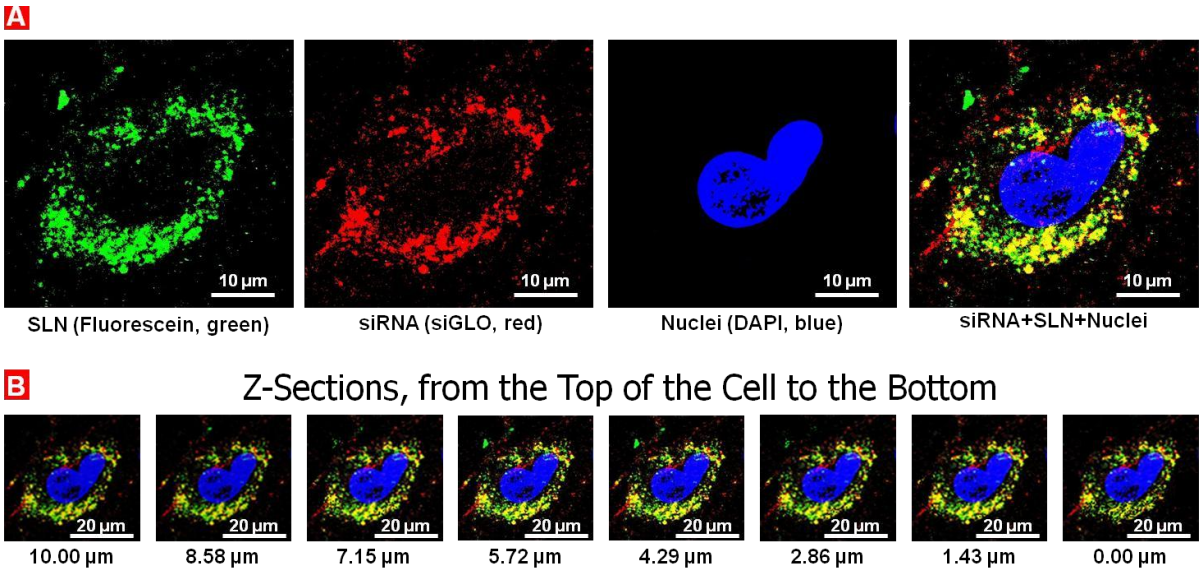

Fig.5.6. Cellular Internalization (A) and co-localization (B, z-Sections) of siRNA (red fluorescence) delivered by SLN (green, fluorescnece). Human lung fibroblasts (CCD-34Lu) were incubated for 24 h and visualized under confocal microscope (Leica G-STED SP8). Superimposition of red and green colors gives yellow color.

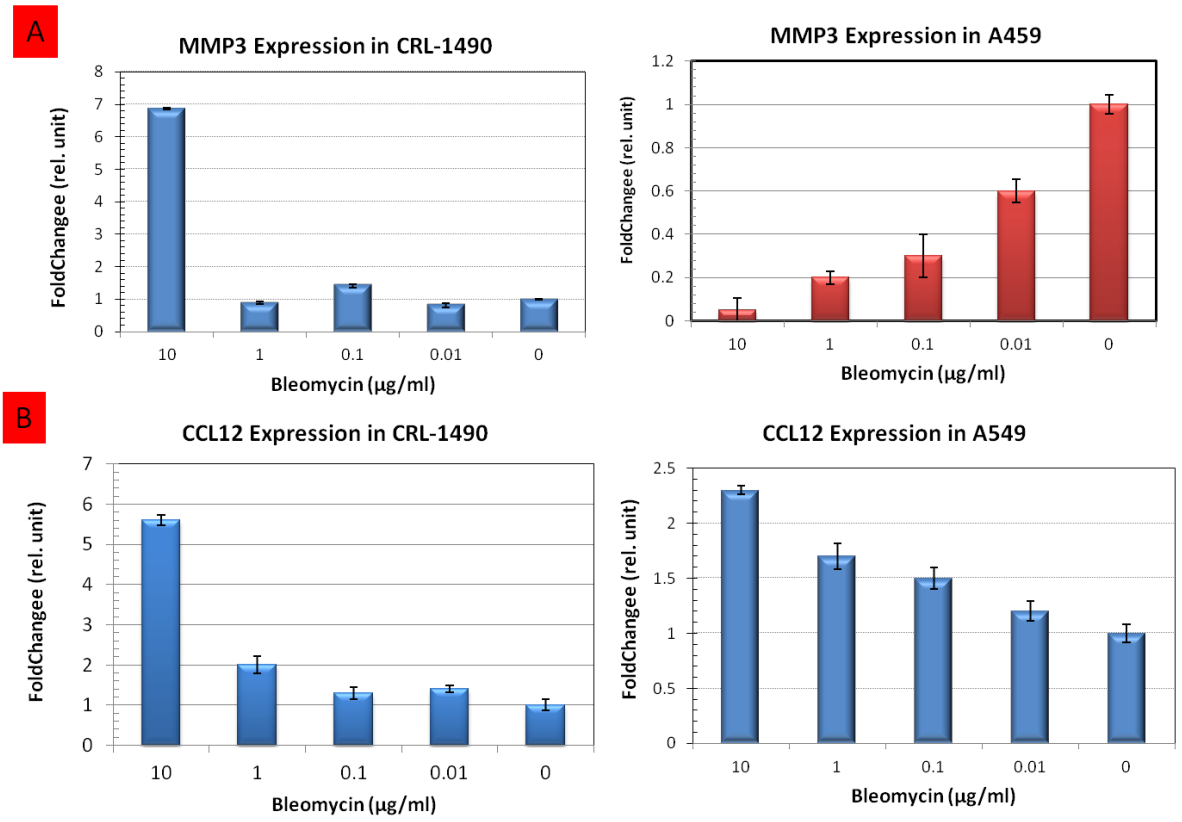

Fig. 5.7. *In vitro* expression of MMP3 and CCL12 genes. A549 and CRL-1490 cells incubated with 10-0.01 µg/ml bleomycin. A) qPCR of MMP3 gene in A549 and CRL-1490 cells treated with bleomycin B) qPCR of CCL12 gene in A549 and CRL-1490 cells treated with bleomycin.

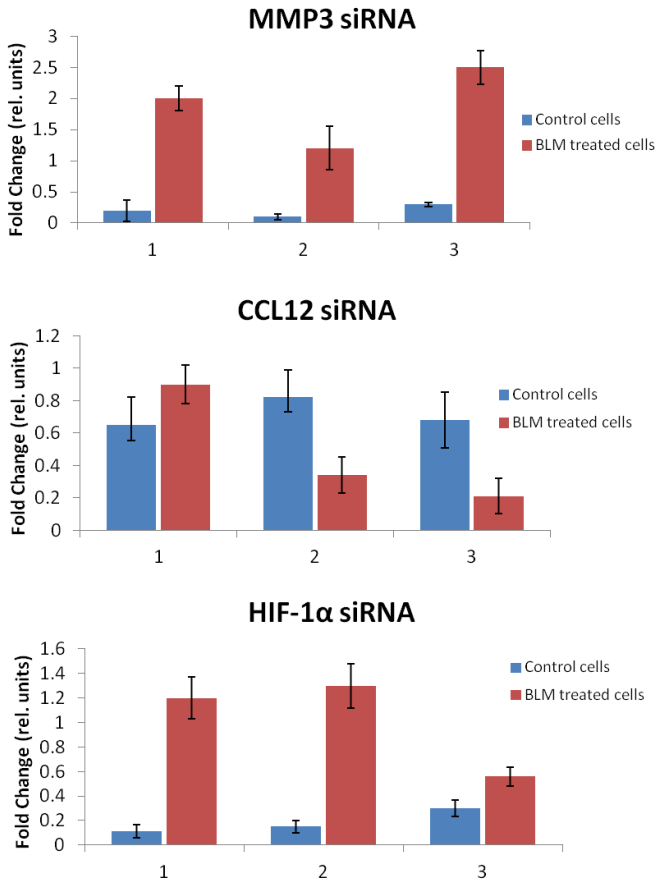

Fig.5.8. A549 cells were incubated with SLN with three different sequences of siRNA to see which siRNA sequence has better silence effect. siRNA -1, siRNA-2, siRNA-3 for HIF1-a. siRNA-1, siRNA-2, siRNA-3 for MMP3, and likewise for CCL2. One of each was selected for in vivo studies.

6 TO STUDY NANOSTRUCTURED LIPID CARRIERS FOR INHALATION CO-DELIVERY OF TWO DRUGS FOR INHIBITION OF TRANSMEMBRANE CONDUCTANCE REGULATOR (CFTR) PATHWAY OF CYSTIC FIBROSIS

6.1 Introduction

Cystic fibrosis (CF) is debilitating disease that affects newborns very shortly after birth. Early diagnosis and treatment with supportive therapies and antibiotics have prolonged survival to almost 40 years of age. However, there is no cure for the disease and finally patients succumb to worsening prognosis and ultimately mortality. The primary cause of CF is mutation of the cystic fibrosis transmembrane conductance regulator (CFTR) gene, which plays a key role in homeostasis. The CFTR protein is a chloride ion transporter and also has a role in transport of sodium ions. There are over 1,800 mutations in the CFTR gene identified (256, 257). The most common mutation is the F508del, which results in the deletion of a phenylalanine residue at the 508 position (2, 258, 259). The severity of CF symptoms is correlated with decreased activity of the CFTR protein. Because of the ubiquitous nature of the CFTR protein, patients lack the ability to recover chloride in sweat and suffer from many pancreatic and reproductive deficiencies (32). However, the most problematic symptoms resulting in increased morbidity and mortality are attributed to respiratory manifestations. The lack of chloride regulation results in production of viscous and purulent mucus, which cannot be efficiently cleared from

the lungs and provides breeding ground for bacteria. Patients experience shortness of breath, chest pain, which severely affects quality of life.

The discovery of the CFTR mutations spearheaded the development of drugs for CF. The first approved drug, ivacaftor, targets the G551D mutation, which affects 4-5% of patients (260-263). It is also being studied in combination with lumacaftor, which targets the F508del mutation seen in 80% of CFTR mutations (136, 258, 259, 264). Patients may be heterozygous for CFTR gene mutation and combination treatment may result in optimal outcomes.

Because morbidity and mortality are mostly due to respiratory manifestations, an inhalation delivery of these targeted CFTR drugs may substantially improve treatment efficacy and outcome. Furthermore, this approach would allow for the delivery of the smallest dose to achieve improved respiratory function. In addition, local inhalation delivery directly to the site of action can enhance a drug accumulation in the lungs and significantly limit possible adverse side effects of the treatment upon unaffected organs. Different nanocarriers may potentially be employed as drug carriers for the inhalation delivery. Biocompatible and biodegradable nanocarriers have been used for 1) targeting drug to the site of action, 2) reducing toxicity of the drug to other organs, and 3) controlled drug delivery and sustained release. Several nanomedicines are already currently used in the clinic such as liposomal doxorubicin, liposomal amphotericin B, albumin bound paclitaxel (265-267). Currently there are numerous drug delivery systems being evaluated for preclinical studies, such as dendrimers, liposomes, solid lipid

nanoparticles, various polymers with combinations of PEG. Recently, several attempts have been made in order to develop nanoparticle-based systems for inhalation delivery of various drugs (256, 268-277). Nanostructured liquid carriers (NLCs) are relatively new colloidal drug delivery system which is composed of physiological lipids that are biocompatible and biodegradable. One of the main advantages of NLCs is that they can readily incorporate lipophilic drugs, improve drug stability, and have higher safety due to avoidance of organic solvents in the manufacturing process.

The application of NLCs as drug carriers is promising especially for pulmonary administration. NLCs are relatively stable and can be used readily for nebulization. They can be synthesized to achieve a desirable size in order to penetrate well into deepest regions of the lungs after the inhalation delivery (275). The nanoparticle formulation can also allow for controlled release of drug as well as penetration through the mucus. To ensure biocompatibility, the lipid composition of NLCs can reflect that of endogenous lipids.

The objective of our studies was to design NLCs loaded with new drugs ivacaftor and lumacaftor for pulmonary treatment of cystic fibrosis. NLCs formulation was attenuated to have optimal size, highest loading efficiency, efficient nebulization, and prolonged release. Furthermore, several physiological aspects such as efficient mucus penetration and cellular internalization, safety of epithelial cellular layer and efficient restoration of CFTR at the membrane by combinatorial treatment of ivacaftor and lumacaftor drugs were also considered.

6.2 Materials and methods

6.2.1 Materials

Precirol ATO 5 was kindly donated by Gattefosse (Paramus, NJ). Tween 80 and squalene were purchased from Sigma-Aldrich (St. Louis, MO). Dimethyl sulfoxide (DMSO), sodium dodecyl sulfate (SDS), sodium hydroxide (10 N solution, 30% w/w), phosphate buffered saline (PBS) were purchased from Fisher Scientific (Fair Lawn, NJ). SYBR® Gold nucleic acid gel stain was purchased from Life Technologies (Carlsbad, CA). Isopropyl myristate (96%) was purchased from Acros Organics (Pittsburgh, PA). 1,2-distearoyl-s n-glycero-3-phosphoethanolamine-N-[Amino(Polyethylene Glycol) 2000] ammonium salt (DSPE-PEG-NH2), and soy L-α-phosphatidylcholine (soy PC) were purchased from Avanti Polar Lipids (Alabaster, AL). Ivacaftor and lumacaftor were purchased from Selleckchem (Houston, TX).

6.2.2 Synthesis of NLC formulations

NLCs were prepared by hot melt homogenization method (Fig. 5.1) previously developed by our group (275). High shear homogenization and sonication were used to reduce particle size. Further NLCs were allowed to solidify by cooling under gentle stirring. Varying different lipid/emulsifier concentrations and sonication/homogenization time and speed optimized production of NLCs. Ivacaftor and lumacaftor were first dissolved in DMSO and added to a lipid phase consisting of 100 mg Precirol ATO 5 (solid lipid), 100 mg isopropyl myristate or 100 mg

squalene (as liquid lipid), and 5 mg soy PC. The aqueous phase was composed of 250 mg Tween® 80 and 10 mg DSPE-PEG-NH_2 in 10 mL deionized water. Both phases were heated to 10 °C above the melting point for Precirol ATO 5 in a silicone oil bath. Afterwards the hot lipid phase was added dropwise to the aqueous phase. This mixture was homogenized at 12,000 rpm for 5 min using a high-speed homogenizer (PRO Scientific Inc., Oxford, CT). The formed emulsion was further subjected to ultrasonication (Model 120 Sonic Dismembrator, Fisher Scientific, Fairlawn, NJ) for 5 min at 3 W while being cooled to 4 °C in ice. The NLC emulsion was purified by overnight dialysis (membrane MWCO of 15 kDa) in deionized water at 4 °C overnight. The purified NLC emulsion was stored at 4 °C. Control NLCs were prepared using equal volume of DMSO instead of ivacaftor and lumacaftor. Optimized formulations are presented in Table 5.1.

6.2.3 Characterization of NLCs

The size distributions and zeta potentials of control and drug-loaded NLCs were characterized by Malvern Zetasizer NanoSeries (Malvern Instruments, Malvern, UK). Samples were diluted in deionized water and measurements were performed at 25 °C. The parameters were measured five times and mean values were calculated. The particle morphology was evaluated by scanning electron microscopy (SEM; model S-3400N, Hitachi, Tokyo, Japan). Samples were prepared by air-drying a drop of nanoparticles in water on 300-mesh copper grid. During microscopic

visualization, sample in the chamber was maintained at -70 °C by circulating liquid nitrogen around the chamber.

6.2.4 HPLC Method for Ivacaftor and Lumacaftor

HPLC was performed to establish calibration curves for both drugs and to measure concentration of ivacaftor and lumacaftor in NLCs. The chromatography system consisted of a Waters 1525 with a Binary pump, Waters 2487 Dual wavelength absorbance detector, Waters 717 plus autosampler, and Breeze workstation (Waters Corp, Milford, USA). The stationary phase consisted of a C8 Xterra® MS (250 mm 4.6 mm, 5 µm; Waters Corp, Milford, USA) column with a guard column. The mobile phase was 0.01% phosphoric acid (0.01%):acetonitrile (30:70) with an isocratic flow rate of 1.0 mL/min at 30 °C. The average retention time for ivacaftor was around 6.6 min and for lumacaftor was 13.3 min. The percentage recovery was calculated. Both drugs were quantified at 228 nm.

6.2.5 Drug loading (DL) and encapsulation efficiency (EE)

Due to the high hydrophobic natures of ivacaftor and lumacaftor, the amount of free drugs in the water phase drug is negligible. In order to measure the amount of encapsulated drugs, the NLC formulations were mixed with 4× volume of methanol and centrifuged at 3,500 rpm for 15 min. The supernatant was collected and the concentrations of both drugs were analyzed as described above. The DL and EE were calculated using the following equations:

Where: , and denote weight of drug encapsulated within NLCs, weight of drug added during synthesis, and weight of lipids (Precirol ATO 5 and isopropyl myristate/ squalene), respectively.

6.2.6 In vitro release

Drug release from NLCs was evaluated in phosphate buffer saline (PBS) and simulated lung fluid (SLF) at pH 7.4, 100 mL, at 37 °C over 48 h. Samples were placed in Spectra/Por® (Spectrum Laboratories, Rancho Dominguez, CA). Sample dialysate was withdrawn at 2 h, 4 h, 6 h, 8 h, 10 h, 24 h, 48 h intervals. Then sample NLCs were mixed with methanol and centrifuged. The supernatant was collected and evaluated by HPLC.

6.2.7 Cell Culture

Human lung (A549), CRL-4015 (CuFi4), and Chinese hamster ovary cells (CHOK1) were purchased from ATCC (Manassas, VA). The A549 cells were grown in RPMI

1640 medium (Lonza, Walkersville, MD) supplemented with 10% fetal bovine serum (Life Technologies, Carlsbad, CA) and 1.2 mL/100 mL penicillin-streptomycin (Life Technologies, Carlsbad, CA). CHO-K1 cells were grown in F12-K medium supplemented with 10% fetal bovine serum (Life Technologies, Carlsbad, CA). CRL 4015 cells were grown in serum free BEBM media supplemented with SingleQuot additives (BEGM Bullet Kit, CC-3170) from Lonza, Walkersville, MD, and with 50 µg/mL G-418 (gentamycin-amphotericin B) from Life Technologies, Grand Island, NY. All cells were grown in a humidified atmosphere of 5% CO2 (v/v) at 37 °C. All experiments were performed on the cells in the exponential growth phase.

6.2.8 Cellular internalization

Nanoparticles were incubated with lung epithelial cells A549 and CuFi4 cells. A549 cells were seeded at a density of 10^5 cells/well in 6 well-plates at 37 °C and 5% CO_2 for 24 h. Cells were incubated with nanoparticles for 24 h with 50 µL of NLC-drug samples. Afterwards, the medium was removed from each well, cells were washed with DPBS buffer, and fresh medium was added to each well. Cell nucleus was stained with DAPI (emission at 461 nm).

6.2.9 Cytotoxicity and Genotoxicity

The cytotoxicities of NLC formulations were assessed using a modified MTT (3-(4,5-dimethylthiazol-2-yl)-2,5-diphenyltetrazolium bromide) assay as previously described (242). Briefly, A549 cells were seeded in a 96 well plate at a density of 10,000

cells/well. Twenty-four hours after seeding, different concentrations of NLC formulations (0.1-5.0 mg/mL lipid concentration) were added to the cells. Control cells were treated with an equal volume of fresh medium. Twenty-four hours after treatment, the medium was removed and replaced with fresh medium and MTT solution. After further 3 h incubation, a solubilizing solution was added and the plates were stored overnight. The absorbance intensity was measured the following day by Tecan infinite M200Pro (Grudig, Austria). The CometAssay® HT kit (Trevigen, Gaithersburg, MD) was used as a sensitive genotoxicity test for the detection of DNA damage induced by non-cytotoxic concentrations of NLCs as previously described (243). The extent of DNA breakage was calculated as the percent of DNA in the comet tail using CometScore™ software (TriTek Corp., Sumerduck, VA).

6.2.10 Nebulization

NLCs in deionized water were nebulized using an ultrasonic nebulizer (eFlow, PARI Pharma GmbH, Starnberg, Germany). The stock NLC suspension was diluted and 10 mL were added to the nebulization holding chamber. The mist was collected in a 50 mL centrifuge tube. The volume was adjusted to 10 mL and the particle size was measured as above described.

6.2.11 Gene expression

CRL-4015 cells were seeded in 6-well plates at a density of 1×10^5 cells/well. After attachment cells were incubated with different nanoparticle formulations with the

concentration of 500 µg/mL for 72 h. Then cells were washed twice with PBS. RNA was isolated from CRL-4015 cells using RNeasy kit (Qiagen, Frederick, MA) following the manufacturer's protocol. Further, RNA samples were subjected to RQ1 RNase free DNase treatment at 37 °C for 30 min to avoid genomic DNA contamination. Then 3 µg of each RNA were used to convert into cDNA following Qiagen Protocol. cDNA was diluted with nuclease free water. Five µL of each cDNA sample were added to each well in microAmp Optical 96 well reaction plate (Applied Biosystems). The reaction mixture was subjected to quantitative polymerase chain reaction (qPCR) using SYBR® Green Master Mix as a detection agent. SDS software (Applied Biosystems) was used to calculate difference in CFTR gene expression between each treatment by first normalizing the CFTR gene expression with that of β-actin, a housekeeping gene.

6.2.12 Statistical analysis

Data were analyzed using descriptive statistics and single factor ANOVA, and are presented as a mean ± SD from five to ten independent measurements. We analyzed data sets for significance with Student's t test and considered *P* values of less than 0.05 as statistically significant.

6.3 Results

6.3.1 Physicochemical characterization of NLCs

Various synthesized NLC formulations had similar size distribution profiles in the range of 150-200 nm. The NLCs were very uniform as seen with their narrow size distribution (Fig. 5.2A). The narrow size distribution is very important for the respiratory delivery because airway and lung deposition is heavily dependent on the size of the particles. Due to the nature of CF, drug-loaded particles need to reach deeper airways of the bronchioles and alveoli. SEM micrographs show particles in the size range of 100-200 nm that are in accordance with the size measurements by light scattering, spherical shape, smooth surface and homogeneous distribution (Fig. 5.2B).

6.3.2 Effects of nebulization on particle size

After nebulization, the NLCs were shown to be relatively stable and did not appreciably form agglomerates. The size distribution of nebulized NLCs was slightly wider and shifted towards the higher side (Fig. 5.2A). Whereas, the non-nebulized NLCs had a peak around 180 nm, the nebulized NLCs have a distribution peak around 215 nm. This may indicate a slight aggregation of small number of nanoparticles.

6.3.3 Drug loading and Encapsulation efficiency

Lipid drugs can be easily incorporated into the lipid core of the nanoparticles. Ivacaftor was encapsulated using different liquid lipids. At 10 mg ivacaftor dose, the encapsulation efficiency was 100% for both liquid lipids (Table 5.1). The highest drug loading registered in this study was equal to 5%. The drug loading depends on the solubility in the liquid lipid and the results show that ivacaftor has excellent solubility in squalene and isopropyl myristate.

6.3.4 NLC Cytotoxicity and Genotoxicity

The various NLC formulations using isopropyl myristate were shown to be safe for use. They did not exhibit any cytotoxicity at NLC concentrations ranging from 0.01-1.0 mg/mL of lipids (Fig. 5.3A). At the highest concentration, the NLCs loaded with 5 mg ivacaftor were slightly less cytotoxic when compared with the other formulations, but the difference was not statistically significant. The commercially available COMET Assay was performed to ensure that non-toxic amounts of NLC did not damage cellular genetic material. On this assay, damaged nucleic acid is broken into smaller fragments and appears as tails on the slide images after electrophoresis. The negative and positive controls set the baseline genetic damage and the upper level of highly induced DNA damage, respectively. Hydrogen peroxide was used as the positive control and induced a median of 50% DNA in the tail. The negative control showed a median of approximately 25% DNA in the comet tail, which can be considered the normal genetic makeup of non-treated cells (Fig.

5.3B). At non-cytotoxic concentrations, treatment with NLCs resulted in approximately 40% of DNA in the tail.

6.3.5 Gene expression

We have incubated CuFi-4 cells with various combinations of nanoparticles with the drug. Our results indicate that all tested nanoparticles containing the drug did not statistically significantly change CFTR gene expression.

6.4 Discussion

Inhalation therapy is commonly used for respiratory diseases such as asthma and chronic obstructive pulmonary disease. Tobramycin Inhalation solution (TOBI®) and dornase alfa (Pulmozyme®) are administered by nebulization for treatment of Pseudomonas infection and break down DNA in mucus in cystic fibrosis patients, respectively (244). Combination oral treatment of ivacaftor with lumacaftor is currently in Phase III clinical trials to assess efficacy in heterozygous patients as well as examine if there is any synergistic capacity of co-administration (278, 279).

Although ivacaftor and lumacaftor are leading the march of bringing CFTR-targeted agents to patients, there are certain enhancements that can further improve patient outcome and quality of life. Because CF-associated morbidity and mortality is predominately the result of pulmonary manifestations, local inhalation treatment may present the most effective route of drug delivery to improve efficacy and minimize

adverse side effects (280, 281). Ivacaftor is a substrate of CYP 3A4 and has the potential to interact with other medications patients may be taking. This represents a substantial concern in CF because patients started therapy during childhood and will likely require lifelong therapy increasing a probability of severe adverse side effects of the treatment (10, 282). Pulmonary administration would also minimize hepatic drug metabolism and drug-to-drug interactions. By eliminating the first- and second-pass liver drug metabolism after oral or systemic administration, respectively, local administration also has a potential to decrease the effective drug dose.

Although some drugs such as beta agonists can be administered as free molecules via nebulization, this usually results in significant amounts of drug loss. Encapsulation within a nanocarrier can ensure higher deposition of drug at the sites of disease. In addition, nanoparticles can allow for mucus penetration, controlled release, and protection of drug from the environment (7, 32, 281, 283). Lipid nanoparticles such as NLCs represent an attractive option as delivery vehicles for pulmonary drugs.

This investigation describes the development and preliminary evaluation of formulation of ivacaftor and lumacaftor as single drugs or their co-encapsulation within a NLC. It was found that the physicochemical properties of the NLCs were not affected by drug encapsulation. All formulations possessed similar narrow size distribution centered on 150 and 200 nm. The particles also possessed smooth surfaces and were of spherical shape. These properties were not significantly altered after nebulization, which indicates that NLC-based formulations may be highly suitable for the pulmonary administration by inhalation. Both drugs in doses of

5 and 10 mg and provided for 100% encapsulation efficiency. A lower dose was used to assess the feasibility of encapsulating the drugs using our synthesis method without affecting the physicochemical properties of the lipid matrix. Future studies needed to assess the maximum amount of drug incorporation into NLCs. It would be ideal to achieve as a drug loading as high as possible. The high drug loading efficiency would also lead to the decrease in the exposure to excipients on the respiratory system. With NLCs, the liquid lipid component enhances dry solubility and resides within the solid lipid matrix. It is better to use a spatially incompatible liquid lipid. Further studies are needed to compare squalene with isopropyl myristate. The liquid lipid also prevents burst release of drug, which may cause toxicity concerns. Combined with the sustained release nature of Precirol, we observed very little drug release. Furthermore, the cold sonication step may have resulted in Precirol being in a stable ß-form. In the unstable α-form, there would have seen release of ivacaftor (284). However, further studies during transition are needed to support this claims.

Since chronic therapy is required for CF patients, safety plays a very important role. The drug encapsulated NLC formulations were shown to be non-cytotoxic. Even at non-cytotoxic doses, the drug formulation may possess some detrimental effects, especially genotoxicity. Therefore, the COMET Assay was performed and showed that NLCs did not demonstrate significant genotoxicity. The safety profile of NLCs arises from the use of biocompatible lipid excipients. In addition, the synthesis of the NLCs does not require the use of organic solvents, as is the case of synthesizing other nanoparticle formulation. The formulations were stable in PBS buffer and

simulated lung fluid. The purulent mucus filled environment of CF lungs is a harsh environment for local drug delivery and a sturdy nanoparticle formulation must withstand the assault (283). The NLCs demonstrated attractive propensity to be internalized into cells. There were no statistically significant changes in CFTR gene expression in CF cells after treatment with NLC formulations containing the drug. This is not a surprising finding because neither drug works at the gene/mRNA level; rather they interact with the mutated CFTR protein. Furthermore, studies have revealed that there is no correlation between CFTR mRNA levels in normal and mutant samples (263, 285). The preservation of gene expression may indicate the absence of any negative feedback mechanism induced by the formulation.

6.5 Conclusion

It was found that synthesized nanoparticles possessed a narrow size distribution, spherical shape and low cyto- and genotoxicity. Nebulization led to minimal changes in the size and dispersion of nanoparticles. It was concluded that the proposed NLCs are perspective candidates for the inhalation delivery of one or several drugs for treatment of pulmonary manifestations of cystic fibrosis.

Table 6.1. Encapsulation and drug loading of ivacaftor into NLCs with different liquid lipids.

NLC Formulation	**% Encapsulation Efficiency**	**Drug Loading (%)**
Squalene-Ivacaftor (10 mg)	100%	5%
Iso. Myristate- Ivacaftor (5 mg)	100%	2.50%
Iso. Myristate- Ivacaftor (10 mg)	100%	5%

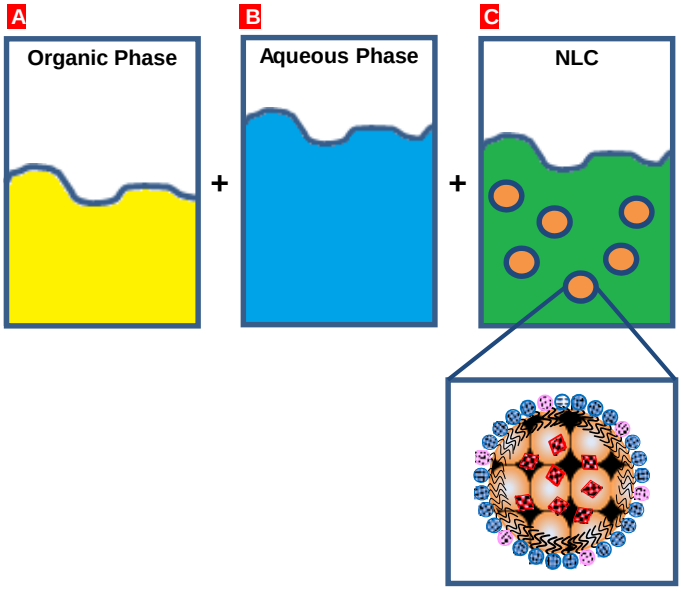

Fig. 6.1. Scheme of NLC preparation. Hot lipid phase consisting of Precirol ATO 5, liquid lipid (isopropyl myristate or squalene), soy PC and drug (A) is added to aqueous phase consisting of water, Tween 80, and DSPE-PEG-NH2 (B). A formed emulsion (C) is subjected to homogenization and sonication to yield NLC (C).

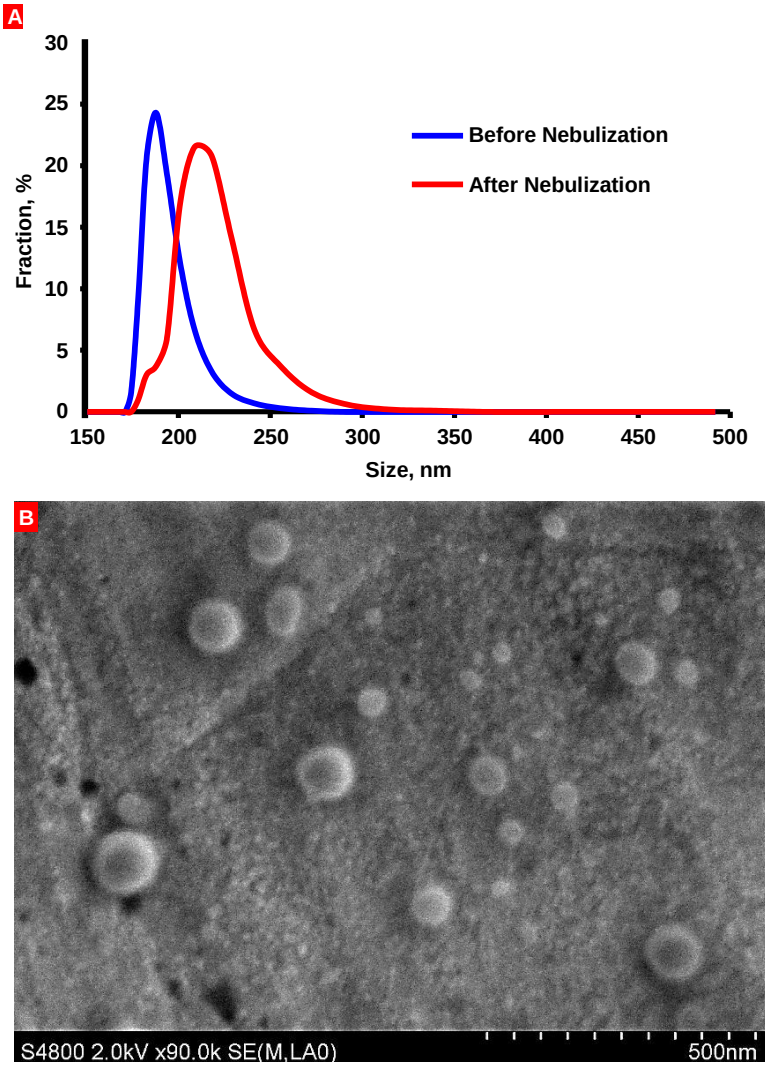

Fig. 6.2. NLC characterization. A) Typical dynamic light scattering curves of size distribution of NLC before and after nebulization. B) A representative scanning electron microscope image of NLC before nebulization.

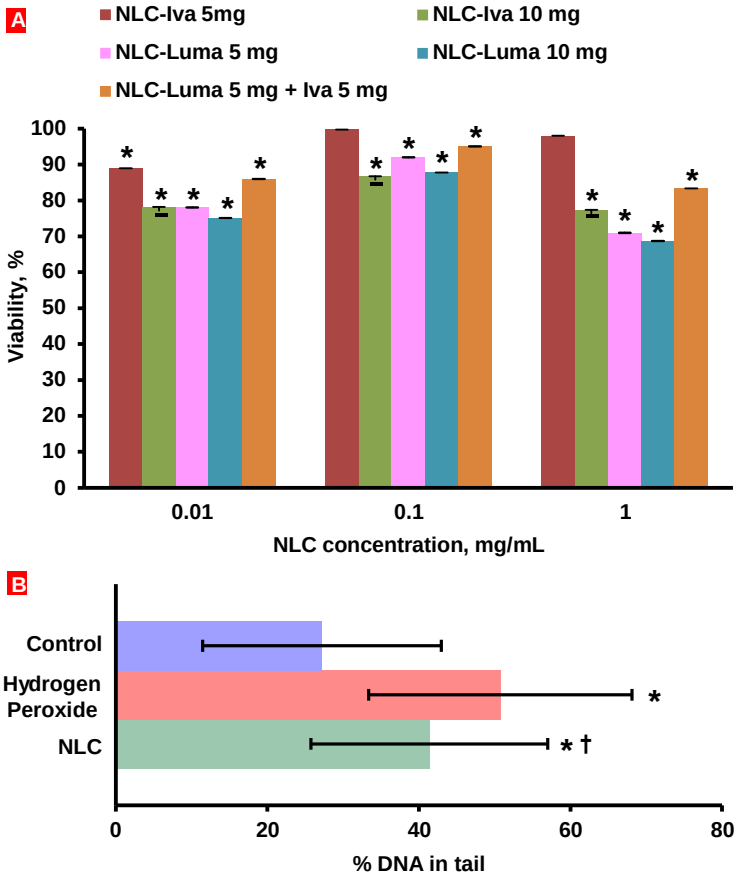

Fig. 6.3. Biocompatibility of NLC formulations. A) Cytotoxicity of various drugs (Ivacaftor - Iva and Lumacaftor – Luma) encapsulated into NLC with two different concentrations. B) Genotoxicity of NLC. Cystic fibrosis epithelial CuFi-4 cells were incubated within 24 hours with the substances indicated. Means ± SD are shown. *P < 0.05 when compared with control (cells incubated with fresh media). $^{\dagger}P$ < 0.05 when compared with positive control (cells incubated with hydrogen peroxide).

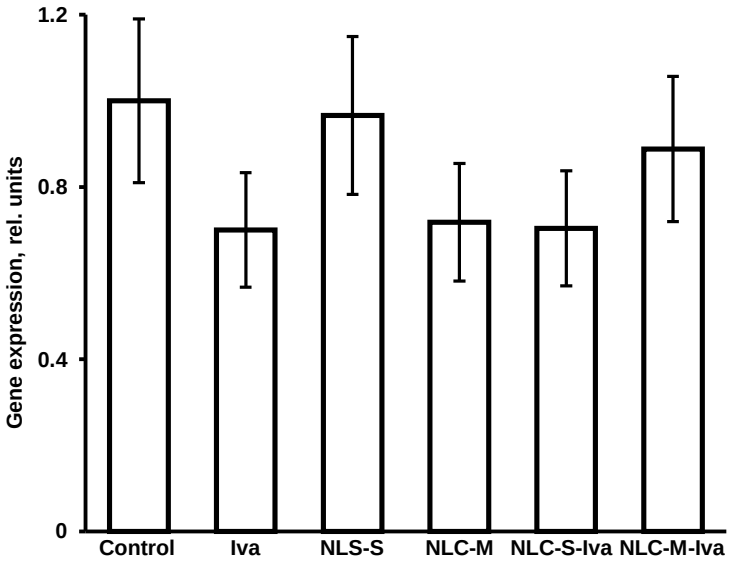

Fig. 6.4: CFTR mRNA expression by quantitative polymerase chain reaction (qPCR). Cystic fibrosis epithelial CuFi-4 cells were incubated within 72 hours with the following substances: fresh media (control), free non-emcapsulated ivacaftor drug (Iva), empty NLC containing squalene (NLC-S) or isopropyl myristate (NLC-M) as liquid lipid, NLC-M containing ivacaftor drug (NLC-M-Iva), and NLC-S containing ivacaftor drug (NLC-S-Iva). No statistically significant differences between the control and all experimental groups in the expression of the targeted mRNA were registered. Means ± SD are shown.

7 References

1. Meyer KC, Nathan SD. Idiopathic pulmonary fibrosis : a comprehensive clinical guide. New York: Humana Press; 2014. xv, 451 p.
2. Amaral MD, Kunzelmann K. Molecular targeting of CFTR as a therapeutic approach to cystic fibrosis. Trends in pharmacological sciences. 2007;28(7):334-41.
3. Schwartz D, Helmers R, Galvin J, Van Fossen D, Frees K, Dayton C, et al. Determinants of survival in idiopathic pulmonary fibrosis. American journal of respiratory and critical care medicine. 1994;149(2):450-4.
4. Gavrilov LA, Gavrilova NS. Early-life factors modulating lifespan. Modulating aging and longevity. 2003:27-50.
5. Farrell PM, Koscik RE. Sweat chloride concentrations in infants homozygous or heterozygous for F508 cystic fibrosis. Pediatrics. 1996;97(4):524-8.
6. Rubin BK. Mucus structure and properties in cystic fibrosis. Paediatric respiratory reviews. 2007;8(1):4-7.
7. Thelin WR, Boucher RC. The epithelium as a target for therapy in cystic fibrosis. Current opinion in pharmacology. 2007;7(3):290-5.
8. Döring G, Conway S, Heijerman H, Hodson M, Høiby N, Smyth A, et al. Antibiotic therapy against Pseudomonas aeruginosa in cystic fibrosis: a European consensus. European Respiratory Journal. 2000;16(4):749-67.
9. Tomkiewicz R, App E, Zayas J, Ramirez O, Church N, Boucher R, et al. Amiloride inhalation therapy in cystic fibrosis: influence on ion content, hydration, and rheology of sputum. American Review of Respiratory Disease. 1993;148(4_pt_1):1002-7.
10. Van Goor F, Hadida S, Grootenhuis PD, Burton B, Cao D, Neuberger T, et al. Rescue of CF airway epithelial cell function in vitro by a CFTR potentiator, VX-770. Proceedings of the National Academy of Sciences. 2009;106(44):18825-30.
11. Van Goor F, Hadida S, Grootenhuis PD, Burton B, Stack JH, Straley KS, et al. Correction of the F508del-CFTR protein processing defect in vitro by the investigational drug VX-809. Proceedings of the National Academy of Sciences. 2011;108(46):18843-8.
12. Chapman HA. Epithelial-mesenchymal interactions in pulmonary fibrosis. Annual review of physiology. 2011;73:413-35.
13. Moore BB, Murray L, Das A, Wilke CA, Herrygers AB, Toews GB. The role of CCL12 in the recruitment of fibrocytes and lung fibrosis. Am J Resp Cell Mol. 2006;35(2):175-81.
14. Tzouvelekis A, Harokopos V, Paparountas T, Oikonomou N, Chatziioannou A, Vilaras G, et al. Comparative expression profiling in pulmonary fibrosis suggests a role of hypoxia-inducible factor-1α in disease pathogenesis. American journal of respiratory and critical care medicine. 2007;176(11):1108-19.
15. Yamashita CM, Dolgonos L, Zemans RL, Young SK, Robertson J, Briones N, et al. Matrix metalloproteinase 3 is a mediator of pulmonary fibrosis. The American journal of pathology. 2011;179(4):1733-45.

16. Richeldi L, Davies HR, Ferrara G, Franco F. Corticosteroids for idiopathic pulmonary fibrosis. The Cochrane database of systematic reviews. 2003(3):CD002880.
17. Beyer C, Distler JH. Tyrosine kinase signaling in fibrotic disorders: Translation of basic research to human disease. Biochimica et biophysica acta. 2013;1832(7):897-904.
18. Ghofrani HA, Wiedemann R, Rose F, Schermuly RT, Olschewski H, Weissmann N, et al. Sildenafil for treatment of lung fibrosis and pulmonary hypertension: a randomised controlled trial. Lancet. 2002;360(9337):895-900.
19. Jain R, Shaul PW, Borok Z, Willis BC. Endothelin-1 induces alveolar epithelial-mesenchymal transition through endothelin type a receptor-mediated production of TGF-beta 1. Am J Resp Cell Mol. 2007;37(1):38-47.
20. Kubo H, Nakayama K, Yanai M, Suzuki T, Yamaya M, Watanabe M, et al. Anticoagulant therapy for idiopathic pulmonary fibrosis. Chest. 2005;128(3):1475-82.
21. Albera C, Bradford W, Costabel U, Du Bois R, Fagan E, Glaspole I, et al. Effect Of Continued Treatment With Pirfenidone Following A Clinically Meaningful Decline In Percent Predicted Forced Vital Capacity In Patients With Idiopathic Pulmonary Fibrosis (ipf). American journal of respiratory and critical care medicine. 2015;191:A1016.
22. Azuma A, Nukiwa T, Tsuboi E, Suga M, Abe S, Nakata K, et al. Double-blind, placebo-controlled trial of pirfenidone in patients with idiopathic pulmonary fibrosis. American journal of respiratory and critical care medicine. 2005;171(9):1040-7.
23. Costabel U, Selman M, Xu Z, Kimura T, Stowasser S, Hallmann C, et al. Efficacy And Safety Of Nintedanib In Patients With Ipf Beyond Week 52: Data From The Phase Ii Tomorrow Trial. American journal of respiratory and critical care medicine. 2015;191:A1019.
24. Cipolla DC, Gonda I. Formulation technology to repurpose drugs for inhalation delivery. Drug Discovery Today: Therapeutic Strategies. 2012;8(3):123-30.
25. Al-Hallak MK, Sarfraz MK, Azarmi S, Roa WH, Finlay WH, Löbenberg R. Pulmonary delivery of inhalable nanoparticles: dry powder inhalers. Therapeutic delivery. 2011;2(10):1313-24.
26. Manunta MD, McAnulty RJ, Tagalakis AD, Bottoms SE, Campbell F, Hailes HC, et al. Nebulisation of receptor-targeted nanocomplexes for gene delivery to the airway epithelium. PloS one. 2011;6(10):e26768.
27. Fink JB. Metered-dose inhalers, dry powder inhalers, and transitions. Respiratory care. 2000;45(6):623-35.
28. Burri RV, Bellucci S. Public perception of nanotechnology. Journal of Nanoparticle Research. 2008;10(3):387-91.
29. Farokhzad OC, Langer R. Impact of nanotechnology on drug delivery. ACS nano. 2009;3(1):16-20.
30. Dykxhoorn DM, Lieberman J. The silent revolution: RNA interference as basic biology, research tool, and therapeutic. Annual review of medicine. 2005;56:401-23.
31. Selman M, Thannickal VJ, Pardo A, Zisman DA, Martinez FJ, Lynch Iii JP. Idiopathic pulmonary fibrosis. Drugs. 2004;64(4):405-30.
32. Boucher RC. An overview of the pathogenesis of cystic fibrosis lung disease. Advanced drug delivery reviews. 2002;54(11):1359-71.

33. Thomas AQ, Lane K, Phillips J, 3rd, Prince M, Markin C, Speer M, et al. Heterozygosity for a surfactant protein C gene mutation associated with usual interstitial pneumonitis and cellular nonspecific interstitial pneumonitis in one kindred. American journal of respiratory and critical care medicine. 2002;165(9):1322-8.
34. Chandler PW, Shin MS, Friedman SE, Myers JL, Katzenstein AL. Radiographic manifestations of bronchiolitis obliterans with organizing pneumonia vs usual interstitial pneumonia. AJR American journal of roentgenology. 1986;147(5):899-906.
35. Hunninghake GW, Lynch DA, Galvin JR, Gross BH, Muller N, Schwartz DA, et al. Radiologic findings are strongly associated with a pathologic diagnosis of usual interstitial pneumonia. Chest. 2003;124(4):1215-23.
36. Mathieson JR, Mayo JR, Staples CA, Muller NL. Chronic diffuse infiltrative lung disease: comparison of diagnostic accuracy of CT and chest radiography. Radiology. 1989;171(1):111-6.
37. Lynch DA, Godwin JD, Safrin S, Starko KM, Hormel P, Brown KK, et al. High-resolution computed tomography in idiopathic pulmonary fibrosis: diagnosis and prognosis. American journal of respiratory and critical care medicine. 2005;172(4):488-93.
38. Mayo JR. CT evaluation of diffuse infiltrative lung disease: dose considerations and optimal technique. Journal of thoracic imaging. 2009;24(4):252-9.
39. Flume PA, Van Devanter DR. State of progress in treating cystic fibrosis respiratory disease. BMC medicine. 2012;10:88.
40. Nishimura K, Kitaichi M, Izumi T, Nagai S, Kanaoka M, Itoh H. Usual interstitial pneumonia: histologic correlation with high-resolution CT. Radiology. 1992;182(2):337-42.
41. West JB, Mathieu-Costello O. Structure, strength, failure, and remodeling of the pulmonary blood-gas barrier. Annual review of physiology. 1999;61:543-72.
42. Sverzellati N, Wells AU, Tomassetti S, Desai SR, Copley SJ, Aziz ZA, et al. Biopsy-proved idiopathic pulmonary fibrosis: spectrum of nondiagnostic thin-section CT diagnoses. Radiology. 2010;254(3):957-64.
43. Davies HR, Richeldi L, Walters EH. Immunomodulatory agents for idiopathic pulmonary fibrosis. The Cochrane database of systematic reviews. 2003(3):CD003134.
44. Wynn TA. Common and unique mechanisms regulate fibrosis in various fibroproliferative diseases. The Journal of clinical investigation. 2007;117(3):524-9.
45. Crystal RG, Bitterman PB, Rennard SI, Hance AJ, Keogh BA. Interstitial lung diseases of unknown cause. Disorders characterized by chronic inflammation of the lower respiratory tract. The New England journal of medicine. 1984;310(4):235-44.
46. Keogh BA, Crystal RG. Alveolitis: the key to the interstitial lung disorders. Thorax. 1982;37(1):1-10.
47. Selman M, King TE, Pardo A, American Thoracic S, European Respiratory S, American College of Chest P. Idiopathic pulmonary fibrosis: prevailing and evolving hypotheses about its pathogenesis and implications for therapy. Annals of internal medicine. 2001;134(2):136-51.
48. Thannickal VJ, Toews GB, White ES, Lynch JP, 3rd, Martinez FJ. Mechanisms of pulmonary fibrosis. Annual review of medicine. 2004;55:395-417.
49. Bhaskaran M, Kolliputi N, Wang Y, Gou D, Chintagari NR, Liu L. Trans-differentiation of alveolar epithelial type II cells to type I cells involves autocrine signaling by transforming

growth factor beta 1 through the Smad pathway. The Journal of biological chemistry. 2007;282(6):3968-76.
50. Myers JL, Katzenstein AL. Epithelial necrosis and alveolar collapse in the pathogenesis of usual interstitial pneumonia. Chest. 1988;94(6):1309-11.
51. Barbas-Filho JV, Ferreira MA, Sesso A, Kairalla RA, Carvalho CR, Capelozzi VL. Evidence of type II pneumocyte apoptosis in the pathogenesis of idiopathic pulmonary fibrosis (IFP)/usual interstitial pneumonia (UIP). Journal of clinical pathology. 2001;54(2):132-8.
52. Kawanami O, Ferrans VJ, Crystal RG. Structure of alveolar epithelial cells in patients with fibrotic lung disorders. Laboratory investigation; a journal of technical methods and pathology. 1982;46(1):39-53.
53. Demling N, Ehrhardt C, Kasper M, Laue M, Knels L, Rieber EP. Promotion of cell adherence and spreading: a novel function of RAGE, the highly selective differentiation marker of human alveolar epithelial type I cells. Cell and tissue research. 2006;323(3):475-88.
54. Englert JM, Hanford LE, Kaminski N, Tobolewski JM, Tan RJ, Fattman CL, et al. A role for the receptor for advanced glycation end products in idiopathic pulmonary fibrosis. The American journal of pathology. 2008;172(3):583-91.
55. Fehrenbach H, Kasper M, Tschernig T, Shearman MS, Schuh D, Muller M. Receptor for advanced glycation endproducts (RAGE) exhibits highly differential cellular and subcellular localisation in rat and human lung. Cellular and molecular biology. 1998;44(7):1147-57.
56. Queisser MA, Kouri FM, Konigshoff M, Wygrecka M, Schubert U, Eickelberg O, et al. Loss of RAGE in pulmonary fibrosis: molecular relations to functional changes in pulmonary cell types. Am J Respir Cell Mol Biol. 2008;39(3):337-45.
57. Adamson IY, Young L, Bowden DH. Relationship of alveolar epithelial injury and repair to the induction of pulmonary fibrosis. The American journal of pathology. 1988;130(2):377-83.
58. Bitterman PB, Wewers MD, Rennard SI, Adelberg S, Crystal RG. Modulation of alveolar macrophage-driven fibroblast proliferation by alternative macrophage mediators. The Journal of clinical investigation. 1986;77(3):700-8.
59. Chauncey JB, Petersgolden M, Simon RH. Arachidonic-Acid Metabolism by Rat Alveolar Epithelial-Cells. Laboratory Investigation. 1988;58(2):133-40.
60. Lama V, Moore BB, Christensen P, Toews GB, Peters-Golden M. Prostaglandin E2 synthesis and suppression of fibroblast proliferation by alveolar epithelial cells is cyclooxygenase-2-dependent. Am J Respir Cell Mol Biol. 2002;27(6):752-8.
61. Lipchik RJ, Chauncey JB, Paine R, Simon RH, Peters-Golden M. Arachidonate metabolism increases as rat alveolar type II cells differentiate in vitro. The American journal of physiology. 1990;259(2 Pt 1):L73-80.
62. Borok Z, Gillissen A, Buhl R, Hoyt RF, Hubbard RC, Ozaki T, et al. Augmentation of functional prostaglandin E levels on the respiratory epithelial surface by aerosol administration of prostaglandin E. The American review of respiratory disease. 1991;144(5):1080-4.

63. Goldstein RH, Polgar P. The effect and interaction of bradykinin and prostaglandins on protein and collagen production by lung fibroblasts. The Journal of biological chemistry. 1982;257(15):8630-3.
64. Huang SK, Wettlaufer SH, Hogaboam CM, Flaherty KR, Martinez FJ, Myers JL, et al. Variable prostaglandin E2 resistance in fibroblasts from patients with usual interstitial pneumonia. American journal of respiratory and critical care medicine. 2008;177(1):66-74.
65. Kohyama T, Ertl RF, Valenti V, Spurzem J, Kawamoto M, Nakamura Y, et al. Prostaglandin E(2) inhibits fibroblast chemotaxis. American journal of physiology Lung cellular and molecular physiology. 2001;281(5):L1257-63.
66. Korn JH, Halushka PV, LeRoy EC. Mononuclear cell modulation of connective tissue function: suppression of fibroblast growth by stimulation of endogenous prostaglandin production. The Journal of clinical investigation. 1980;65(2):543-54.
67. Brody AR, Soler P, Basset F, Haschek WM, Witschi H. Epithelial-mesenchymal associations of cells in human pulmonary fibrosis and in BHT-oxygen-induced fibrosis in mice. Experimental lung research. 1981;2(3):207-20.
68. Kasper M, Haroske G. Alterations in the alveolar epithelium after injury leading to pulmonary fibrosis. Histology and histopathology. 1996;11(2):463-83.
69. Thiery JP, Sleeman JP. Complex networks orchestrate epithelial-mesenchymal transitions. Nature reviews Molecular cell biology. 2006;7(2):131-42.
70. Kim KK, Kugler MC, Wolters PJ, Robillard L, Galvez MG, Brumwell AN, et al. Alveolar epithelial cell mesenchymal transition develops in vivo during pulmonary fibrosis and is regulated by the extracellular matrix. Proceedings of the National Academy of Sciences of the United States of America. 2006;103(35):13180-5.
71. Marmai C, Sutherland RE, Kim KK, Dolganov GM, Fang X, Kim SS, et al. Alveolar epithelial cells express mesenchymal proteins in patients with idiopathic pulmonary fibrosis. American journal of physiology Lung cellular and molecular physiology. 2011;301(1):L71-8.
72. Bridges RS, Kass D, Loh K, Glackin C, Borczuk AC, Greenberg S. Gene expression profiling of pulmonary fibrosis identifies Twist1 as an antiapoptotic molecular "rectifier" of growth factor signaling. The American journal of pathology. 2009;175(6):2351-61.
73. Jayachandran A, Konigshoff M, Yu H, Rupniewska E, Hecker M, Klepetko W, et al. SNAI transcription factors mediate epithelial-mesenchymal transition in lung fibrosis. Thorax. 2009;64(12):1053-61.
74. Rowe RG, Lin Y, Shimizu-Hirota R, Hanada S, Neilson EG, Greenson JK, et al. Hepatocyte-derived Snail1 propagates liver fibrosis progression. Molecular and cellular biology. 2011;31(12):2392-403.
75. Thiery JP, Acloque H, Huang RY, Nieto MA. Epithelial-mesenchymal transitions in development and disease. Cell. 2009;139(5):871-90.
76. Zavadil J, Bottinger EP. TGF-beta and epithelial-to-mesenchymal transitions. Oncogene. 2005;24(37):5764-74.
77. Willis BC, Borok Z. TGF-beta-induced EMT: mechanisms and implications for fibrotic lung disease. American journal of physiology Lung cellular and molecular physiology. 2007;293(3):L525-34.
78. Xu J, Lamouille S, Derynck R. TGF-beta-induced epithelial to mesenchymal transition. Cell research. 2009;19(2):156-72.

79. Koli K, Myllarniemi M, Vuorinen K, Salmenkivi K, Ryynanen MJ, Kinnula VL, et al. Bone morphogenetic protein-4 inhibitor gremlin is overexpressed in idiopathic pulmonary fibrosis. The American journal of pathology. 2006;169(1):61-71.
80. Kim KK, Wei Y, Szekeres C, Kugler MC, Wolters PJ, Hill ML, et al. Epithelial cell alpha3beta1 integrin links beta-catenin and Smad signaling to promote myofibroblast formation and pulmonary fibrosis. The Journal of clinical investigation. 2009;119(1):213-24.
81. Masszi A, Fan L, Rosivall L, McCulloch CA, Rotstein OD, Mucsi I, et al. Integrity of cell-cell contacts is a critical regulator of TGF-beta 1-induced epithelial-to-myofibroblast transition: role for beta-catenin. The American journal of pathology. 2004;165(6):1955-67.
82. Antoniades HN, Bravo MA, Avila RE, Galanopoulos T, Neville-Golden J, Maxwell M, et al. Platelet-derived growth factor in idiopathic pulmonary fibrosis. The Journal of clinical investigation. 1990;86(4):1055-64.
83. Antoniades HN, Neville-Golden J, Galanopoulos T, Kradin RL, Valente AJ, Graves DT. Expression of monocyte chemoattractant protein 1 mRNA in human idiopathic pulmonary fibrosis. Proceedings of the National Academy of Sciences of the United States of America. 1992;89(12):5371-5.
84. Dancer RC, Wood AM, Thickett DR. Metalloproteinases in idiopathic pulmonary fibrosis. The European respiratory journal. 2011;38(6):1461-7.
85. Giaid A, Yanagisawa M, Langleben D, Michel RP, Levy R, Shennib H, et al. Expression of endothelin-1 in the lungs of patients with pulmonary hypertension. The New England journal of medicine. 1993;328(24):1732-9.
86. Kapanci Y, Desmouliere A, Pache JC, Redard M, Gabbiani G. Cytoskeletal protein modulation in pulmonary alveolar myofibroblasts during idiopathic pulmonary fibrosis. Possible role of transforming growth factor beta and tumor necrosis factor alpha. American journal of respiratory and critical care medicine. 1995;152(6 Pt 1):2163-9.
87. Pan LH, Yamauchi K, Uzuki M, Nakanishi T, Takigawa M, Inoue H, et al. Type II alveolar epithelial cells and interstitial fibroblasts express connective tissue growth factor in IPF. The European respiratory journal. 2001;17(6):1220-7.
88. Piguet PF, Ribaux C, Karpuz V, Grau GE, Kapanci Y. Expression and localization of tumor necrosis factor-alpha and its mRNA in idiopathic pulmonary fibrosis. The American journal of pathology. 1993;143(3):651-5.
89. Gross TJ, Simon RH, Sitrin RG. Tissue factor procoagulant expression by rat alveolar epithelial cells. Am J Respir Cell Mol Biol. 1992;6(4):397-403.
90. Kotani I, Sato A, Hayakawa H, Urano T, Takada Y, Takada A. Increased procoagulant and antifibrinolytic activities in the lungs with idiopathic pulmonary fibrosis. Thrombosis research. 1995;77(6):493-504.
91. Gunther A, Mosavi P, Ruppert C, Heinemann S, Temmesfeld B, Velcovsky HG, et al. Enhanced tissue factor pathway activity and fibrin turnover in the alveolar compartment of patients with interstitial lung disease. Thrombosis and haemostasis. 2000;83(6):853-60.
92. Chambers RC, Scotton CJ. Coagulation cascade proteinases in lung injury and fibrosis. Proceedings of the American Thoracic Society. 2012;9(3):96-101.
93. Howell DC, Johns RH, Lasky JA, Shan B, Scotton CJ, Laurent GJ, et al. Absence of proteinase-activated receptor-1 signaling affords protection from bleomycin-induced lung inflammation and fibrosis. The American journal of pathology. 2005;166(5):1353-65.

94. Scotton CJ, Krupiczojc MA, Konigshoff M, Mercer PF, Lee YC, Kaminski N, et al. Increased local expression of coagulation factor X contributes to the fibrotic response in human and murine lung injury. The Journal of clinical investigation. 2009;119(9):2550-63.
95. Wygrecka M, Kwapiszewska G, Jablonska E, von Gerlach S, Henneke I, Zakrzewicz D, et al. Role of protease-activated receptor-2 in idiopathic pulmonary fibrosis. American journal of respiratory and critical care medicine. 2011;183(12):1703-14.
96. Huang SK, Fisher AS, Scruggs AM, White ES, Hogaboam CM, Richardson BC, et al. Hypermethylation of PTGER2 confers prostaglandin E2 resistance in fibrotic fibroblasts from humans and mice. The American journal of pathology. 2010;177(5):2245-55.
97. Zhang K, Rekhter MD, Gordon D, Phan SH. Myofibroblasts and their role in lung collagen gene expression during pulmonary fibrosis. A combined immunohistochemical and in situ hybridization study. The American journal of pathology. 1994;145(1):114-25.
98. Hinz B, Phan SH, Thannickal VJ, Galli A, Bochaton-Piallat ML, Gabbiani G. The myofibroblast: one function, multiple origins. The American journal of pathology. 2007;170(6):1807-16.
99. King TE, Jr., Pardo A, Selman M. Idiopathic pulmonary fibrosis. Lancet. 2011;378(9807):1949-61.
100. Raghu G, Collard HR, Egan JJ, Martinez FJ, Behr J, Brown KK, et al. An official ATS/ERS/JRS/ALAT statement: idiopathic pulmonary fibrosis: evidence-based guidelines for diagnosis and management. American journal of respiratory and critical care medicine. 2011;183(6):788-824.
101. Spagnolo P, Del Giovane C, Luppi F, Cerri S, Balduzzi S, Walters EH, et al. Non-steroid agents for idiopathic pulmonary fibrosis. The Cochrane database of systematic reviews. 2010(9):CD003134.
102. King TE, Jr., Albera C, Bradford WZ, Costabel U, Hormel P, Lancaster L, et al. Effect of interferon gamma-1b on survival in patients with idiopathic pulmonary fibrosis (INSPIRE): a multicentre, randomised, placebo-controlled trial. Lancet. 2009;374(9685):222-8.
103. Ziesche R, Hofbauer E, Wittmann K, Petkov V, Block LH. A preliminary study of long-term treatment with interferon gamma-1b and low-dose prednisolone in patients with idiopathic pulmonary fibrosis. The New England journal of medicine. 1999;341(17):1264-9.
104. Swigris JJ, Brown KK. The Role of Endothelin-1 in the Pathogenesis of Idiopathic Pulmonary Fibrosis. Biodrugs. 2010;24(1):49-54.
105. King TE, Behr J, Brown KK, du Bois RM, Lancaster L, de Andrade JA, et al. BUILD-1: A randomized placebo-controlled trial of bosentan in idiopathic pulmonary fibrosis. American journal of respiratory and critical care medicine. 2008;177(1):75-81.
106. King TE, Brown KK, Raghu G, du Bois RM, Lynch DA, Martinez F, et al. BUILD-3: A Randomized, Controlled Trial of Bosentan in Idiopathic Pulmonary Fibrosis. American journal of respiratory and critical care medicine. 2011;184(1):92-9.
107. Collard HR, Anstrom KJ, Schwarz MI, Zisman DA. Sildenafil improves walk distance in idiopathic pulmonary fibrosis. Chest. 2007;131(3):897-9.
108. Noth I, Anstrom KJ, Calvert SB, de Andrade J, Flaherty KR, Glazer C, et al. A placebo-controlled randomized trial of warfarin in idiopathic pulmonary fibrosis. American journal of respiratory and critical care medicine. 2012;186(1):88-95.

109. Grimminger F, Schermuly RT, Ghofrani HA. Targeting non-malignant disorders with tyrosine kinase inhibitors. Nature reviews Drug discovery. 2010;9(12):956-70.
110. Richeldi L, Costabel U, Selman M, Kim DS, Hansell DM, Nicholson AG, et al. Efficacy of a tyrosine kinase inhibitor in idiopathic pulmonary fibrosis. The New England journal of medicine. 2011;365(12):1079-87.
111. Daniels CE, Wilkes MC, Edens M, Kottom TJ, Murphy SJ, Limper AH, et al. Imatinib mesylate inhibits the profibrogenic activity of TGF-beta and prevents bleomycin-mediated lung fibrosis. The Journal of clinical investigation. 2004;114(9):1308-16.
112. Daniels CE, Lasky JA, Limper AH, Mieras K, Gabor E, Schroeder DR, et al. Imatinib treatment for idiopathic pulmonary fibrosis: Randomized placebo-controlled trial results. American journal of respiratory and critical care medicine. 2010;181(6):604-10.
113. Sagana RL, Yan M, Cornett AM, Tsui JL, Stephenson DA, Huang SK, et al. Phosphatase and tensin homologue on chromosome 10 (PTEN) directs prostaglandin E2-mediated fibroblast responses via regulation of E prostanoid 2 receptor expression. The Journal of biological chemistry. 2009;284(47):32264-71.
114. Charbeneau RP, Peters-Golden M. Eicosanoids: mediators and therapeutic targets in fibrotic lung disease. Clinical science. 2005;108(6):479-91.
115. Qu W, Graves LM, Thurman RG. PGE(2) stimulates O(2) uptake in hepatic parenchymal cells: involvement of the cAMP-dependent protein kinase. The American journal of physiology. 1999;277(5 Pt 1):G1048-54.
116. Zhang A, Wang MH, Dong Z, Yang T. Prostaglandin E2 is a potent inhibitor of epithelial-to-mesenchymal transition: interaction with hepatocyte growth factor. American journal of physiology Renal physiology. 2006;291(6):F1323-31.
117. Dillon CP, Sandy P, Nencioni A, Kissler S, Rubinson DA, Van Parijs L. Rnai as an experimental and therapeutic tool to study and regulate physiological and disease processes. Annual review of physiology. 2005;67:147-73.
118. Elbashir SM, Lendeckel W, Tuschl T. RNA interference is mediated by 21- and 22-nucleotide RNAs. Genes & development. 2001;15(2):188-200.
119. Cogoni C, Macino G. Homology-dependent gene silencing in plants and fungi: a number of variations on the same theme. Current opinion in microbiology. 1999;2(6):657-62.
120. Svoboda P, Stain P, Hayashi H, Schultz RM. Selective reduction of dormant maternal mRNAs in mouse oocytes by RNA interference. Development. 2000;127(19):4147-56.
121. Fire A, Xu S, Montgomery MK, Kostas SA, Driver SE, Mello CC. Potent and specific genetic interference by double-stranded RNA in Caenorhabditis elegans. Nature. 1998;391(6669):806-11.
122. Ketting RF, Plasterk RH. A genetic link between co-suppression and RNA interference in C. elegans. Nature. 2000;404(6775):296-8.
123. Kennerdell JR, Carthew RW. Use of dsRNA-mediated genetic interference to demonstrate that frizzled and frizzled 2 act in the wingless pathway. Cell. 1998;95(7):1017-26.
124. Sharp PA, Zamore PD. Molecular biology. RNA interference. Science. 2000;287(5462):2431-3.

125. Oelgeschlager M, Larrain J, Geissert D, De Robertis EM. The evolutionarily conserved BMP-binding protein Twisted gastrulation promotes BMP signalling. Nature. 2000;405(6788):757-63.
126. Zamore PD, Tuschl T, Sharp PA, Bartel DP. RNAi: double-stranded RNA directs the ATP-dependent cleavage of mRNA at 21 to 23 nucleotide intervals. Cell. 2000;101(1):25-33.
127. Chiu YL, Ali A, Chu CY, Cao H, Rana TM. Visualizing a correlation between siRNA localization, cellular uptake, and RNAi in living cells. Chemistry & biology. 2004;11(8):1165-75.
128. Choung S, Kim YJ, Kim S, Park HO, Choi YC. Chemical modification of siRNAs to improve serum stability without loss of efficacy. Biochemical and biophysical research communications. 2006;342(3):919-27.
129. Dominska M, Dykxhoorn DM. Breaking down the barriers: siRNA delivery and endosome escape. Journal of cell science. 2010;123(Pt 8):1183-9.
130. Ratjen FA. Cystic fibrosis: pathogenesis and future treatment strategies. Respiratory care. 2009;54(5):595-605.
131. O'Sullivan BP, Freedman SD. Cystic fibrosis. Lancet. 2009;373(9678):1891-904.
132. Loo TW, Bartlett MC, Shi L, Clarke DM. Corrector-mediated rescue of misprocessed CFTR mutants can be reduced by the P-glycoprotein drug pump. Biochemical pharmacology. 2012;83(3):345-54.
133. Oakland M, Sinn PL, McCray PB, Jr. Advances in cell and gene-based therapies for cystic fibrosis lung disease. Molecular therapy : the journal of the American Society of Gene Therapy. 2012;20(6):1108-15.
134. Griesenbach U, Alton EW. Current status and future directions of gene and cell therapy for cystic fibrosis. BioDrugs : clinical immunotherapeutics, biopharmaceuticals and gene therapy. 2011;25(2):77-88.
135. Van Goor F, Hadida S, Grootenhuis PD, Burton B, Cao D, Neuberger T, et al. Rescue of CF airway epithelial cell function in vitro by a CFTR potentiator, VX-770. Proceedings of the National Academy of Sciences of the United States of America. 2009;106(44):18825-30.
136. Boyle MP, Bell SC, Konstan MW, McColley SA, Rowe SM, Rietschel E, et al. A CFTR corrector (lumacaftor) and a CFTR potentiator (ivacaftor) for treatment of patients with cystic fibrosis who have a phe508del CFTR mutation: a phase 2 randomised controlled trial. The Lancet Respiratory medicine. 2014;2(7):527-38.
137. Van Goor F, Hadida S, Grootenhuis PD, Burton B, Stack JH, Straley KS, et al. Correction of the F508del-CFTR protein processing defect in vitro by the investigational drug VX-809. Proceedings of the National Academy of Sciences of the United States of America. 2011;108(46):18843-8.
138. Kumar TP, Vani MI, Yamini D, Raju PN, Reddy GN. RECENT ADVANCES IN NASAL FORMULATIONS AND DEVICES USED IN PULMONARY DRUG DELIVERY. 2013.
139. Schleh C, Hohlfeld JM. Interaction of nanoparticles with the pulmonary surfactant system. Inhalation toxicology. 2009;21(S1):97-103.
140. Card JW, Zeldin DC, Bonner JC, Nestmann ER. Pulmonary applications and toxicity of engineered nanoparticles. American journal of physiology Lung cellular and molecular physiology. 2008;295(3):L400-11.

141. Rubin BK, Williams RW. Emerging aerosol drug delivery strategies: from bench to clinic. Advanced drug delivery reviews. 2014;75:141-8.
142. Cryan SA. Carrier-based strategies for targeting protein and peptide drugs to the lungs. The AAPS journal. 2005;7(1):E20-41.
143. Al-Hallak MH, Sarfraz MK, Azarmi S, Roa WH, Finlay WH, Lobenberg R. Pulmonary delivery of inhalable nanoparticles: dry powder inhalers. Therapeutic delivery. 2011;2(10):1313-24.
144. Healy AM, Amaro MI, Paluch KJ, Tajber L. Dry powders for oral inhalation free of lactose carrier particles. Advanced drug delivery reviews. 2014;75:32-52.
145. Hoppentocht M, Hagedoorn P, Frijlink HW, de Boer AH. Technological and practical challenges of dry powder inhalers and formulations. Advanced drug delivery reviews. 2014;75:18-31.
146. Garcia-Contreras L, Hickey AJ. Pharmaceutical and biotechnological aerosols for cystic fibrosis therapy. Advanced drug delivery reviews. 2002;54(11):1491-504.
147. Muhlfeld C, Rothen-Rutishauser B, Blank F, Vanhecke D, Ochs M, Gehr P. Interactions of nanoparticles with pulmonary structures and cellular responses. American journal of physiology Lung cellular and molecular physiology. 2008;294(5):L817-29.
148. Gessler T, Seeger W, Schmehl T. Inhaled prostanoids in the therapy of pulmonary hypertension. Journal of aerosol medicine and pulmonary drug delivery. 2008;21(1):1-12.
149. Vyas S, Kannan M, Jain S, Mishra V, Singh P. Design of liposomal aerosols for improved delivery of rifampicin to alveolar macrophages. International journal of pharmaceutics. 2004;269(1):37-49.
150. Zaru M, Mourtas S, Klepetsanis P, Fadda AM, Antimisiaris SG. Liposomes for drug delivery to the lungs by nebulization. European journal of pharmaceutics and biopharmaceutics : official journal of Arbeitsgemeinschaft fur Pharmazeutische Verfahrenstechnik eV. 2007;67(3):655-66.
151. Cipolla D, Wu H, Gonda I, Chan H-K. Aerosol Performance and Long-Term Stability of Surfactant-Associated Liposomal Ciprofloxacin Formulations with Modified Encapsulation and Release Properties. AAPS PharmSciTech. 2014;15(5):1218-27.
152. Hullmann A. The economic development of nanotechnology-An indicators based analysis. EU report. 2006.
153. Hunter RJ. Foundations of colloid science. 2001.
154. Stein HN. The preparation of dispersions in liquids: CRC Press; 1995.
155. Gabellieri C, Frima H. Nanomedicine in the European Commission policy for nanotechnology. Nanomedicine: Nanotechnology, Biology and Medicine. 2011;7(5):519-20.
156. Jesorka A, Orwar O. Liposomes: technologies and analytical applications. Annual review of analytical chemistry. 2008;1:801-32.
157. Bangham AD, Standish MM, Watkins JC. Diffusion of univalent ions across the lamellae of swollen phospholipids. Journal of molecular biology. 1965;13(1):238-52.
158. Lasch J, Weissig V, Brandl M. Preparation of liposomes. Liposomes: a practical approach. 2003;2:24-5.
159. Lee J-H, Agarwal V, Bose A, Payne GF, Raghavan SR. Transition from unilamellar to bilamellar vesicles induced by an amphiphilic biopolymer. Physical review letters. 2006;96(4):048102.

160. Szoka F, Jr., Papahadjopoulos D. Procedure for preparation of liposomes with large internal aqueous space and high capture by reverse-phase evaporation. Proceedings of the National Academy of Sciences of the United States of America. 1978;75(9):4194-8.
161. Torchilin VP. Recent advances with liposomes as pharmaceutical carriers. Nature reviews Drug discovery. 2005;4(2):145-60.
162. Chatterjee S, Banerjee DK. Preparation, isolation, and characterization of liposomes containing natural and synthetic lipids. Liposome Methods and Protocols: Springer; 2002. p. 3-16.
163. Shimomura M, Sawadaishi T. Bottom-up strategy of materials fabrication: a new trend in nanotechnology of soft materials. Current opinion in colloid & interface science. 2001;6(1):11-6.
164. Torchilin VP, Weissig V. Liposomes: a practical approach: Oxford University Press; 2003.
165. Helm CA, Israelachvili JN, McGuiggan PM. Role of hydrophobic forces in bilayer adhesion and fusion. Biochemistry. 1992;31(6):1794-805.
166. Damen J, Regts J, Scherphof G. Transfer and exchange of phospholipid between small unilamellar liposomes and rat plasma high density lipoproteins Dependence on cholesterol content and phospholipid composition. Biochimica et Biophysica Acta (BBA)-Lipids and Lipid Metabolism. 1981;665(3):538-45.
167. Gurr MI, Harwood JL, Frayn KN. Lipid biochemistry: Springer; 2002.
168. Immordino ML, Dosio F, Cattel L. Stealth liposomes: review of the basic science, rationale, and clinical applications, existing and potential. International journal of nanomedicine. 2006;1(3):297.
169. Ishida T, Harashima H, Kiwada H. Liposome clearance. Bioscience reports. 2002;22(2):197-224.
170. Chonn A, Semple SC, Cullis PR. Beta 2 glycoprotein I is a major protein associated with very rapidly cleared liposomes in vivo, suggesting a significant role in the immune clearance of "non-self" particles. The Journal of biological chemistry. 1995;270(43):25845-9.
171. Veerareddy PR, Vobalaboina V. Lipid-based formulations of amphotericin B. Drugs of today. 2004;40(2):133-45.
172. Harashima H, Sakata K, Funato K, Kiwada H. Enhanced hepatic uptake of liposomes through complement activation depending on the size of liposomes. Pharmaceutical research. 1994;11(3):402-6.
173. Patel HM. Serum opsonins and liposomes: their interaction and opsonophagocytosis. Critical reviews in therapeutic drug carrier systems. 1992;9(1):39-90.
174. Senior J, Gregoriadis G. Is half-life of circulating liposomes determined by changes in their permeability? FEBS letters. 1982;145(1):109-14.
175. Powell G. Polyethylene glycol. Handbook of water soluble gums and resins. 1980;18:1-31.
176. Needham D, McIntosh T, Lasic D. Repulsive interactions and mechanical stability of polymer-grafted lipid membranes. Biochimica et Biophysica Acta (BBA)-Biomembranes. 1992;1108(1):40-8.

177. BOULIKAS T, STATHOPOULOS GP, VOLAKAKIS N, VOUGIOUKA M. Systemic Lipoplatin infusion results in preferential tumor uptake in human studies. Anticancer Research. 2005;25(4):3031-9.
178. Mehnert W, Mader K. Solid lipid nanoparticles: production, characterization and applications. Advanced drug delivery reviews. 2001;47(2-3):165-96.
179. Ohl F, Sillaber I, Binder E, Keck ME, Holsboer F. Differential analysis of behavior and diazepam-induced alterations in C57BL/6N and BALB/c mice using the modified hole board test. Journal of psychiatric research. 2001;35(3):147-54.
180. Muller RH, Mader K, Gohla S. Solid lipid nanoparticles (SLN) for controlled drug delivery - a review of the state of the art. European journal of pharmaceutics and biopharmaceutics : official journal of Arbeitsgemeinschaft fur Pharmazeutische Verfahrenstechnik eV. 2000;50(1):161-77.
181. Dingler A, Gohla S. Production of solid lipid nanoparticles (SLN): scaling up feasibilities. Journal of microencapsulation. 2002;19(1):11-6.
182. Trotta M, Debernardi F, Caputo O. Preparation of solid lipid nanoparticles by a solvent emulsification–diffusion technique. International journal of pharmaceutics. 2003;257(1):153-60.
183. How CW, Abdullah R, Abbasalipourkabir R. Physicochemical properties of nanostructured lipid carriers as colloidal carrier system stabilized with polysorbate 20 and polysorbate 80. African Journal of Biotechnology. 2013;10(9):1684-9.
184. Kovacevic A, Savic S, Vuleta G, Muller RH, Keck CM. Polyhydroxy surfactants for the formulation of lipid nanoparticles (SLN and NLC): effects on size, physical stability and particle matrix structure. Int J Pharm. 2011;406(1-2):163-72.
185. Abbasalipurkabir R, Salehzadeh A, Abdullah R. Delivering tamoxifen within solid lipid nanoparticles. Pharmaceutical Technology. 2011;35(4):74-9.
186. Das S, Ng WK, Tan RB. Are nanostructured lipid carriers (NLCs) better than solid lipid nanoparticles (SLNs): development, characterizations and comparative evaluations of clotrimazole-loaded SLNs and NLCs? European journal of pharmaceutical sciences : official journal of the European Federation for Pharmaceutical Sciences. 2012;47(1):139-51.
187. Purevdorj E, Zscheppang K, Hoymann HG, Braun A, von Mayersbach D, Brinkhaus MJ, et al. ErbB4 deletion leads to changes in lung function and structure similar to bronchopulmonary dysplasia. American journal of physiology Lung cellular and molecular physiology. 2008;294(3):L516-22.
188. Andrade-Lima M, Pereira LFF, Fernandes ALG. Pharmaceutical equivalence of the combination formulation of budesonide and formoterol in a single capsule with a dry powder inhaler. Jornal Brasileiro de Pneumologia. 2012;38(6):748-56.
189. Patel CJ, Asija R, Asija S, Dhruv M, Patel P, Patel K. Formulation and Evaluation of Solid Dispersion of Aceclofenac Sodium for Enhancement of Dissolution Rate. Research Journal of Pharmaceutical Dosage Forms and Technology. 2012;4(4):221-6.
190. Gharaee-Kermani M, Gyetko MR, Hu B, Phan SH. New insights into the pathogenesis and treatment of idiopathic pulmonary fibrosis: a potential role for stem cells in the lung parenchyma and implications for therapy. Pharmaceutical research. 2007;24(5):819-41.
191. Sime PJ, O'Reilly KM. Fibrosis of the lung and other tissues: new concepts in pathogenesis and treatment. Clin Immunol. 2001;99(3):308-19.

192. Frankel SK, Schwarz MI. Update in idiopathic pulmonary fibrosis. Curr Opin Pulm Med. 2009;15(5):463-9.
193. Williams TJ, Wilson JW. Challenges in pulmonary fibrosis: 7--Novel therapies and lung transplantation. Thorax. 2008;63(3):277-84.
194. Vancheri C, Mastruzzo C, Sortino MA, Crimi N. The lung as a privileged site for the beneficial actions of PGE2. Trends Immunol. 2004;25(1):40-6.
195. Bozyk PD, Moore BB. Prostaglandin E2 and the pathogenesis of pulmonary fibrosis. American journal of respiratory cell and molecular biology. 2011;45(3):445-52.
196. Huang SK, Wettlaufer SH, Chung J, Peters-Golden M. Prostaglandin E2 inhibits specific lung fibroblast functions via selective actions of PKA and Epac-1. American journal of respiratory cell and molecular biology. 2008;39(4):482-9.
197. Huang SK, Wettlaufer SH, Hogaboam CM, Flaherty KR, Martinez FJ, Myers JL, et al. Variable prostaglandin E2 resistance in fibroblasts from patients with usual interstitial pneumonia. Am J Respir Crit Care Med. 2008;177(1):66-74.
198. Ghosh M, Stewart A, Tucker DE, Bonventre JV, Murphy RC, Leslie CC. Role of cytosolic phospholipase A(2) in prostaglandin E(2) production by lung fibroblasts. American journal of respiratory cell and molecular biology. 2004;30(1):91-100.
199. Failla M, Genovese T, Mazzon E, Fruciano M, Fagone E, Gili E, et al. 16,16-Dimethyl prostaglandin E2 efficacy on prevention and protection from bleomycin-induced lung injury and fibrosis. American journal of respiratory cell and molecular biology. 2009;41(1):50-8.
200. Garbuzenko OB, Saad M, Betigeri S, Zhang M, Vetcher AA, Soldatenkov VA, et al. Intratracheal versus intravenous liposomal delivery of siRNA, antisense oligonucleotides and anticancer drug. Pharmaceutical research. 2009;26(2):382-94.
201. Garbuzenko OB, Saad M, Pozharov VP, Reuhl KR, Mainelis G, Minko T. Inhibition of lung tumor growth by complex pulmonary delivery of drugs with oligonucleotides as suppressors of cellular resistance. Proceedings of the National Academy of Sciences of the United States of America. 2010;107(23):10737-42.
202. Minko T, Stefanov A, Pozharov V. Selected contribution: Lung hypoxia: antioxidant and antiapoptotic effects of liposomal alpha-tocopherol. J Appl Physiol. 2002;93(4):1550-60; discussion 49.
203. Taratula O, Garbuzenko OB, Chen AM, Minko T. Innovative strategy for treatment of lung cancer: targeted nanotechnology-based inhalation co-delivery of anticancer drugs and siRNA. J Drug Target. 2011;19(10):900-14.
204. Betigeri S, Zhang M, Garbuzenko O, Minko T. Non-viral systemic delivery of siRNA or antisense oligonucleotides targeted to Jun N-terminal kinase 1 prevents cellular hypoxic damage. Drug Deliv Transl Res. 2011;1(1):13-24.
205. Wang Y, Saad M, Pakunlu RI, Khandare JJ, Garbuzenko OB, Vetcher AA, et al. Nonviral nanoscale-based delivery of antisense oligonucleotides targeted to hypoxia-inducible factor 1 alpha enhances the efficacy of chemotherapy in drug-resistant tumor. Clin Cancer Res. 2008;14(11):3607-16.
206. Lu G, Liao J, Yang G, Reuhl KR, Hao X, Yang CS. Inhibition of adenoma progression to adenocarcinoma in a 4-(methylnitrosamino)-1-(3-pyridyl)-1-butanone-induced lung tumorigenesis model in A/J mice by tea polyphenols and caffeine. Cancer Res. 2006;66(23):11494-501.

207. Minko T, Pakunlu RI, Wang Y, Khandare JJ, Saad M. New generation of liposomal drugs for cancer. Anticancer Agents Med Chem. 2006;6(6):537-52.
208. Pakunlu RI, Wang Y, Saad M, Khandare JJ, Starovoytov V, Minko T. In vitro and in vivo intracellular liposomal delivery of antisense oligonucleotides and anticancer drug. J Control Release. 2006;114(2):153-62.
209. Huaux F, Gharaee-Kermani M, Liu T, Morel V, McGarry B, Ullenbruch M, et al. Role of Eotaxin-1 (CCL11) and CC chemokine receptor 3 (CCR3) in bleomycin-induced lung injury and fibrosis. The American journal of pathology. 2005;167(6):1485-96.
210. Awad M, Pravica V, Perrey C, El Gamel A, Yonan N, Sinnott PJ, et al. CA repeat allele polymorphism in the first intron of the human interferon-gamma gene is associated with lung allograft fibrosis. Hum Immunol. 1999;60(4):343-6.
211. Lee CG, Homer RJ, Cohn L, Link H, Jung S, Craft JE, et al. Transgenic overexpression of interleukin (IL)-10 in the lung causes mucus metaplasia, tissue inflammation, and airway remodeling via IL-13-dependent and -independent pathways. The Journal of biological chemistry. 2002;277(38):35466-74.
212. Blackburn MR, Lee CG, Young HW, Zhu Z, Chunn JL, Kang MJ, et al. Adenosine mediates IL-13-induced inflammation and remodeling in the lung and interacts in an IL-13-adenosine amplification pathway. The Journal of clinical investigation. 2003;112(3):332-44.
213. Fichtner-Feigl S, Strober W, Kawakami K, Puri RK, Kitani A. IL-13 signaling through the IL-13alpha2 receptor is involved in induction of TGF-beta1 production and fibrosis. Nat Med. 2006;12(1):99-106.
214. Kuperman DA, Huang X, Koth LL, Chang GH, Dolganov GM, Zhu Z, et al. Direct effects of interleukin-13 on epithelial cells cause airway hyperreactivity and mucus overproduction in asthma. Nat Med. 2002;8(8):885-9.
215. Zhu Z, Homer RJ, Wang Z, Chen Q, Geba GP, Wang J, et al. Pulmonary expression of interleukin-13 causes inflammation, mucus hypersecretion, subepithelial fibrosis, physiologic abnormalities, and eotaxin production. The Journal of clinical investigation. 1999;103(6):779-88.
216. Fukuda Y, Ishizaki M, Kudoh S, Kitaichi M, Yamanaka N. Localization of matrix metalloproteinases-1, -2, and -9 and tissue inhibitor of metalloproteinase-2 in interstitial lung diseases. Laboratory investigation; a journal of technical methods and pathology. 1998;78(6):687-98.
217. Selman M, King TE, Pardo A. Idiopathic pulmonary fibrosis: prevailing and evolving hypotheses about its pathogenesis and implications for therapy. Annals of internal medicine. 2001;134(2):136-51.
218. Yaguchi T, Fukuda Y, Ishizaki M, Yamanaka N. Immunohistochemical and gelatin zymography studies for matrix metalloproteinases in bleomycin-induced pulmonary fibrosis. Pathol Int. 1998;48(12):954-63.
219. Ask K, Martin GE, Kolb M, Gauldie J. Targeting genes for treatment in idiopathic pulmonary fibrosis: challenges and opportunities, promises and pitfalls. Proceedings of the American Thoracic Society. 2006;3(4):389-93.
220. Borok Z. Role for alpha3 integrin in EMT and pulmonary fibrosis. The Journal of clinical investigation. 2009;119(1):7-10.

221. Liu H, Peng Y, Liu F, Li J, Chen X, Liu Y, et al. A selective cyclooxygenase-2 inhibitor decreases transforming growth factor-beta1 synthesis and matrix production in human peritoneal mesothelial cells. Cell Biol Int. 2007;31(5):508-15.
222. Zeisberg EM, Tarnavski O, Zeisberg M, Dorfman AL, McMullen JR, Gustafsson E, et al. Endothelial-to-mesenchymal transition contributes to cardiac fibrosis. Nat Med. 2007;13(8):952-61.
223. Oikonomou N, Harokopos V, Zalevsky J, Valavanis C, Kotanidou A, Szymkowski DE, et al. Soluble TNF mediates the transition from pulmonary inflammation to fibrosis. PloS one. 2006;1:e108.
224. Suda T, Takahashi T, Golstein P, Nagata S. Molecular cloning and expression of the Fas ligand, a novel member of the tumor necrosis factor family. Cell. 1993;75(6):1169-78.
225. Zhang K, Gharaee-Kermani M, McGarry B, Remick D, Phan SH. TNF-alpha-mediated lung cytokine networking and eosinophil recruitment in pulmonary fibrosis. J Immunol. 1997;158(2):954-9.
226. Antoniu SA. Targeting the angiotensin pathway in idiopathic pulmonary fibrosis. Expert Opin Ther Targets. 2008;12(12):1587-90.
227. Matsuse T, Fukuchi Y, Eto Y, Matsui H, Hosoi T, Oka T, et al. Expression of immunoreactive and bioactive activin A protein in adult murine lung after bleomycin treatment. American journal of respiratory cell and molecular biology. 1995;13(1):17-24.
228. Sheppard D. The role of integrins in pulmonary fibrosis. Eur Respir Rev. 2008;17(109):157-62.
229. Copple BL, Kaska S, Wentling C. Hypoxia-inducible Factor Activation in Myeloid Cells Contributes to the Development of Liver Fibrosis in Cholestatic Mice. J Pharmacol Exp Ther. 2012.
230. Haase VH. Pathophysiological Consequences of HIF Activation: HIF as a modulator of fibrosis. Ann N Y Acad Sci. 2009;1177:57-65.
231. Halberg N, Khan T, Trujillo ME, Wernstedt-Asterholm I, Attie AD, Sherwani S, et al. Hypoxia-inducible factor 1alpha induces fibrosis and insulin resistance in white adipose tissue. Molecular and cellular biology. 2009;29(16):4467-83.
232. Kimura K, Iwano M, Higgins DF, Yamaguchi Y, Nakatani K, Harada K, et al. Stable expression of HIF-1alpha in tubular epithelial cells promotes interstitial fibrosis. American journal of physiology Renal physiology. 2008;295(4):F1023-9.
233. Moon JO, Welch TP, Gonzalez FJ, Copple BL. Reduced liver fibrosis in hypoxia-inducible factor-1alpha-deficient mice. Am J Physiol Gastrointest Liver Physiol. 2009;296(3):G582-92.
234. Theilig F, Enke AK, Scolari B, Polzin D, Bachmann S, Koesters R. Tubular deficiency of von Hippel-Lindau attenuates renal disease progression in anti-GBM glomerulonephritis. The American journal of pathology. 2011;179(5):2177-88.
235. Tiriveedhi V, Gelman AE, Mohanakumar T. HIF-1alpha signaling by airway epithelial cell K-alpha1-tubulin: Role in fibrosis and chronic rejection of human lung allografts. Cell Immunol. 2012;273(1):59-66.
236. Ueno M, Maeno T, Nomura M, Aoyagi-Ikeda K, Matsui H, Hara K, et al. Hypoxia-inducible factor-1alpha mediates TGF-beta-induced PAI-1 production in alveolar

macrophages in pulmonary fibrosis. American journal of physiology Lung cellular and molecular physiology. 2011;300(5):L740-52.
237. Zhou Q, Pardo A, Konigshoff M, Eickelberg O, Budinger GR, Thavarajah K, et al. Role of von Hippel-Lindau protein in fibroblast proliferation and fibrosis. Faseb J. 2011;25(9):3032-44.
238. Molina-Molina M, Serrano-Mollar A, Bulbena O, Fernandez-Zabalegui L, Closa D, Marin-Arguedas A, et al. Losartan attenuates bleomycin induced lung fibrosis by increasing prostaglandin E2 synthesis. Thorax. 2006;61(7):604-10.
239. Draz MS, Fang BA, Zhang P, Hu Z, Gu S, Weng KC, et al. Nanoparticle-mediated systemic delivery of siRNA for treatment of cancers and viral infections. Theranostics. 2014;4(9):872-92.
240. Trotta M, Debernardi F, Caputo O. Preparation of solid lipid nanoparticles by a solvent emulsification-diffusion technique. Int J Pharm. 2003;257(1-2):153-60.
241. Xue HY, Wong HL. Tailoring nanostructured solid-lipid carriers for time-controlled intracellular siRNA kinetics to sustain RNAi-mediated chemosensitization. Biomaterials. 2011;32(10):2662-72.
242. Pakunlu RI, Wang Y, Tsao W, Pozharov V, Cook TJ, Minko T. Enhancement of the efficacy of chemotherapy for lung cancer by simultaneous suppression of multidrug resistance and antiapoptotic cellular defense: novel multicomponent delivery system. Cancer Res. 2004;64(17):6214-24.
243. Savla R, Garbuzenko OB, Chen S, Rodriguez-Rodriguez L, Minko T. Tumor-targeted responsive nanoparticle-based systems for magnetic resonance imaging and therapy. Pharmaceutical research. 2014;31(12):3487-502.
244. Riordan JR. CFTR function and prospects for therapy. Annu Rev Biochem. 2008;77:701-26.
245. Kugler AJ, Fabbio KL, Pham DQ, Nadeau DA. Inhaled Technosphere Insulin: A Novel Delivery System and Formulation for the Treatment of Types 1 and 2 Diabetes Mellitus. Pharmacotherapy: The Journal of Human Pharmacology and Drug Therapy. 2015;35(3):298-314.
246. Laube BL, Georgopoulos A, Adams G. Preliminary study of the efficacy of insulin aerosol delivered by oral inhalation in diabetic patients. JAmA. 1993;269(16):2106-9.
247. Fleming LW, Fleming JW, Davis CS. Afrezza: An inhaled approach to insulin delivery. Journal of the American Association of Nurse Practitioners. 2015.
248. Dolatabadi JEN, Valizadeh H, Hamishehkar H. Solid Lipid Nanoparticles as Efficient Drug and Gene Delivery Systems: Recent Breakthroughs. 2015.
249. Rahimpour Y, Hamishehkar H, Nokhodchi A. Lipidic Micro-and Nano-Carriers for Pulmonary Drug Delivery—A State-of-the-Art Review. Pulmonary Drug Delivery: Advances and Challenges. 2015:123-42.
250. Della Latta V, Cecchettini A, Del Ry S, Morales M. Bleomycin in the setting of lung fibrosis induction: From biological mechanisms to counteractions. Pharmacological Research. 2015;97:122-30.
251. Wang XM, Zhang Y, Kim HP, Zhou Z, Feghali-Bostwick CA, Liu F, et al. Caveolin-1: a critical regulator of lung fibrosis in idiopathic pulmonary fibrosis. The Journal of experimental medicine. 2006;203(13):2895-906.

252. Moore BB, Murray L, Das A, Wilke CA, Herrygers AB, Toews GB. The role of CCL12 in the recruitment of fibrocytes and lung fibrosis. Am J Respir Cell Mol Biol. 2006;35(2):175-81.
253. Gharaee-Kermani M, Hu B, Phan SH, Gyetko MR. Recent advances in molecular targets and treatment of idiopathic pulmonary fibrosis: focus on TGFbeta signaling and the myofibroblast. Current medicinal chemistry. 2009;16(11):1400-17.
254. Karmouty-Quintana H, Chen N, Davies J, Weng T, Luo F, Molina J, et al. Hypoxia And Macrophage Differentiation Contribute To Idiopathic Pulmonary Fibrosis. American journal of respiratory and critical care medicine. 2015;191:A6128.
255. McClendon J, Redente EF, Ito Y, Colgan SP, Ahmad A, Tuder R, et al. Hypoxia-Inducible Factor–Dependent CXCR4/SDF1 Signaling Promotes Alveolar Type II Cell Spreading and the Resolution of Epithelial Permeability after Lung Injury. Annals of the American Thoracic Society. 2015;12(Supplement 1):S72-S3.
256. Savla R, Minko T. Nanotechnology approaches for inhalation treatment of fibrosis. Journal of drug targeting. 2013;21(10):914-25.
257. Joseph PM, O'Sullivan BP, Lapey A, Dorkin H, Oren J, Balfour R, et al. Aerosol and lobar administration of a recombinant adenovirus to individuals with cystic fibrosis. I. Methods, safety, and clinical implications. Human gene therapy. 2001;12(11):1369-82.
258. Cai ZW, Liu J, Li HY, Sheppard DN. Targeting F508del-CFTR to develop rational new therapies for cystic fibrosis. Acta pharmacologica Sinica. 2011;32(6):693-701.
259. Ren HY, Grove DE, De La Rosa O, Houck SA, Sopha P, Van Goor F, et al. VX-809 corrects folding defects in cystic fibrosis transmembrane conductance regulator protein through action on membrane-spanning domain 1. Molecular biology of the cell. 2013;24(19):3016-24.
260. Hoffman LR, Ramsey BW. Cystic fibrosis therapeutics: the road ahead. Chest. 2013;143(1):207-13.
261. Kreindler JL. Cystic fibrosis: exploiting its genetic basis in the hunt for new therapies. Pharmacology & therapeutics. 2010;125(2):219-29.
262. Chaaban MR, Kejner A, Rowe SM, Woodworth BA. Cystic fibrosis chronic rhinosinusitis: a comprehensive review. American journal of rhinology & allergy. 2013;27(5):387-95.
263. Yu H, Burton B, Huang CJ, Worley J, Cao D, Johnson JP, Jr., et al. Ivacaftor potentiation of multiple CFTR channels with gating mutations. Journal of cystic fibrosis : official journal of the European Cystic Fibrosis Society. 2012;11(3):237-45.
264. Rowe SM, Verkman AS. Cystic fibrosis transmembrane regulator correctors and potentiators. Cold Spring Harbor perspectives in medicine. 2013;3(7).
265. Boswell GW, Buell D, Bekersky I. AmBisome (liposomal amphotericin B): a comparative review. Journal of clinical pharmacology. 1998;38(7):583-92.
266. Green MR, Manikhas GM, Orlov S, Afanasyev B, Makhson AM, Bhar P, et al. Abraxane, a novel Cremophor-free, albumin-bound particle form of paclitaxel for the treatment of advanced non-small-cell lung cancer. Annals of oncology : official journal of the European Society for Medical Oncology / ESMO. 2006;17(8):1263-8.
267. O'Brien ME, Wigler N, Inbar M, Rosso R, Grischke E, Santoro A, et al. Reduced cardiotoxicity and comparable efficacy in a phase III trial of pegylated liposomal doxorubicin HCl (CAELYX/Doxil) versus conventional doxorubicin for first-line treatment of metastatic

breast cancer. Annals of oncology : official journal of the European Society for Medical Oncology / ESMO. 2004;15(3):440-9.
268. Bi R, Shao W, Wang Q, Zhang N. Solid lipid nanoparticles as insulin inhalation carriers for enhanced pulmonary delivery. Journal of biomedical nanotechnology. 2009;5(1):84-92.
269. Feng T, Tian H, Xu C, Lin L, Xie Z, Lam MH, et al. Synergistic co-delivery of doxorubicin and paclitaxel by porous PLGA microspheres for pulmonary inhalation treatment. European journal of pharmaceutics and biopharmaceutics : official journal of Arbeitsgemeinschaft fur Pharmazeutische Verfahrenstechnik eV. 2014;88(3):1086-93.
270. Godugu C, Patel AR, Doddapaneni R, Marepally S, Jackson T, Singh M. Inhalation delivery of Telmisartan enhances intratumoral distribution of nanoparticles in lung cancer models. J Control Release. 2013;172(1):86-95.
271. Ivanova V, Garbuzenko OB, Reuhl KR, Reimer DC, Pozharov VP, Minko T. Inhalation treatment of pulmonary fibrosis by liposomal prostaglandin E2. European journal of pharmaceutics and biopharmaceutics : official journal of Arbeitsgemeinschaft fur Pharmazeutische Verfahrenstechnik eV. 2013;84(2):335-44.
272. Kunda NK, Alfagih IM, Dennison SR, Tawfeek HM, Somavarapu S, Hutcheon GA, et al. Bovine Serum Albumin Adsorbed PGA-co-PDL Nanocarriers for Vaccine Delivery via Dry Powder Inhalation. Pharmaceutical research. 2015;32(4):1341-53.
273. Scalia S, Haghi M, Losi V, Trotta V, Young PM, Traini D. Quercetin solid lipid microparticles: a flavonoid for inhalation lung delivery. European journal of pharmaceutical sciences : official journal of the European Federation for Pharmaceutical Sciences. 2013;49(2):278-85.
274. Taratula O, Garbuzenko OB, Chen AM, Minko T. Innovative strategy for treatment of lung cancer: targeted nanotechnology-based inhalation co-delivery of anticancer drugs and siRNA. J Drug Target. 2011;19(10):900-14.
275. Taratula O, Kuzmov A, Shah M, Garbuzenko OB, Minko T. Nanostructured lipid carriers as multifunctional nanomedicine platform for pulmonary co-delivery of anticancer drugs and siRNA. Journal of controlled release : official journal of the Controlled Release Society. 2013;171(3):349-57.
276. Vadakkan MV, Annapoorna K, Sivakumar KC, Mundayoor S, Kumar GS. Dry powder cationic lipopolymeric nanomicelle inhalation for targeted delivery of antitubercular drug to alveolar macrophage. Int J Nanomedicine. 2013;8:2871-85.
277. Willis L, Hayes D, Jr., Mansour HM. Therapeutic liposomal dry powder inhalation aerosols for targeted lung delivery. Lung. 2012;190(3):251-62.
278. Boyle MP, Bell SC, Konstan MW, McColley SA, Rowe SM, Rietschel E, et al. A CFTR corrector (lumacaftor) and a CFTR potentiator (ivacaftor) for treatment of patients with cystic fibrosis who have a phe508del CFTR mutation: a phase 2 randomised controlled trial. The Lancet Respiratory Medicine. 2014;2(7):527-38.
279. McKone EF, Borowitz D, Drevinek P, Griese M, Konstan MW, Wainwright C, et al. Long-term safety and efficacy of ivacaftor in patients with cystic fibrosis who have the Gly551Asp-CFTR mutation: a phase 3, open-label extension study (PERSIST). The Lancet Respiratory Medicine. 2014;2(11):902-10.
280. Elborn JS, Geller DE, Conrad D, Aaron SD, Smyth AR, Fischer R, et al. A phase 3, open-label, randomized trial to evaluate the safety and efficacy of levofloxacin inhalation solution

(APT-1026) versus tobramycin inhalation solution in stable cystic fibrosis patients. Journal of Cystic Fibrosis. 2015.
281. Geller DE. The science of aerosol delivery in cystic fibrosis. Pediatric Pulmonology. 2008;43(S9):S5-S17.
282. Davis PB. Another Beginning for Cystic Fibrosis Therapy. New England Journal of Medicine. 2015.
283. Sanders NN, DE SMEDT SC, Van Rompaey E, Simoens P, De Baets F, Demeester J. Cystic fibrosis sputum: a barrier to the transport of nanospheres. American journal of respiratory and critical care medicine. 2000;162(5):1905-11.
284. Saupe A, Gordon KC, Rades T. Structural investigations on nanoemulsions, solid lipid nanoparticles and nanostructured lipid carriers by cryo-field emission scanning electron microscopy and Raman spectroscopy. International journal of pharmaceutics. 2006;314(1):56-62.
285. Van Goor F, Yu H, Burton B, Hoffman BJ. Effect of ivacaftor on CFTR forms with missense mutations associated with defects in protein processing or function. Journal of cystic fibrosis : official journal of the European Cystic Fibrosis Society. 2014;13(1):29-36.

8 Acknowledgment of Previous Publications

1. V. Ivanova, R. Savla, T. Minko, Nanostructured lipid carriers for inhalation co-delivery of two drugs for the treatment of cystic fibrosis respiratory manifestations, in preparation.

2. R. Savla, V. Ivanova, T. Minko, Nanoparticle Design Considerations for Various Imaging Purposes, Nanomedicine: Nanotechnology, Biology and Medicine, submitted.

3. R. N. Jain, X. Huang, S. Das, R. Silva, V. Ivanova, T. Minko, T. Asefa, Functionalized Mesoporous Silica Nanoparticles for Glucose- and pH-Stimulated Release of Insulin, Z. Anorg. Allg. Chem. (Zeitschrift fur anorganische und allgemeine Chemie, ZAAC, Journal of inorganic and general chemistry), in press (2015).

4. R. Savla, V. Ivanova, T. Minko, Nanoparticles in the development of therapeutic cancer vaccines, Pharmaceutical Nanotechnology, 2, 2-22 (2014).

5. V. Ivanova, O. B. Garbuzenko, K. R. Reuhl, D. C. Reimer, V. P. Pozharov, T. Minko, Inhalation Inhalation treatment of pulmonary fibrosis by liposomal prostaglandin E2, Eur J Pharm Biopharm, 84, 335-344 (2013).